Low Energy Antikaon-nucleon/nuclei interaction studies by AMADEUS

Excited QCD 2017
Sintra (Portugal) 7-13 May 2017

Kristian Piscicchia*
Laboratori Nazionali di Frascati (INFN)
Museo Storico della Fisica e Centro Studi e Ricerche Enrico Fermi
*kristian.piscicchia@lnf.infn.it

AMADEUS collaboration

Last collaboration meeting: 14 July 2016

Low-energy QCD in the u-d-s sector

$$\mathcal{L}_{eff} = \mathcal{L}_{mesons}(\Phi) + \mathcal{L}_B(\Phi, \Psi_B)$$

- Chiral perturbation theory: interacting systems of N-G bosons (pions, kaons) coupled to baryons works well for ππ, πN, K^+N ..
  NOT for K^-N !!

- $K^- = (s\bar{u})$ strangeness = -1 , $K^+ = (\bar{u}s)$ strangeness = +1

  strange baryons stable respect to strong interaction all have s = -1

- the sub-threshold region is dominated by resonances → complex multichannel dynamics
  Λ(1405) just below $\bar{K}N$ threshold (1432 MeV)

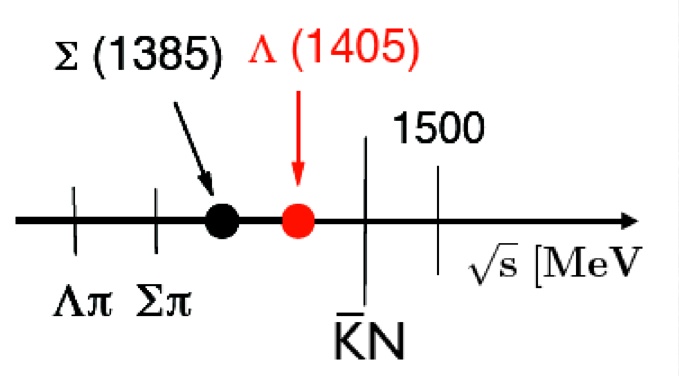

—>

Possible solutions:

- Non-perturbative Coupled Channels approach: Chiral Unitary SU(3) Dynamics
- phenomenological $\bar{K}N$ and NN potentials

The Λ(1405) case

Mass = $1405.1^{+1.3}_{-1.0}$ MeV,
Width = 50.5 ± 2.0 MeV
$I = 0$, $S = -1$, $J^P = 1/2^-$,
Status: **** ,
strong **decay** into Σπ

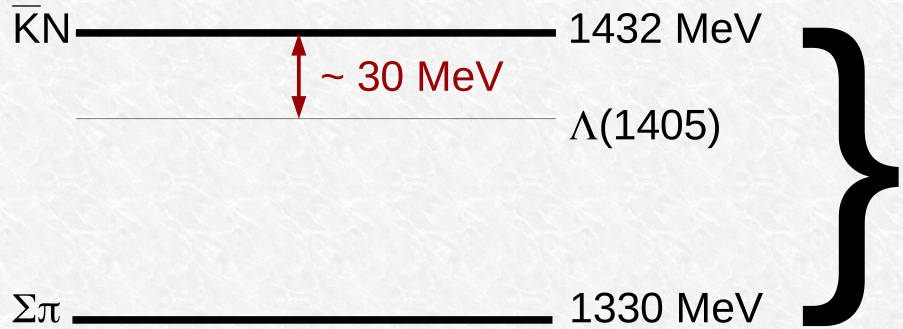

- 3 quark?
- **molecular?**
- **$\bar{K}N$ bound state?**
- pentaquark?

Theoretical prediction Dalitz-Tuan (1959)

First experimental evidence:

M. H. Alston, et al., Phys. Rev. Lett. 6 (1961) 698

$K^- p \rightarrow \pi\pi\pi\Sigma$

Λ(1405)

Λ(1116)

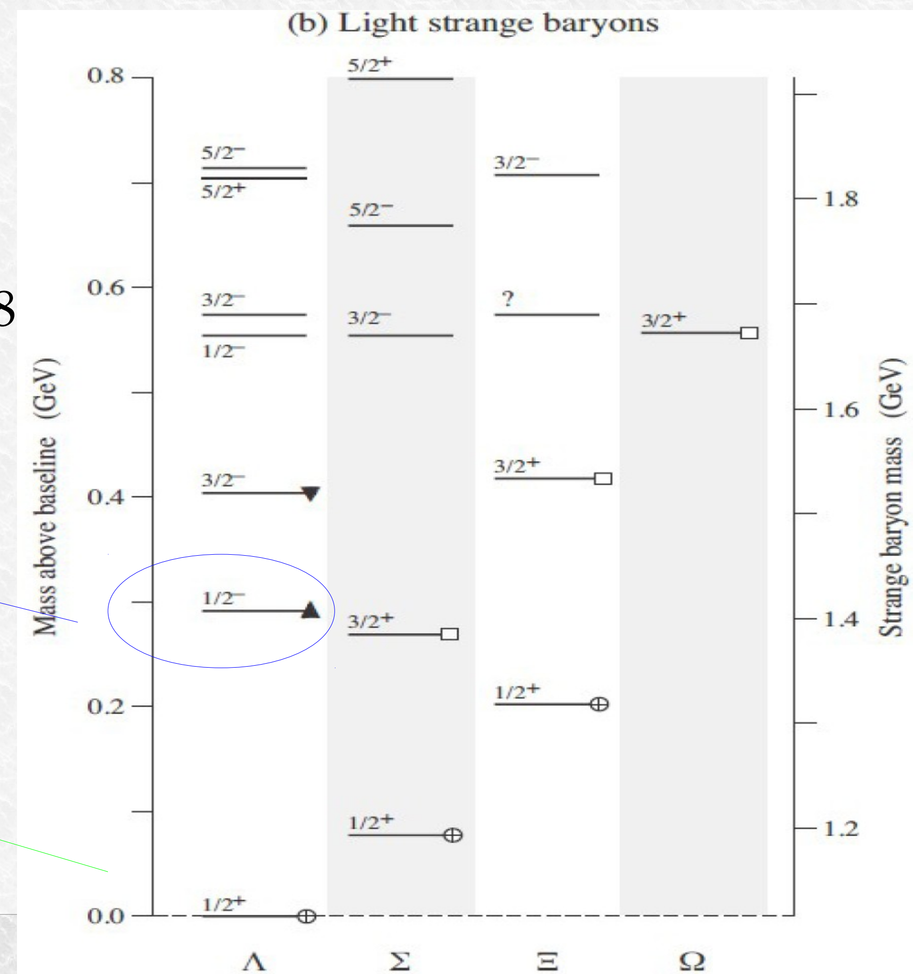

The Λ(1405) case

Λ(1405) is located slightly below the $\bar{K}N$ threshold (1432 MeV)

Three quark model picture difficulties to reproduce the Λ(1405):

- According to its negative parity, one of the quarks has to be excited to $l = 1$
- nucleon sector, we find the N(1535) → the expected mass of the Λ^* is around 1700 MeV
- too big energy splitting observed between the Λ(1405) and the Λ(1520) interpreted as the spin-orbit partner ($J^p = 3/2^-$).
- pentaquark (4q + qbar in $l = 0$), but also predicts other, unobserved, excited baryons,

R. Dalitz and collaborators first suggested to interpret Λ(1405) as an KN quasibound state.

R.H. Dalitz, T.C. Wong and G. Rajasekaran, Phys. Rev. **153** (1967) 1617.

The Λ(1405) case

BUBBLE CHAMBER search of the Λ(1405):

- O. Braun et al. Nucl. Phys. B129 (1977) 1

K- induced reactions on d → $\Sigma^- \pi^+ n$ the resonance is found & 1420 MeV

- D. W. Thomas et al., Nucl. Phys. B56 (1973) 15

pion induced reaction $\pi^- p \rightarrow K^+ \pi \Sigma$ the resonance is found & 1405 MeV

- R. J. Hemingway, Nucl. Phys. B253 (1985) 742

$K^- p \rightarrow \pi^- \Sigma^+(1660) \rightarrow \pi^- (\pi^+ \Lambda(1405)) \rightarrow \pi^- \pi^+ (\pi\Sigma)$ & 4.2 GeV

analysed by Dalitz and Deloff $M = 1406.5 \pm 4.0$ MeV, $\Gamma = 50 \pm 2$MeV

The Λ(1405) case

THE "LINE-SHAPE" OF THE Λ(1405) DEPENDS ON THE OBSERVED CHANNEL !!

$$\frac{d\sigma(\Sigma^-\pi^+)}{dM} \propto \frac{1}{3}\left|T^0\right|^2 + \frac{1}{2}\left|T^1\right|^2 + \frac{2}{\sqrt{6}} Re(T^0 T^{1*})$$

$$\frac{d\sigma(\Sigma^+\pi^-)}{dM} \propto \frac{1}{3}\left|T^0\right|^2 + \frac{1}{2}\left|T^1\right|^2 - \frac{2}{\sqrt{6}} Re(T^0 T^{1*})$$

$$\frac{d\sigma(\Sigma^0\pi^0)}{dM} \propto \frac{1}{3}\left|T^0\right|^2$$

The Λ(1405) case

THE "LINE-SHAPE" OF THE Λ(1405) DEPENDS ON THE OBSERVED CHANNEL !!

$$\frac{d\sigma(\Sigma^-\pi^+)}{dM} \propto \frac{1}{3}\left|T^0\right|^2 + \frac{1}{2}\left|T^1\right|^2 + \frac{2}{\sqrt{6}}Re(T^0T^{1*})$$

$$\frac{d\sigma(\Sigma^+\pi^-)}{dM} \propto \frac{1}{3}\left|T^0\right|^2 + \frac{1}{2}\left|T^1\right|^2 - \frac{2}{\sqrt{6}}Re(T^0T^{1*})$$

$$\frac{d\sigma(\Sigma^0\pi^0)}{dM} \propto \frac{1}{3}\left|T^0\right|^2$$

IS DIFFERENT IN $\Sigma^+\pi^-$ VS $\Sigma^-\pi^+$

DUE TO ISOSPIN INTERFERENCE

The Λ(1405) case

THE "LINE-SHAPE" OF THE Λ(1405) DEPENDS ON THE OBSERVED CHANNEL !!

$$\frac{d\sigma(\Sigma^-\pi^+)}{dM} \propto \frac{1}{3}\left|T^0\right|^2 + \frac{1}{2}\left|T^1\right|^2 + \frac{2}{\sqrt{6}} Re(T^0 T^{1*})$$

$$\frac{d\sigma(\Sigma^+\pi^-)}{dM} \propto \frac{1}{3}\left|T^0\right|^2 + \frac{1}{2}\left|T^1\right|^2 - \frac{2}{\sqrt{6}} Re(T^0 T^{1*})$$

$$\frac{d\sigma(\Sigma^0\pi^0)}{dM} \propto \frac{1}{3}\left|T^0\right|^2$$

IS DIFFERENT IN $\Sigma^+\pi^-$ VS $\Sigma^-\pi^+$

DUE TO ISOSPIN INTERFERENCE

THE CLEANEST SIGNATURE OF THE Λ(1405) IS GIVEN BY THE NEUTRAL CHANNEL:

- is free from isospin interference
- is purely I = 0, no Σ(1385) contamination.

Λ(1405) .. the golden channel

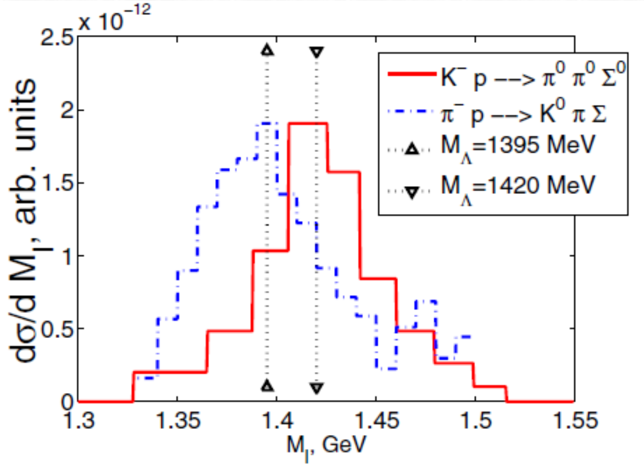

Crystall Ball: K-p $\to \Sigma^0\pi^0\pi^0$ for kaon momentum in the range (514-750 MeV/c). S. Prakhov et al. Phys Rev. C70 (2004) 03465

(**interpreted by Magas et al. PRL 95, 052301 (2005)**)

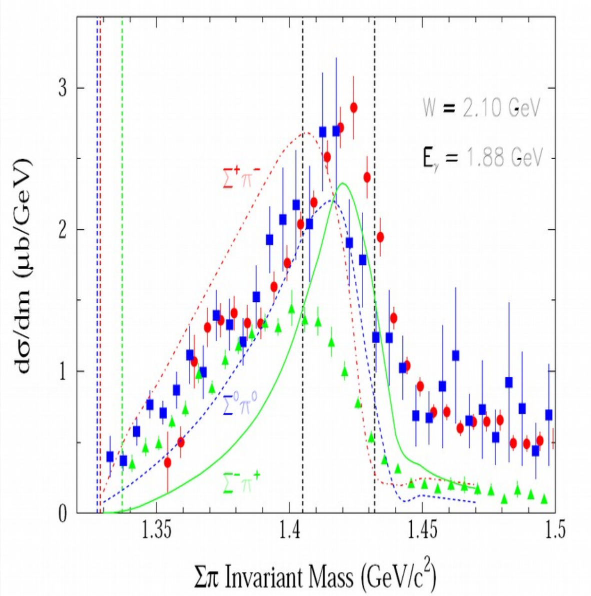

CLAS: $\gamma p \to K^+ \Sigma\pi$

AIP Conf.Proc. 1441 (2012) 296-298

COSY julich: pp $\to$ pK$^+$ $\Sigma^0\pi^0$

(I. Zychor et al., Phys. Lett. B 660 (2008) 167)

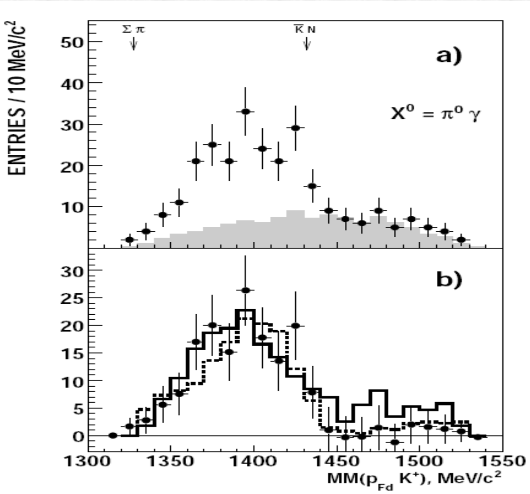

Fig. 4. a) Missing–mass $MM(p_{Fd}K^+)$ distribution for the $pp \to pK^+p\pi^-X^0$ reaction for events with $M(p_{Sd}\pi^-) \approx m(\Lambda)$ and $MM(pK^+p\pi^-) > 190\,\mathrm{MeV}/c^2$. Exper-

Λ(1405) .. the golden channel

Crystall Ball: $K^- p \rightarrow \Sigma^0\pi^0\pi^0$ for kaon momentum in the range (514-750 MeV/c). S. Prakhov et al. Phys Rev. C70 (2004) 03465

(Magas et al. PRL 95, 052301 (2005))

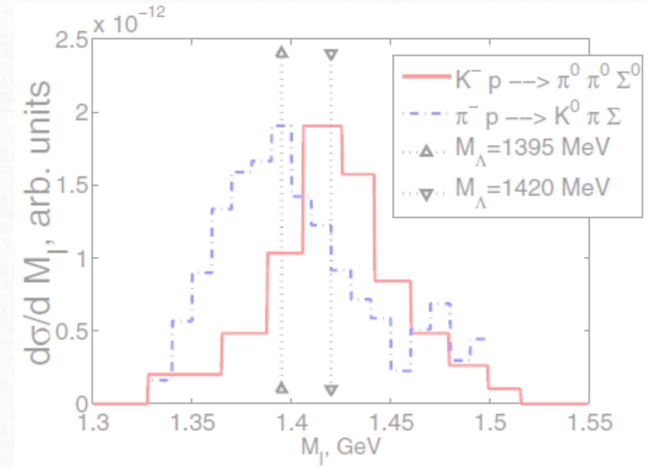

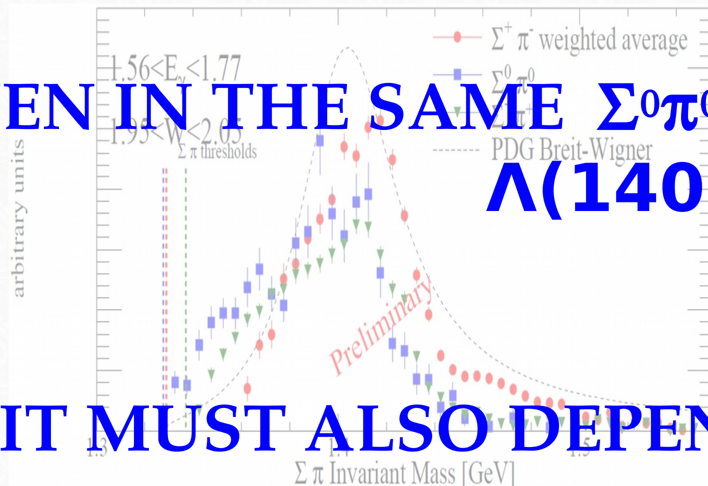

EVEN IN THE SAME $\Sigma^0\pi^0$ THE "LINE-SHAPE" OF THE Λ(1405) CHANGES

CLAS: $\gamma p \rightarrow pK^+ \Sigma\pi$

AIP Conf.Proc. 1441 (2012) 296-298

IT MUST ALSO DEPEND ON THE PRODUCTION MECHANISM

COSY julich: $pp \rightarrow pK^+ \Sigma^0\pi^0$

(I. Zychor et al., Phys. Lett. B 660 (2008) 167)

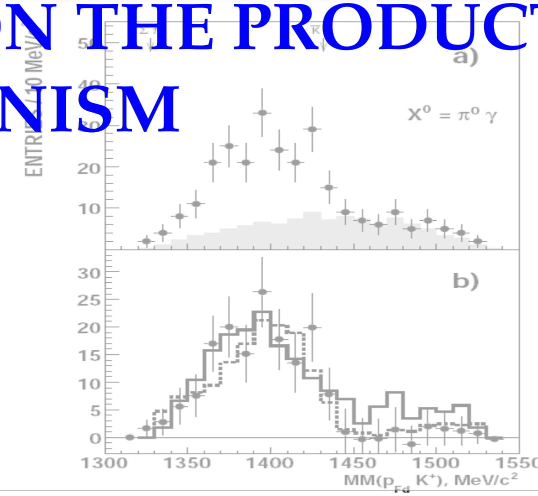

Fig. 4. a) Missing–mass $MM(p_{Fd}K^+)$ distribution for the $pp \rightarrow pK^+p\pi^-X^0$ reaction for events with $M(p_{Sd}\pi^-) \approx m(\Lambda)$ and $MM(pK^+p\pi^-) > 190\,\mathrm{MeV}/c^2$. Exper-

The Λ(1405) case

- Chiral unitary models: Λ(1405) is an I = 0 quasibound state emerging from the coupling between the $\bar{K}N$ and the Σπ channels. Two poles in the neighborhood of the Λ(1405):

two poles: about 1420 ; about = 1380 MeV   Phys. Lett. B 500 (2001), Phys. Rev. C 66 (2002), (Nucl. Phys. A 725(2003) 181) .. many others .. (Nucl. Phys. A881, 98 (2012)) .. others

mainly coupled to $\bar{K}N$ mainly coupled to Σπ → line-shape depends on production mechanism

- Akaishi-Esmaili-Yamazaki phenomenological potential

Phys. Lett. B 686 (2010) 23-28   Confirmation of single pole ansatz? ⟶

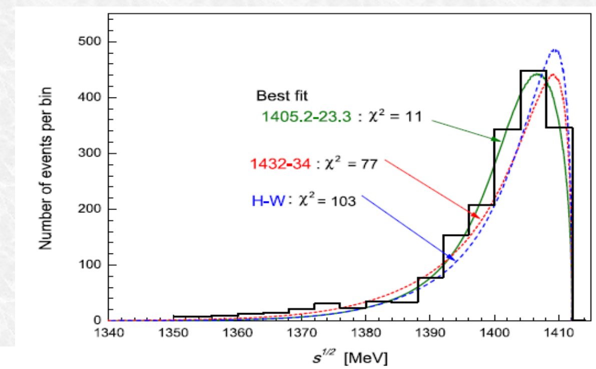

Fig. 6. Detailed differences in $M_{\Sigma\pi}$ spectra among the Hyodo–Weise prediction and the present model predictions.

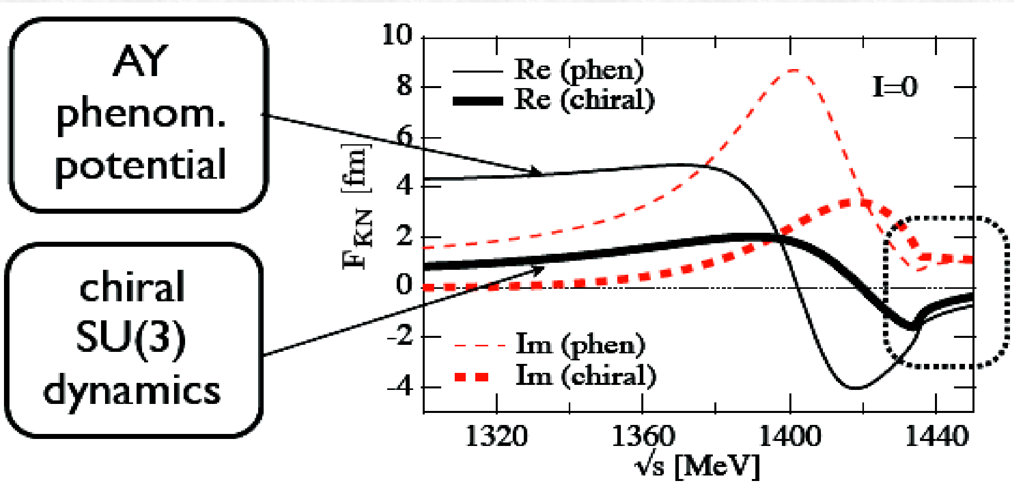

large differences in **subthreshold** extrapolations

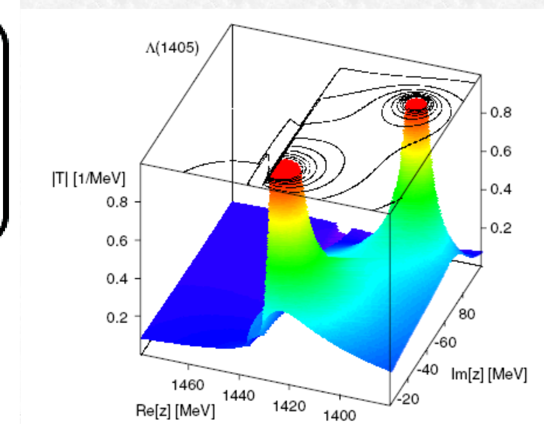

- **Chiral dynamics** predicts significantly **weaker attraction** than AY (local, energy independent) potential in **far-subthreshold** region

The Λ(1405) case

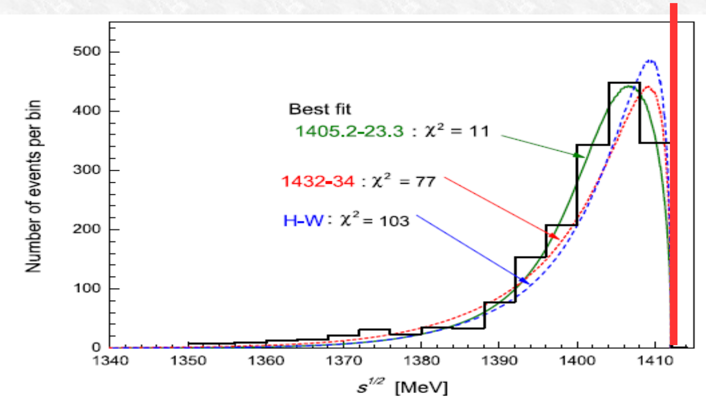

Fig. 6. Detailed differences in $M_{\Sigma\pi}$ spectra among the Hyodo–Weise prediction and the present model predictions.

Two main biases:

- the kinematical energy threshold 1412 MeV

  ($M_K + M_p$ - | BE_p |) the high pole energy region is closed,

- The shape and the amplitude of the NON-RESONANT

  Σ π production below KbarN threshold is unknown.

An ideal experiment:

- Λ(1405) is produced in K- p absorption → mainly coupled to the high mass pole,
- Λ(1405) is observed in the $\Sigma^0\pi^0$ decay channel (pure isospin 0),
- K- is absorbed in-flight on a bound proton with p_K ~ 100 MeV, Σπ invariant mass gain of ~ 10 MeV to open an energy window to the high mass pole.
- Knowledge of the Σπ NON-RESONANT production amplitude.

Why AMADEUS & DAΦNE?

AMADEUS & DAΦNE

DAΦNE

- double ring $e^+ e^-$ collider working at C.M. energy of ϕ, producing **≈ 1000 ϕ /s**

$\phi \rightarrow K^+ K^-$ (BR = (49.2 ± 0.6)%)

- **low momentum** Kaons ≈ 127 Mev/c
- **back to back** $K^+ K^-$ topology

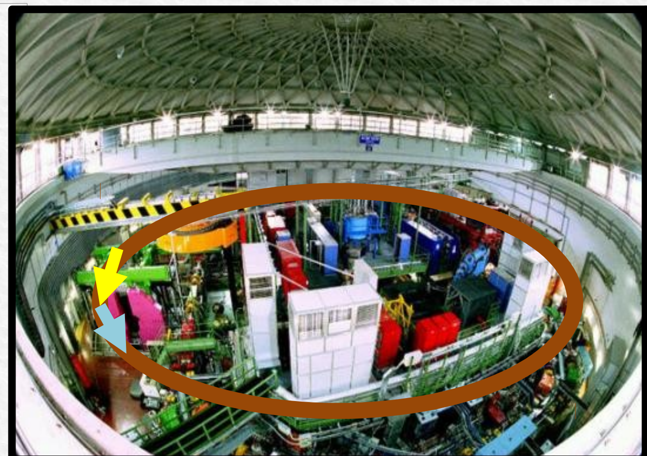

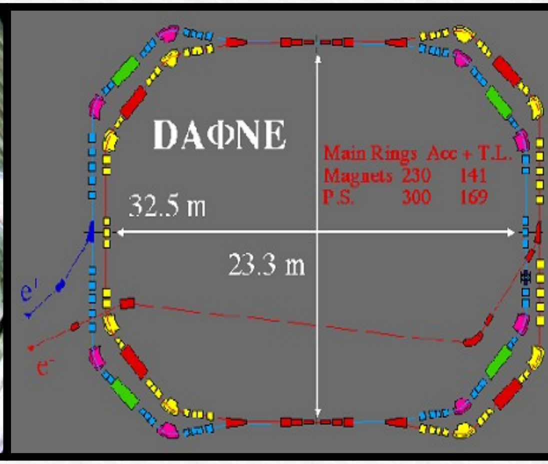

AMADEUS step 0 → KLOE 2004-2005 dataset analysis ($\mathscr{L}$ = 1.74 pb^{-1})

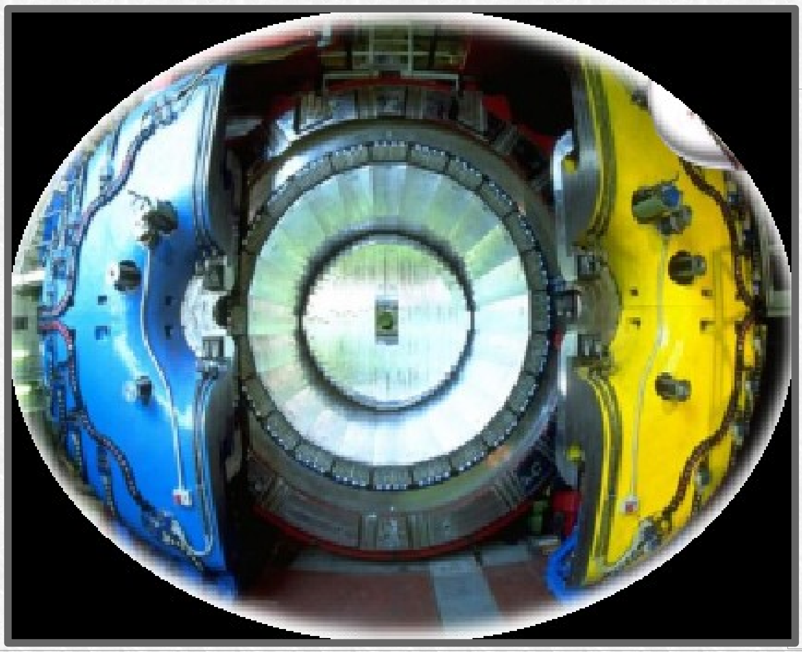

KLOE

- Cilindrical drift chamber with a **4π geometry** and electromagnetic calorimeter
- **96% acceptance**
- optimized in the energy range of all **charged particles** involved
- **good performance** in detecting **photons and neutrons** checked by kloNe group [M. Anelli et al., Nucl Inst. Meth. A 581, 368 (2007)]

K^- absorption on light nuclei

from the materials of the KLOE detector

DC gas (90% He, 10% C_4H_{10}) & DC wall (C + H)

<u>AT-REST</u> (K^- absorbed from atomic orbit) or <u>IN-FLIGHT</u>

(p_K~100MeV)

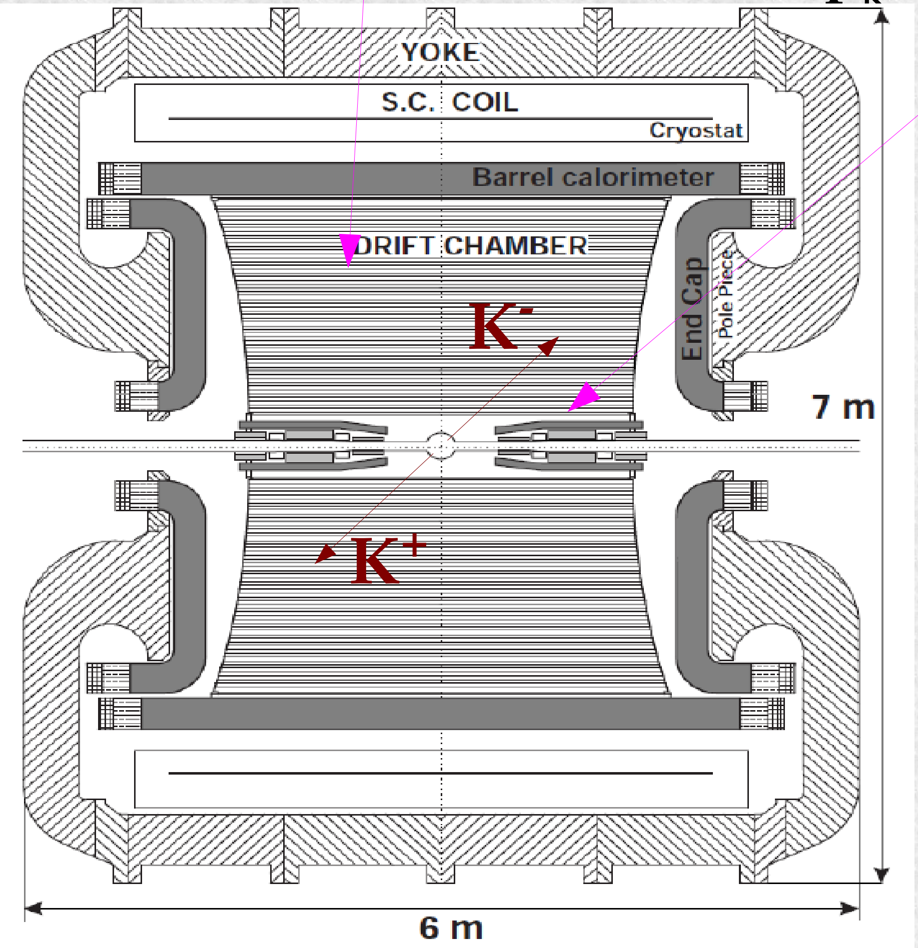

Advantage:

excellent resolution ..

$\sigma_{p\Lambda}$ = 0.49±0.01 MeV/c in DC gas

$\sigma_{m\gamma\gamma}$ = 18.3±0.6 MeV/c^2

Disadvantage:

Not dedicated target → different nuclei contamination → complex interpretation .. but → new features .. K^- in flight absorption.

At-rest VS in-flight K$^-$ captures

AT-REST

K$^-$ absorbed from atomic orbit

(p_K~ 0 MeV)

IN-FLIGHT

(p_K~100MeV)

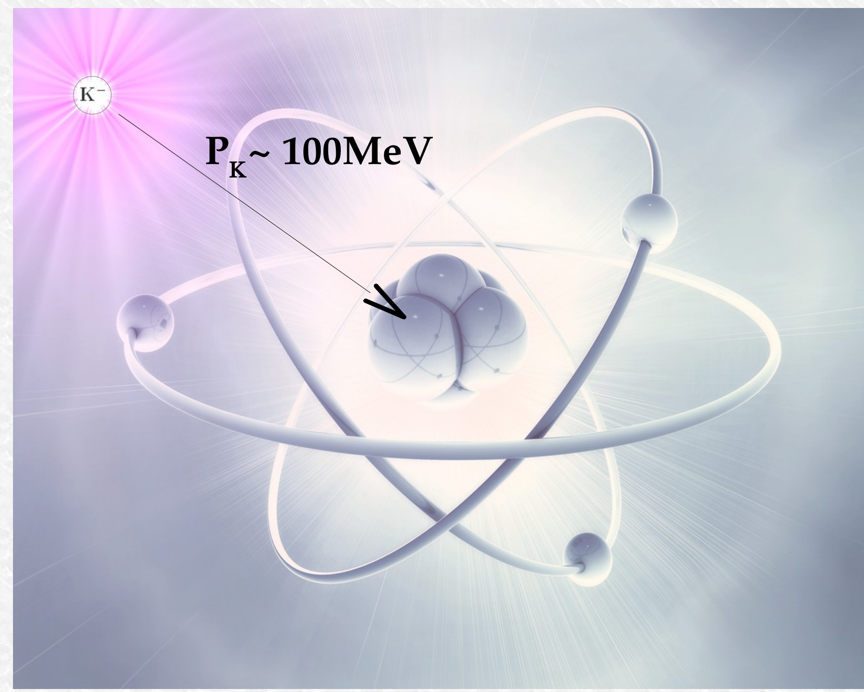

The scientific goal of AMADEUS

Low energy QCD in strangeness sector is still waiting for experimental conclusive constrains on:

1) $\bar{K}$-N potential → how deep can an antikaon be bound in a nucleus?

- U_{KN} strongly affects the position of the $\Lambda(1405)$ state → we investigate it through $(\Sigma-\pi)^0$ decay --- Y π CORRELATION

- if U_{KN} is strongly attractive then K^- NN bound states should appear → we investigate through (Λ/Σ-N) decay --- Y N CORRELATION

2) Y-N potential → extremely poor experimental information from scattering data

- U_{YN} determines the strength of the final state YN (elastic & inelastic) scattering in nuclear environment → could be tested by Y N CORRELATION

K^- - N single nucleon absorption
the case of the $\Lambda(1405)$

Λ(1405) case

Phys.Rev.Lett.95:052301,2005

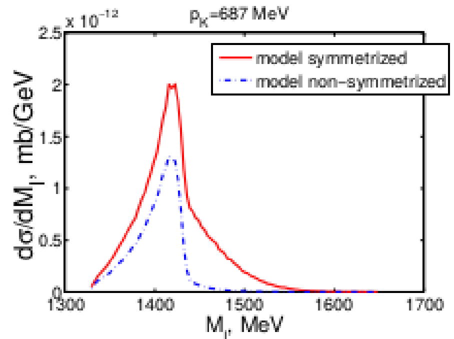

FIG. 4: Theoretical ($\pi^0\Sigma^0$) invariant mass distribution for an initial kaon lab momenta of 687 MeV. The non-symmetrized distribution also contains the factor 1/2 in the cross section.

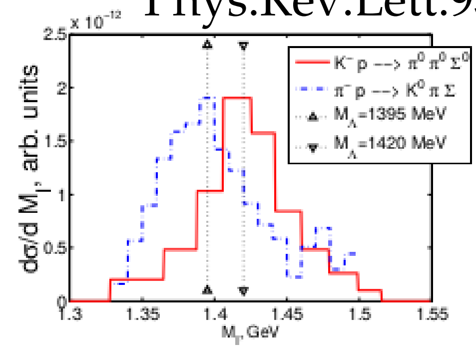

FIG. 5: Two experimental shapes of Λ(1405) resonance. See text for more details.

$p_{\pi 0}$ resolution: $\sigma_p \approx 12$ MeV/c

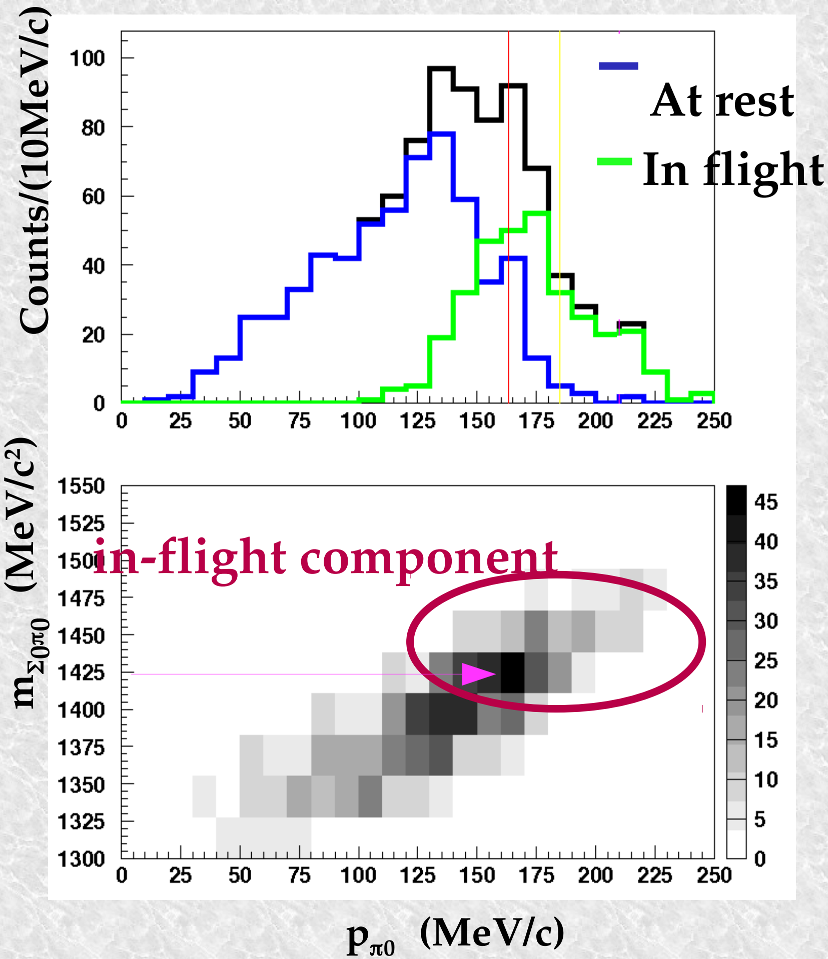

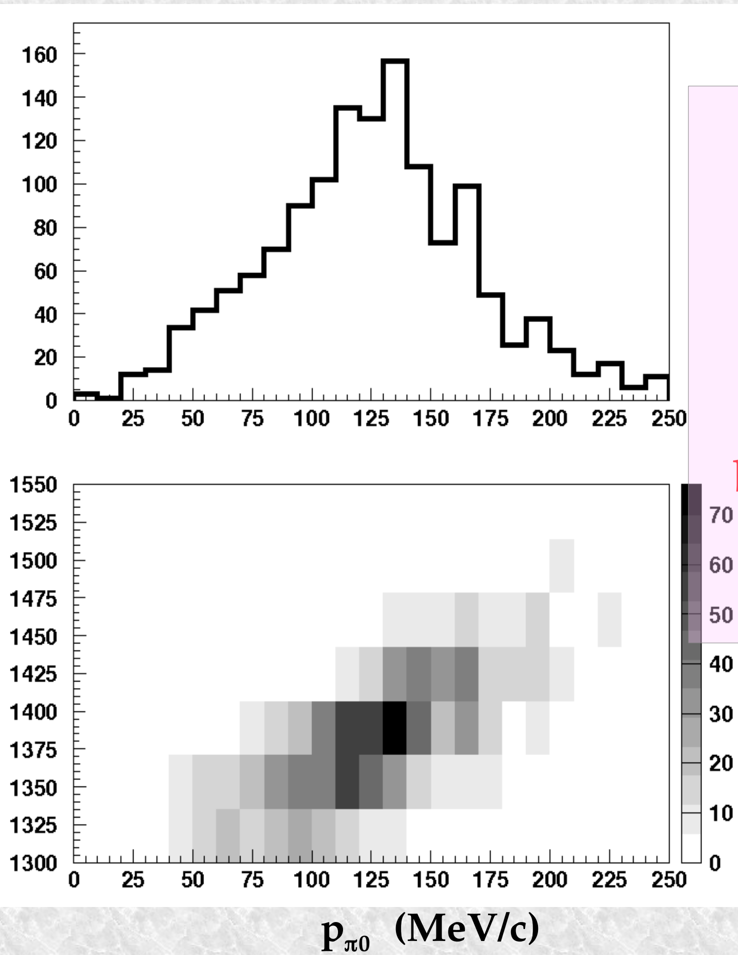

IN-FLIGHT

K- 12C

opens a window

between 1416 MeV

and K-Nth

Complex interpretation due to K- H absorptions ongoing with the collaboration of A. Cieply (UJF, Prague)

$p_{\pi 0}$ **resolution**: $\sigma_p \approx 12$ MeV/c

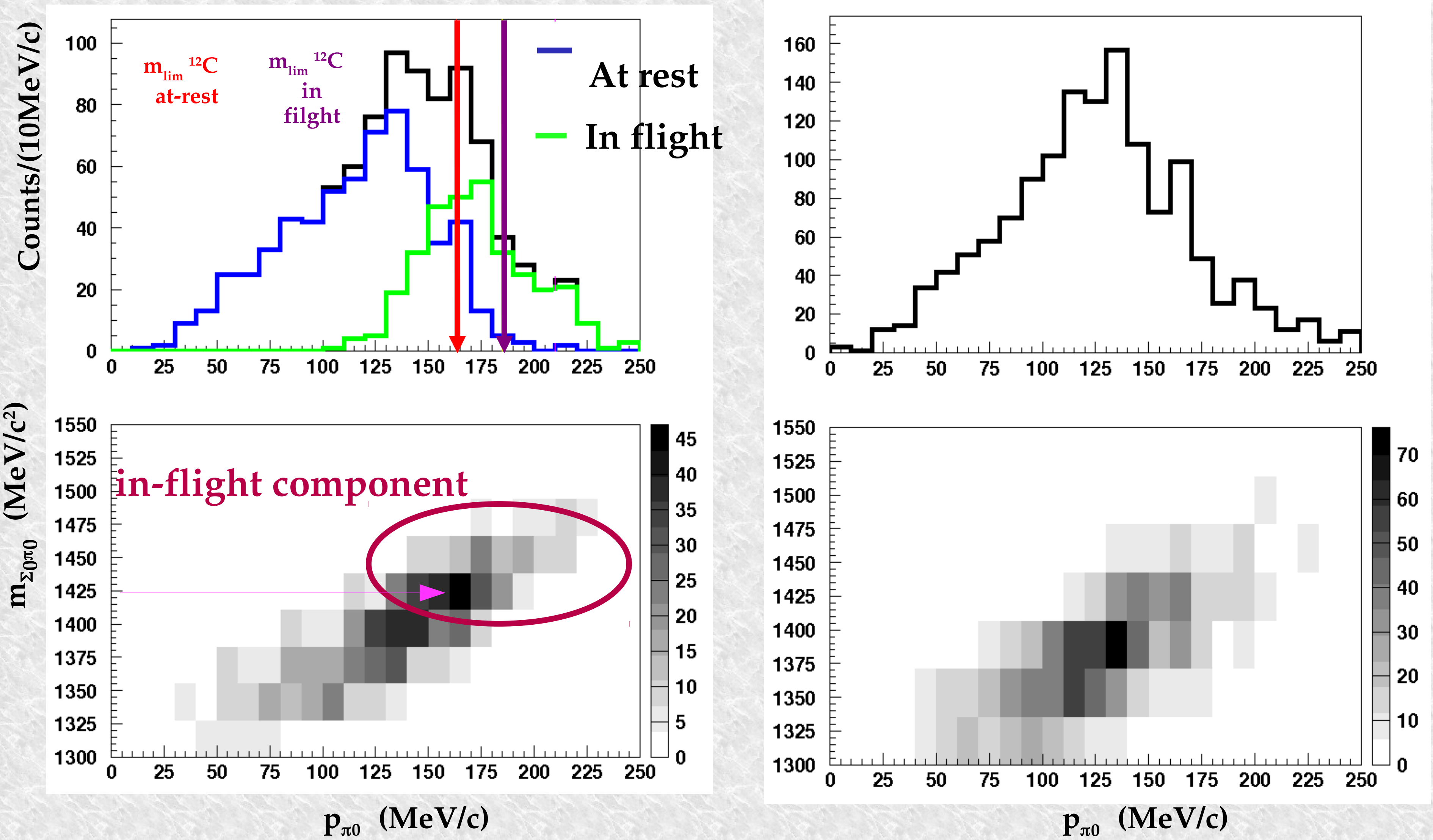

$\Sigma^+\pi^-$ correlation

$K^- p \rightarrow \Sigma^+ \pi^-$ detected via: $(p\pi^0)\ \pi^-$

Possibility to disentangle: Hydrogen, in-flight, at-rest, K^- capture

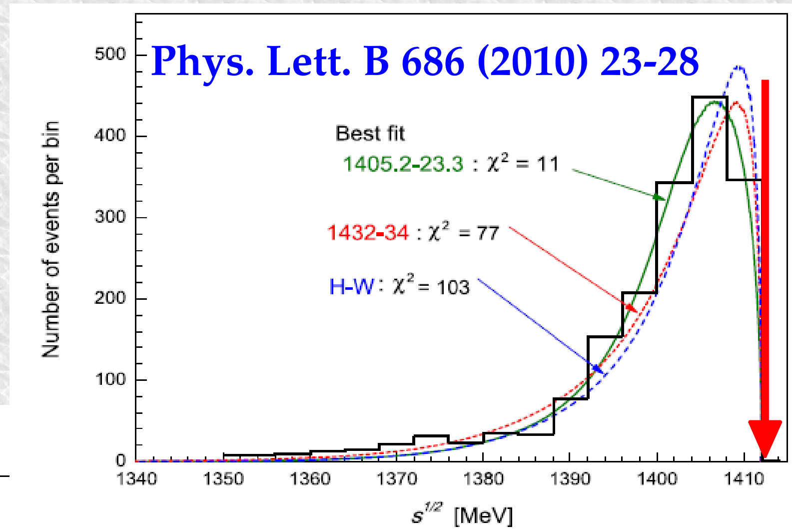

Fig. 6. Detailed differences in $M_{\Sigma\pi}$ spectra among the Hyodo–Weise prediction and the present model predictions.

p_{π^-} resolution: $\sigma_p \approx 1$ MeV/c

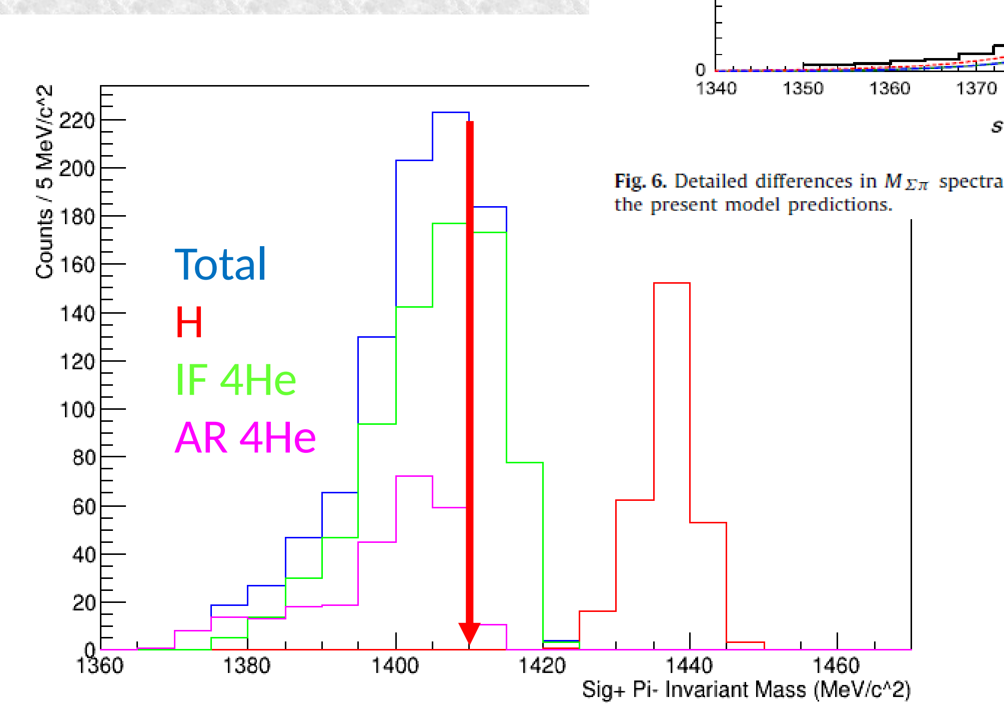

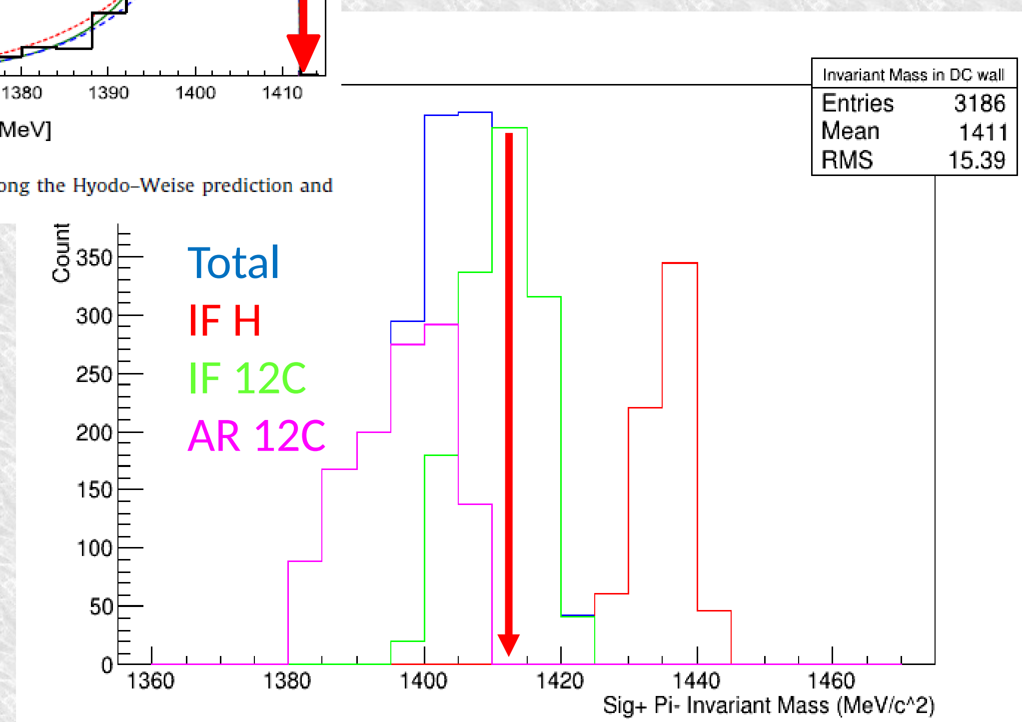

$\Sigma^+\pi^-$ correlation

$K^- p \rightarrow \Sigma^+ \pi^-$ detected via: $(p\pi^0)\ \pi^-$

Possibility to disentangle: Hydrogen, in-flight, at-rest, K^- capture

if resonant production contribution is important a high mass component appears!

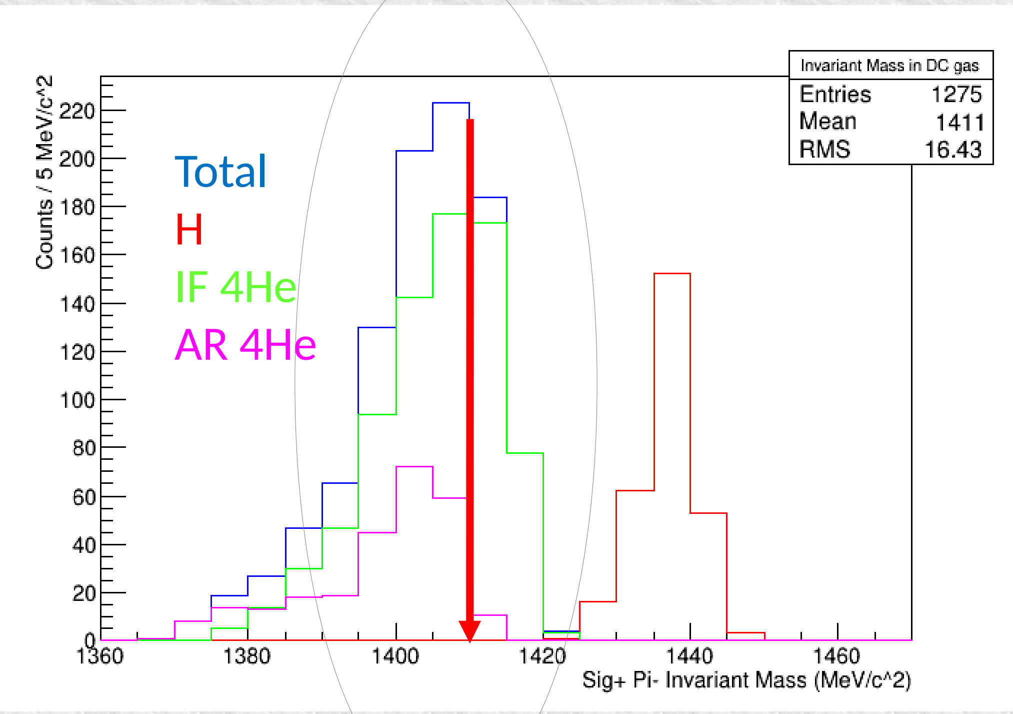

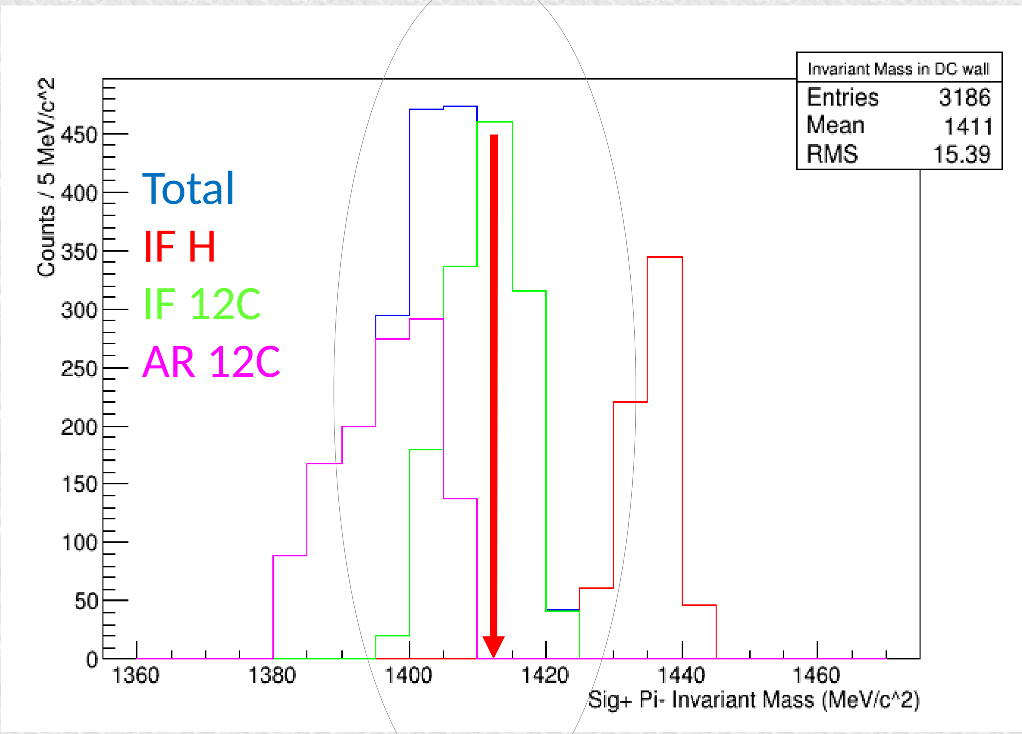

Resonant VS non-resonant

$K^- N \rightarrow (Y^* ?) \rightarrow Y \pi$

in medium, how much comes from resonance ?

Non resonant transition amplitude:

- Never measured before below threshold

(33 MeV below threshold kinetic energy in the Kn CM system):

$$E_{Kn} = -|B_n| - \frac{p_3^2}{2\mu_{\pi,\Lambda,3He}},$$

- few, old theoretical calculations

(Nucl. Phys. B179 (1981) 33-48)

Resonant VS non-resonant

Investigated using:

K^- "n" $\rightarrow \Lambda\pi^-$ direct formation in ^{4}He

the goal is to measure $|f^{N\text{-}R}_{\Lambda\pi}(I=1)|$

to get information on $|f^{N\text{-}R}_{\Sigma\pi}(I=0)|$

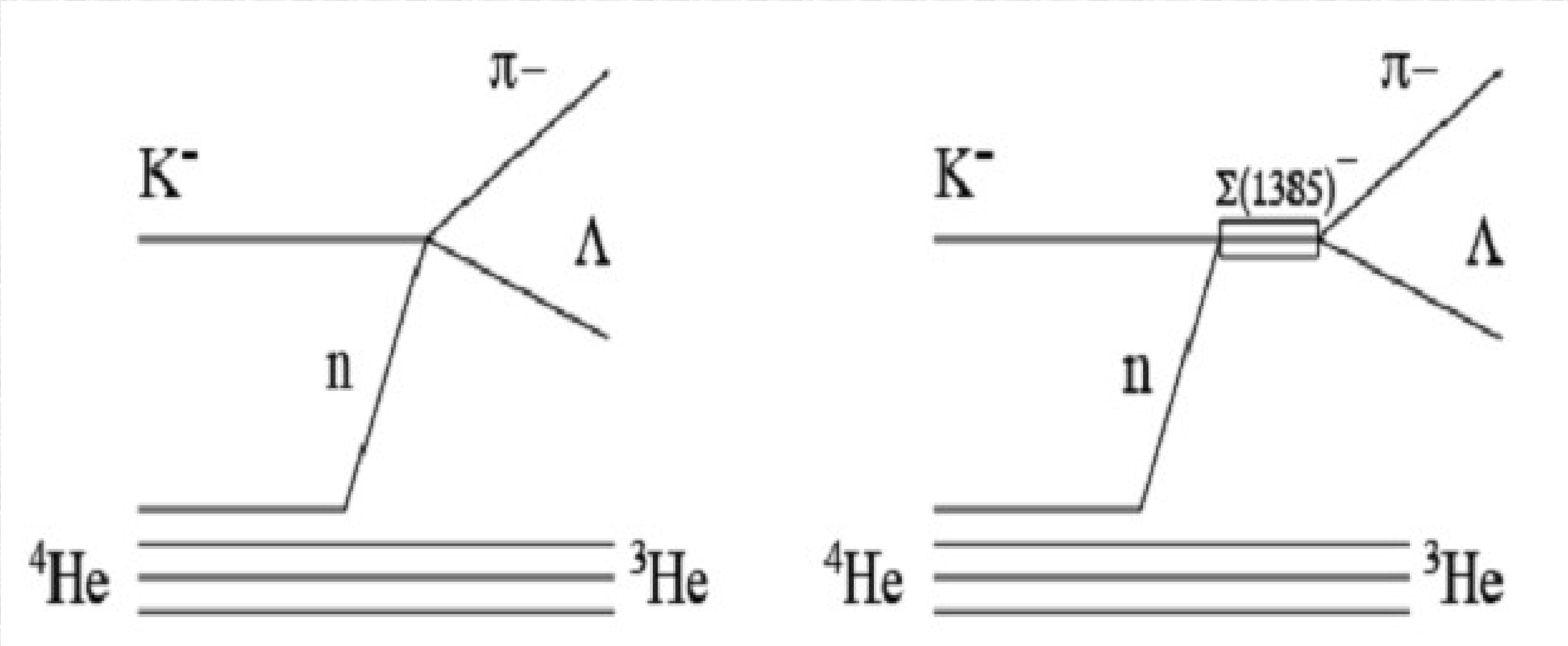

$K^- \, ^4He \rightarrow \Lambda p^- \, ^3He$ resonant and non-resonant processes

Nucl. Phys. A954 (2016) 75-93

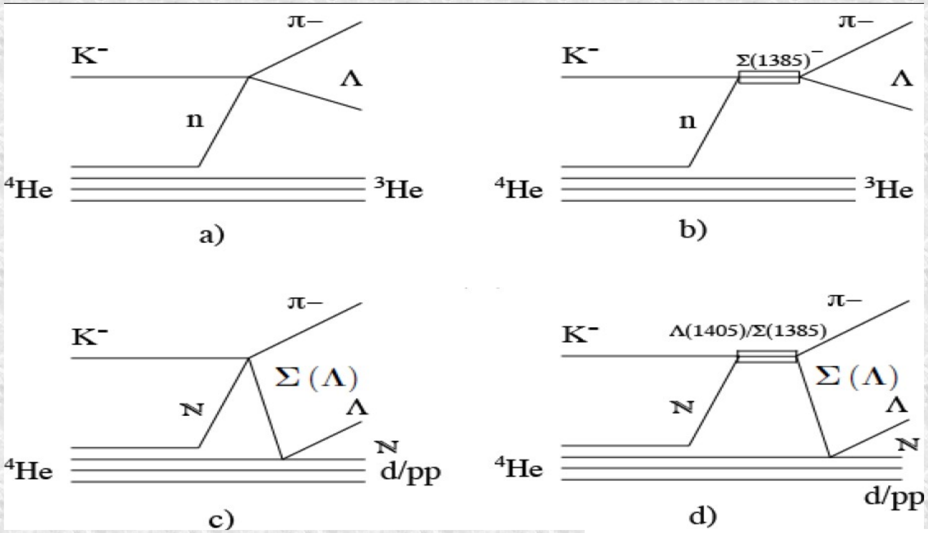

Theoretical shapes for :

total $\Lambda\pi^-$ momentum spectra for the resonant (Σ^{*-}) and non-resonant (I = 1) processes were calculated, for both S-state and P-state K^- capture at-rest and in-flight. Corrections to the amplitudes due to Λ/π final state interactions were estimated.

Collaboration with S. Wycech

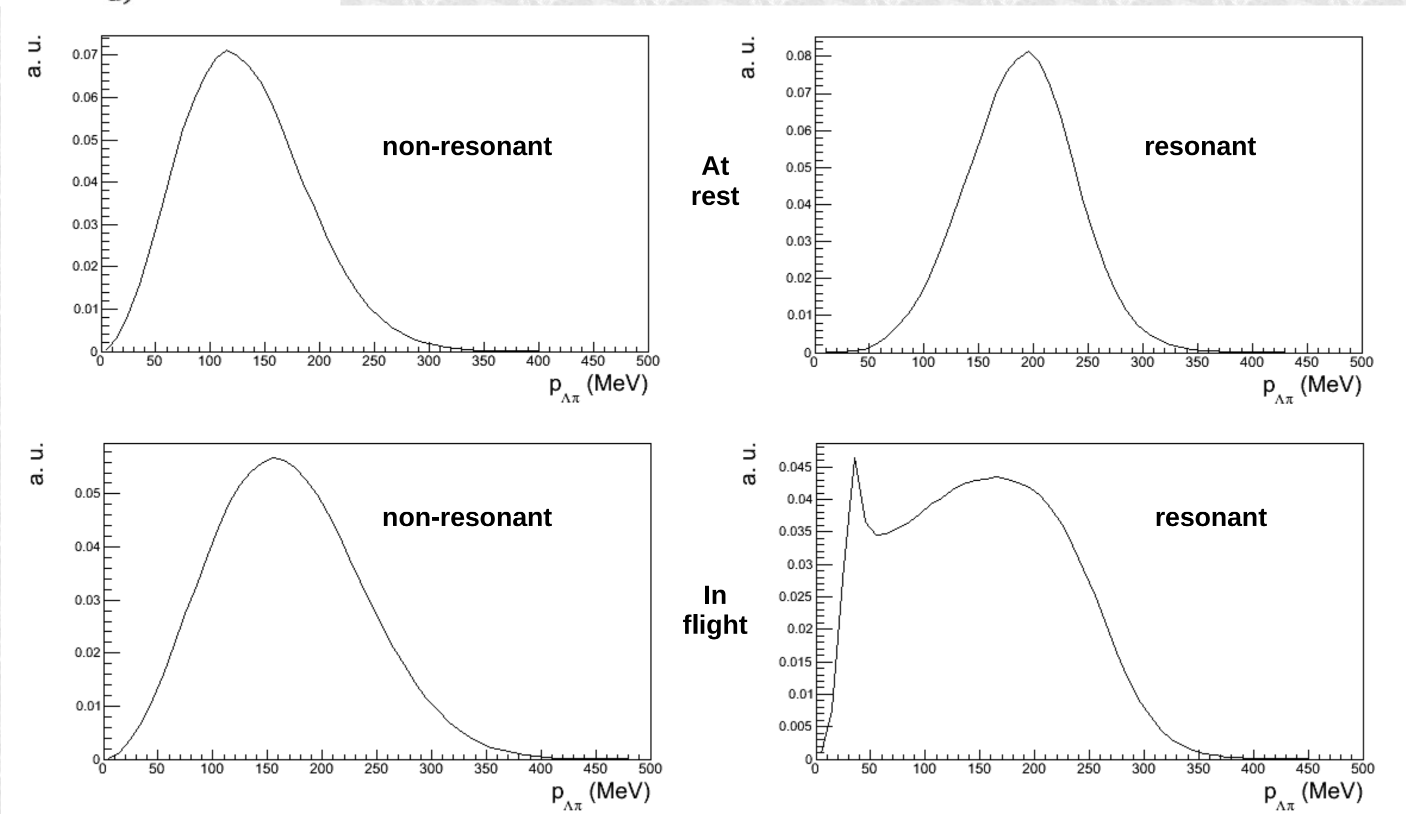

How to extract the $K^- n \to \Lambda\pi^-$ non resonant transition amplitude

simultaneous fit ($p_{\Lambda\pi^-}$ - $m_{\Lambda\pi^-}$ - $\cos(\theta_{\Lambda\pi^-})$) with signal and background processes :

- non resonant K^- capture at-rest from S states in ^{4}He
- resonant K^- capture at-rest from S states in ^{4}He
- non resonant K^- capture in-flight in ^{4}He
- resonant K^- capture in-flight in ^{4}He

- primary $\Sigma\pi^-$ production followed by the $\Sigma N \to \Lambda N'$ conversion process
- K^- capture processes in ^{12}C giving rise to $\Lambda\pi^-$ in the final state

In order to extract:

NR-ar/RES-ar & NR-if/RES-if

Results for the $K^- n \to \Lambda\pi^-$ non resonant transition amplitude

Channels	Ratio/Amplitude	σ_{stat}	σ_{syst}
RES-ar/NR-ar	0.39	$\pm$ 0.04	$^{+0.18}_{-0.07}$
RES-if/NR-if	0.23	$\pm$ 0.03	$^{+0.23}_{-0.22}$
NR-ar	12.00 %	$\pm$ 1.66 %	$^{+1.96}_{-2.77}$ %
NR-if	19.24 %	$\pm$ 4,38 %	$^{+5.90}_{-3.33}$ %
$\Sigma \to \Lambda$ conv.	2.16 %	$\pm$ 0.30 %	$^{+1.62}_{-0.83}$ %
K^{-12}C capture	57.00 %	$\pm$ 1.23 %	$^{+2.21}_{-3.19}$ %

TABLE I. Resonant to non-resonant ratios and amplitude of the different channels extracted from the fit of the $\Lambda\pi^-$ sample. The statistical and systematic errors are also shown. See text for details.

Preliminary

extracted:

NR-ar/RES-ar & NR-if/RES-if

Simultaneous momentum – angle – mass fit

Light band sys err.
Dark band stat. Err.

Σ/Λ nuclear conversion

K-N→Σ **π**

└→ ΣN→**Λ**N'

Absorptions in 12C
(from Carbon wall data)

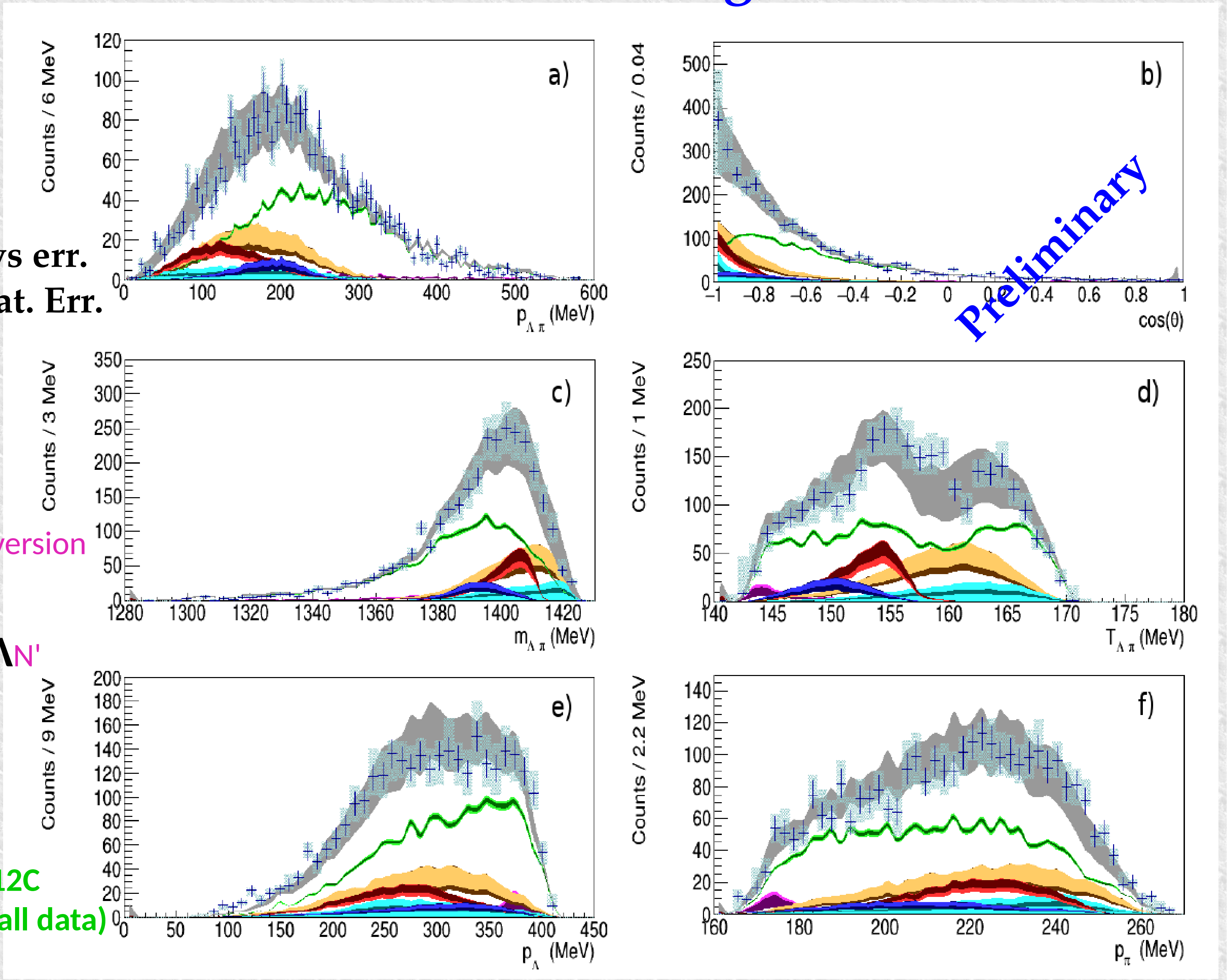

Simultaneous momentum – angle – mass fit

Light band sys err.
Dark band stat. Err.

Non-Resonant
(at-rest)
(in-flight)

Resonant Σ*
(at-rest)
(in-flight)

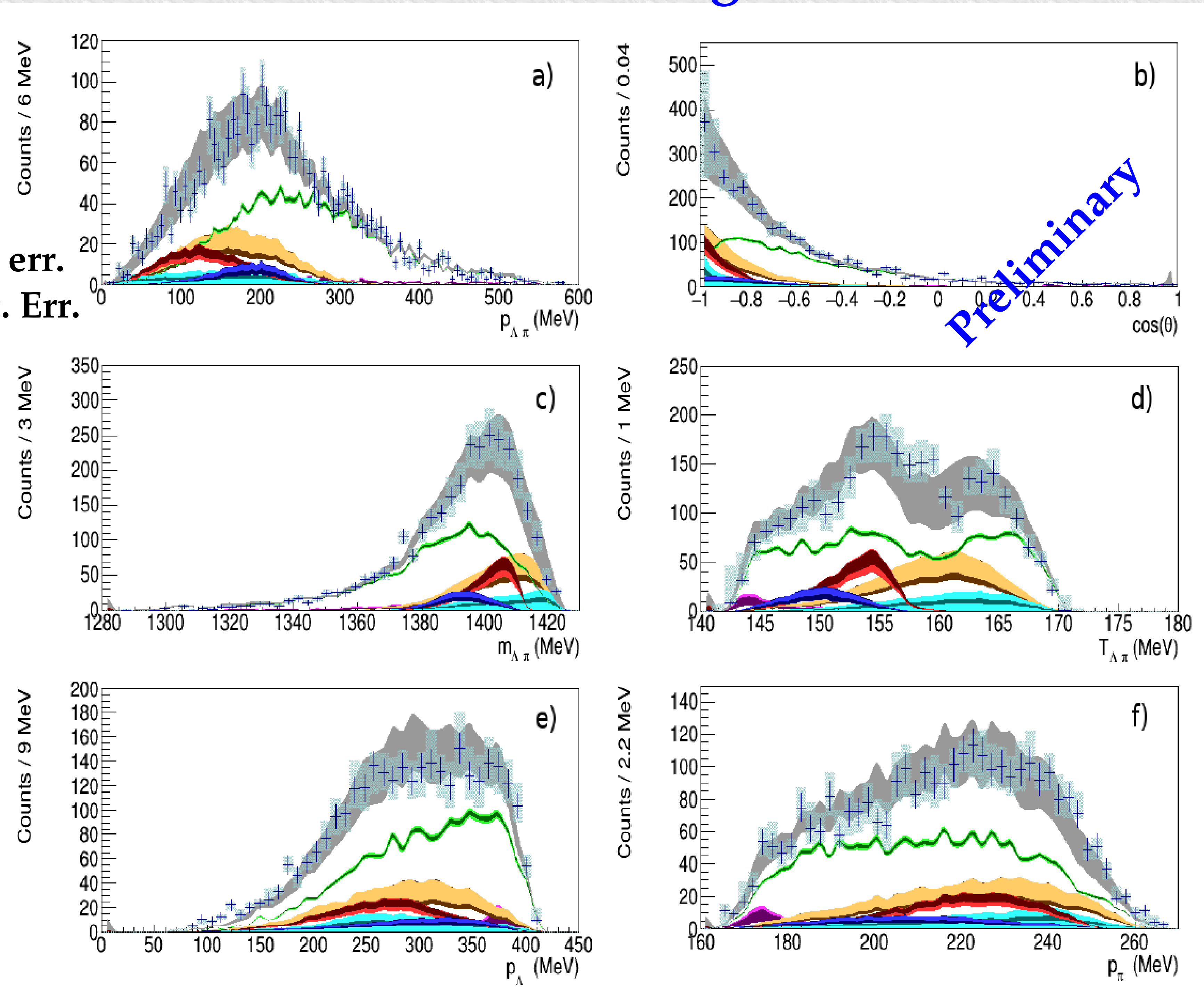

Comparison

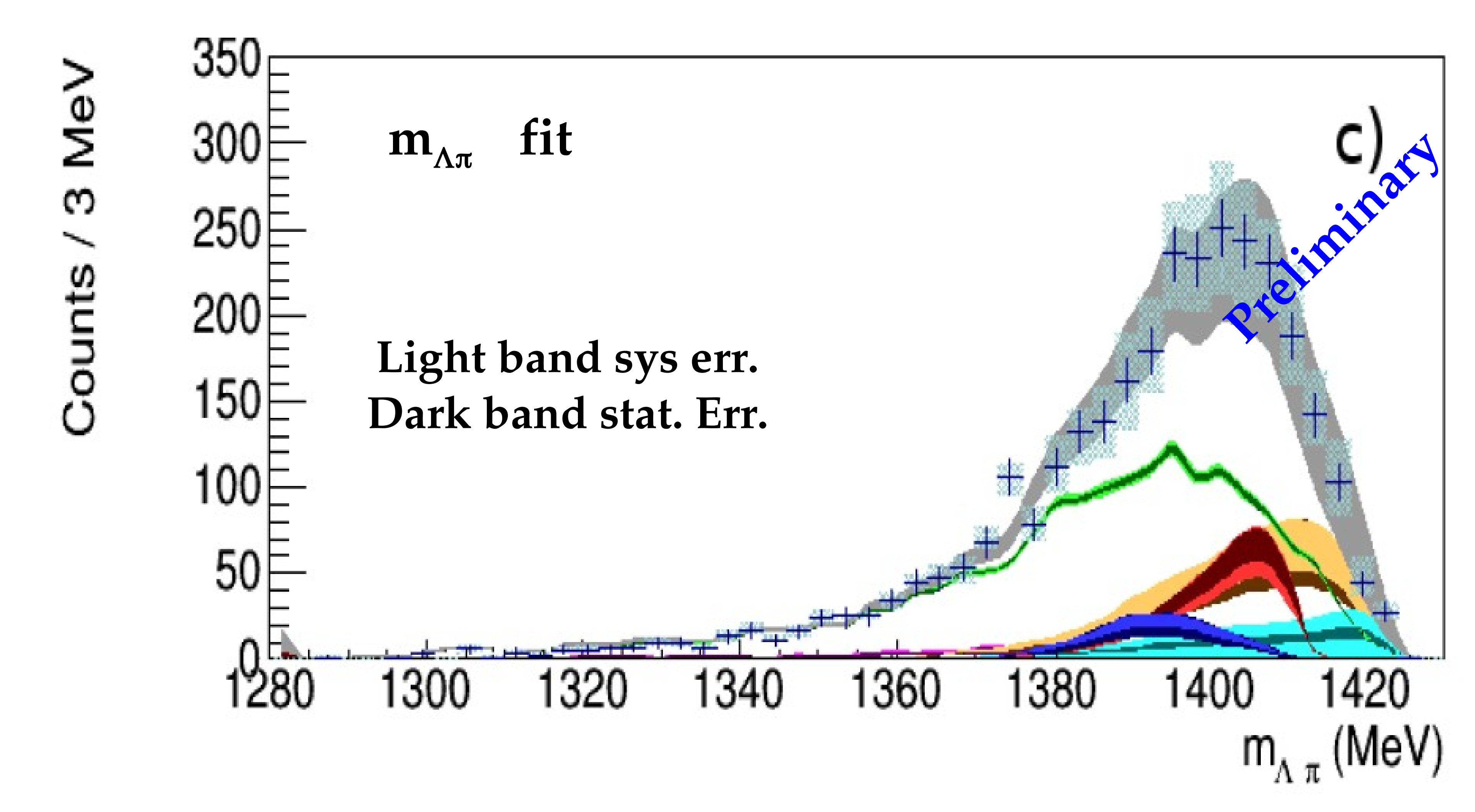

Non-Resonant
(at-rest)
(in-flight)

Resonant $\Sigma*$
(at-rest)
(in-flight)

Outcome of the measurement

From the well known Σ* transition probability:

Preliminary

$$\frac{\mathrm{NR-ar}}{\mathrm{RES-ar}} = \frac{\int_0^{pmax} P_{ar}^{nr}(p_{\Lambda\pi})\,dp_{\Lambda\pi}}{\int_0^{pmax} P_{ar}^{res}(p_{\Lambda\pi})\,dp_{\Lambda\pi}} =$$

$$= |f_{ar}^{s}|^2 \cdot 8,94 \cdot 10^5 \mathrm{MeV}^2 \,.$$

$$\rightarrow \; |f_{ar}^{s}| = (0.334 \pm 0.018\,\mathrm{stat}^{+0.034}_{-0.058}\mathrm{syst})\;\mathrm{fm}\,.$$

The sub-threshold result is compatible with corresponding values extracted from K^- p → $\Lambda\,\pi^0$ cross sections above threshold

J. K. Kim, Columbia University Report, Nevis 149 (1966)

J. K. Kim, Phys Rev Lett, 19 (1977) 1074:

$E = -33$ MeV	$p_{lab} = 120$ MeV	160 MeV	200 MeV	245 MeV
$0.334 \pm 0.018\,\mathrm{stat}^{+0.034}_{-0.058}\mathrm{syst}$	0.33(11)	0.29(10)	0.24 (6)	0.28(2)

K^- - multiN absorption and search for bound states

How deep can an antikaon be bound in a nucleus?

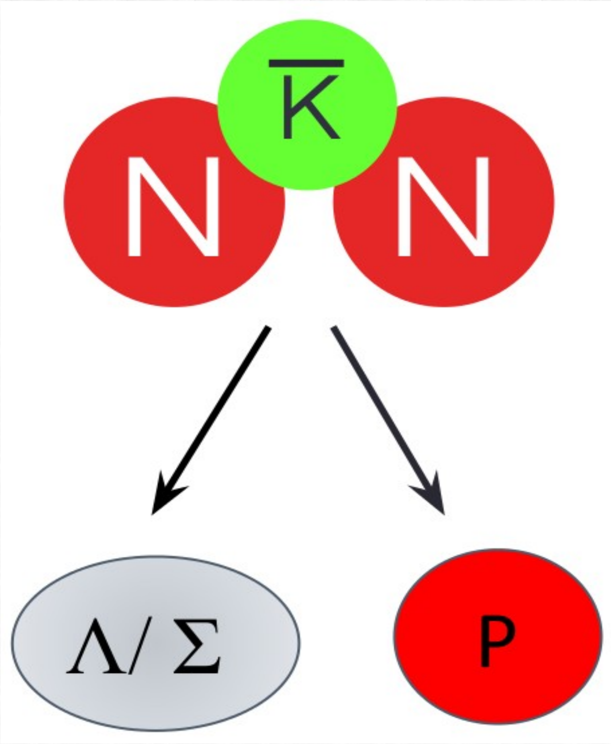

Possible Bound States:

$(K^- pp) \rightarrow \Lambda\, p$
$\rightarrow \Sigma^0\, p$

$(K^- ppn) \rightarrow \Lambda\, d$
$\rightarrow \Sigma^0\, d$

predicted due to the strong $\bar{K}N$ interaction in the I=0 channel.

[Wycech (1986) - Akaishi & Yamazaki (2002)]

K^-pp bound state

....at the end of 2015

	Dote,Hyodo, Weise	Akaishi, Yamazaki	Barnea, Gal, Liverts	Ikeda, Sato	Ikeda, Kamano,Sato	Schevchenko ,Gal, Mares	Revai, Schevchenko	Maeda, Akaishi, Yamazaki
B (MeV)	17-23	48	16	60-95	9-16	50-70	32	51.5
Γ(MeV)	40-70	61	41	45-80	34-46	90-110	49	61
Method	Variational	Variational	Variational	Faddeev-AGS	Faddeev-AGS	Faddeev-AGS	Faddeev-AGS	Faddeev-Yakubovsky
Interaction	Chiral	Phenom.	Chiral	Chiral	Chiral	Phenom.	Chiral	Phenom.

Experiments reporting DBKNS		
KEK-PS E549	T. Suzuki at al. MPLA23, 2520-2523 (2008)	
FINUDA	M. Agnello et al. PRL94, 212303 (2005)	Extraction of a **signal**
DISTO	T. Yamazaki et al. PRL104 (2010)	Extraction of a **signal**
OBELIX	G. Bendiscioli et al. NPA789, 222 (2007)	Extraction of a **signal**
HADES	G. Agakishiev et al. PLB742, 242-248 (2015)	**Upper limit**
LEPS/SPring-8	A.O. Tokiyasu et al. PLB728, 616-621 (2014)	**Upper limit**
J-PARC E15	T. Hashimoto et al. PTEP, 061D01 (2015)	**Upper limit**
J-PARC E27	Y. Ichikawa et al. PTEP, 021D01 (2015)	Extraction of a **signal**

How deep can an antikaon be bound in a nucleus?

K^-pp bound state.....the theory

Chiral SU(3)-based (Energy dependent) → Shallow~20 MeV
Phenomenological (Energy independent) → Deep~40-70 MeV

	Dote,Hyodo, Weise	Akaishi, Yamazaki	Barnea, Gal, Liverts	Ikeda, Sato	Ikeda, Kamano,Sato	Schevchenko ,Gal, Mares	Revai, Schevchenko	Maeda, Akaishi, Yamazaki
B (MeV)	17-23	48	16	60-95	9-16	50-70	32	51.5
Γ(MeV)	40-70	61	41	45-80	34-46	90-110	49	61
Method	Variational	Variational	Variational	Faddeev-AGS	Faddeev-AGS	Faddeev-AGS	Faddeev-AGS	Faddeev-Yakubovsky
Interaction	Chiral	Phenom.	Chiral	Chiral	Chiral	Phenom.	Chiral	Phenom.

Large width means short-life state → hard to measure
Small width means long-life state → easy to measure

How deep can an antikaon be bound in a nucleus?

K^-pp bound state

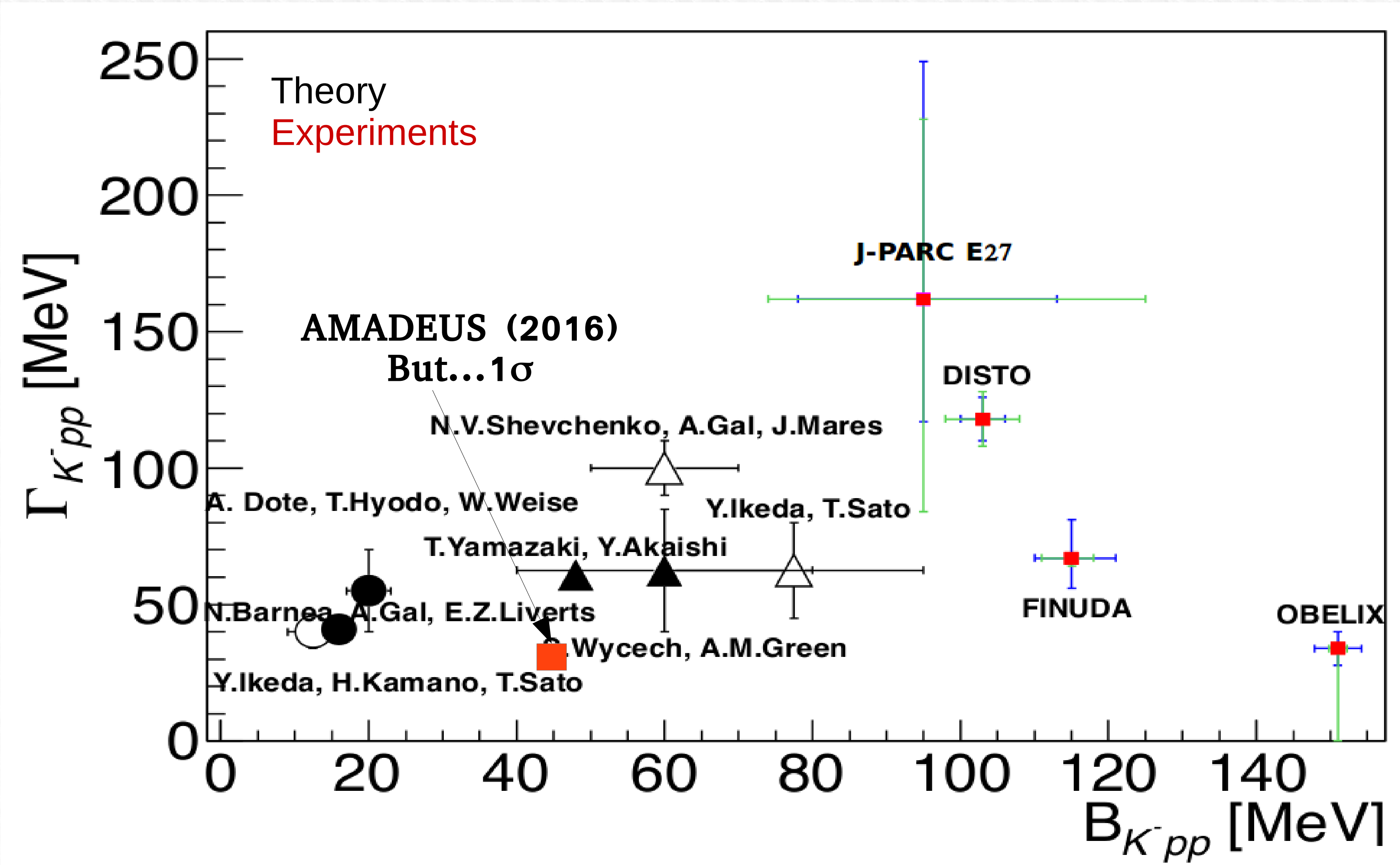

How deep can an antikaon be bound in a nucleus?

interpreted in
T. Sekihara, E. Oset, A. Ramos, Prog. Theor. Exp. Phys (2016) (12): 123D03

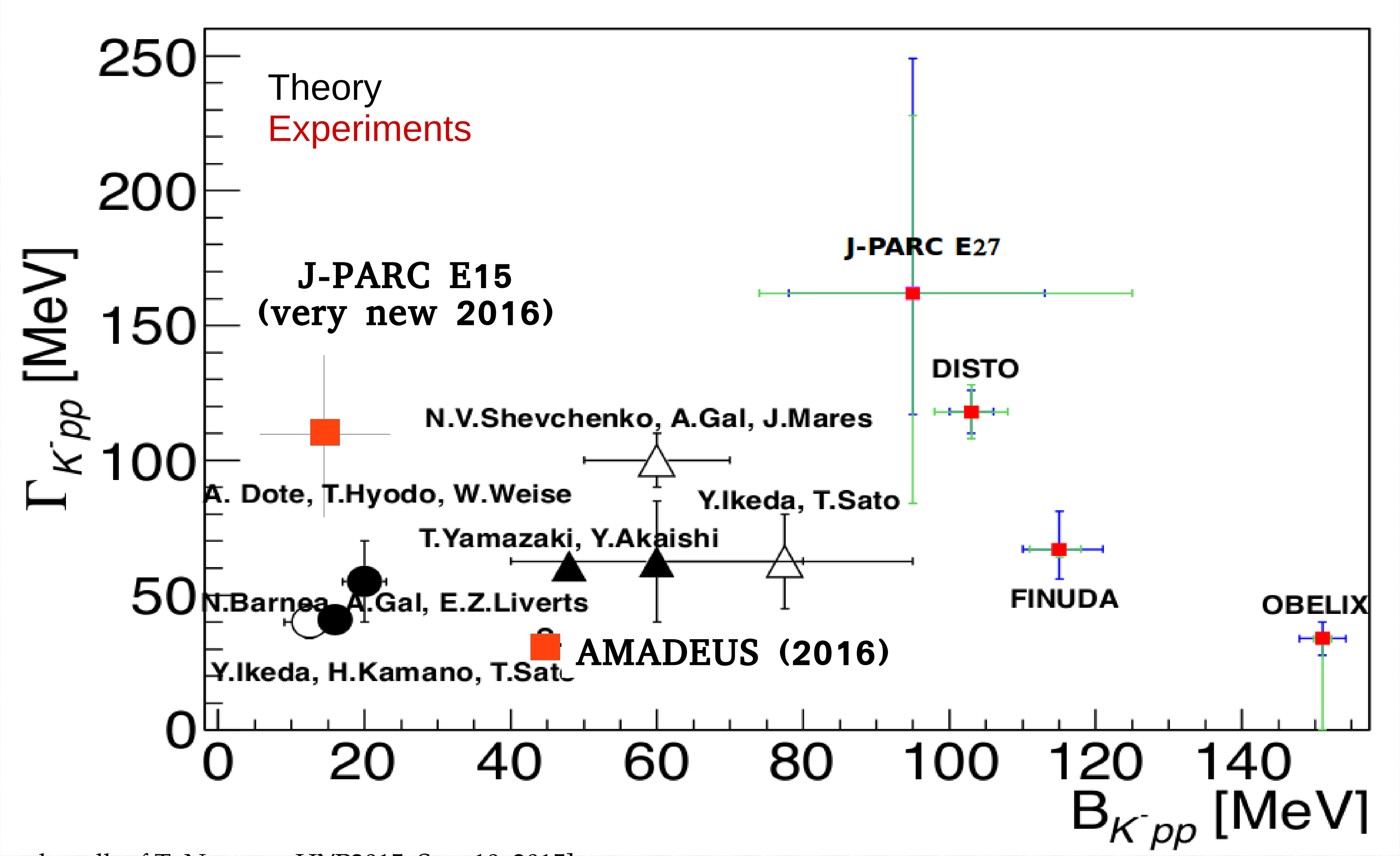

[from the talk of T. Nagae at HYP2015, Sep. 10, 2015]

J-PARC E15

K⁻ + ³He → Λ + p + n

Invariant mass spectroscopy

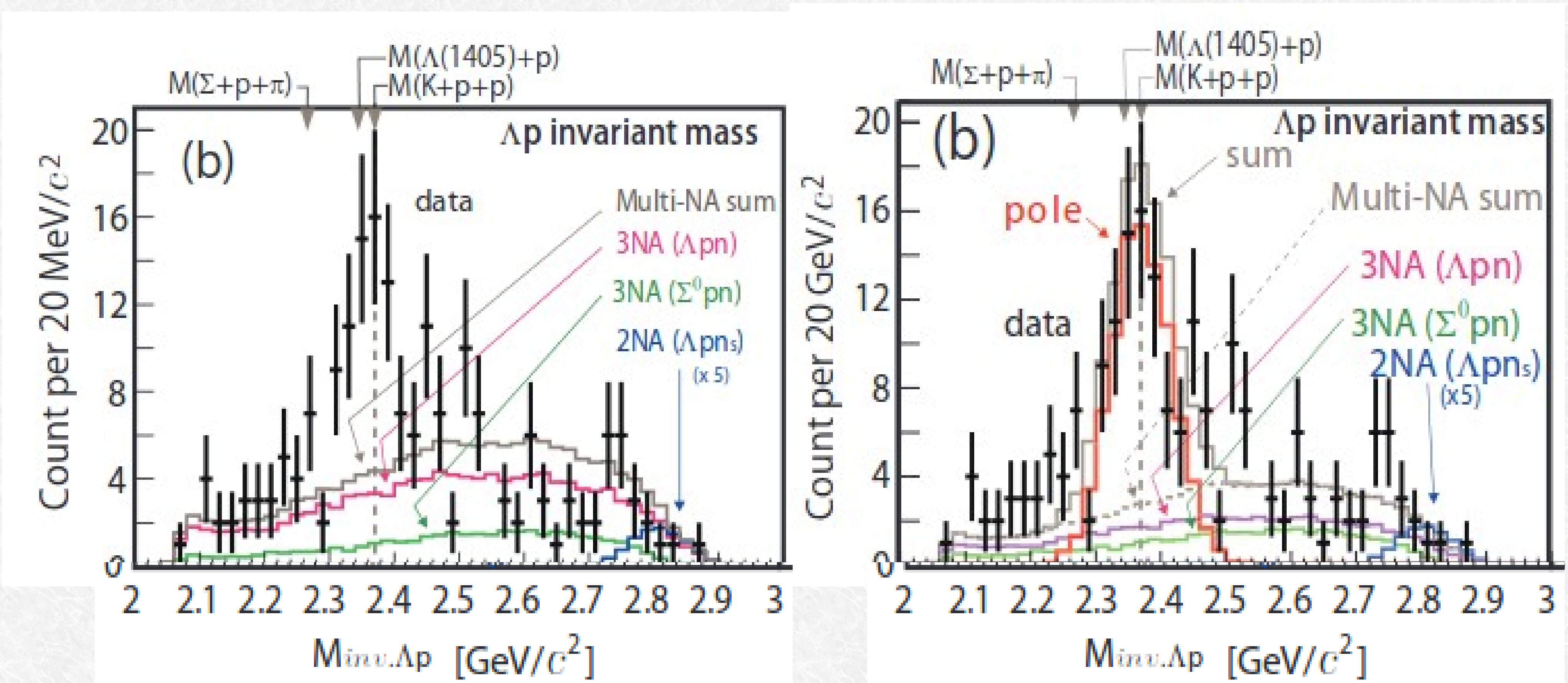

[J-PARC E15 Collaboration: arXiv:1601.06876 [nucl-ex]]

M = 2355 +6 −8 (stat.) ± 12 (syst.) MeV/c2
Γ = 110 +19 −17 (stat.) ± 27 (syst.) MeV/c2

BE = 15 MeV

Σ0 p correlated production, goals of this analysis

K- Absorption

- Pin down the contribution of the process:

$$K^- + NN \rightarrow \Sigma^0 + p$$

with respect to processes as:

$$K^- + NN \rightarrow \Sigma^0 + p \rightarrow p\text{''} + \Sigma^0\text{''}\ (FSI)$$

$$K^- + NNN \rightarrow \Sigma^0 + p + X$$

$$K^- + NNNN \rightarrow \Sigma^0 + p + X$$

Kaonic Bound States

$$ppK^- \rightarrow \Sigma^0 + p$$

- Yield Extraction and Significance

Final fit

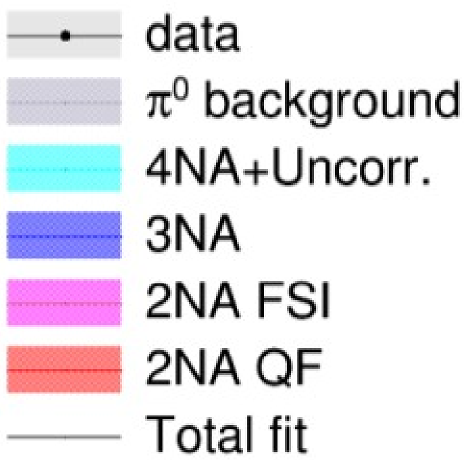

$$\chi^2 = 0.85$$

2NA-QF clearly separated From other processes

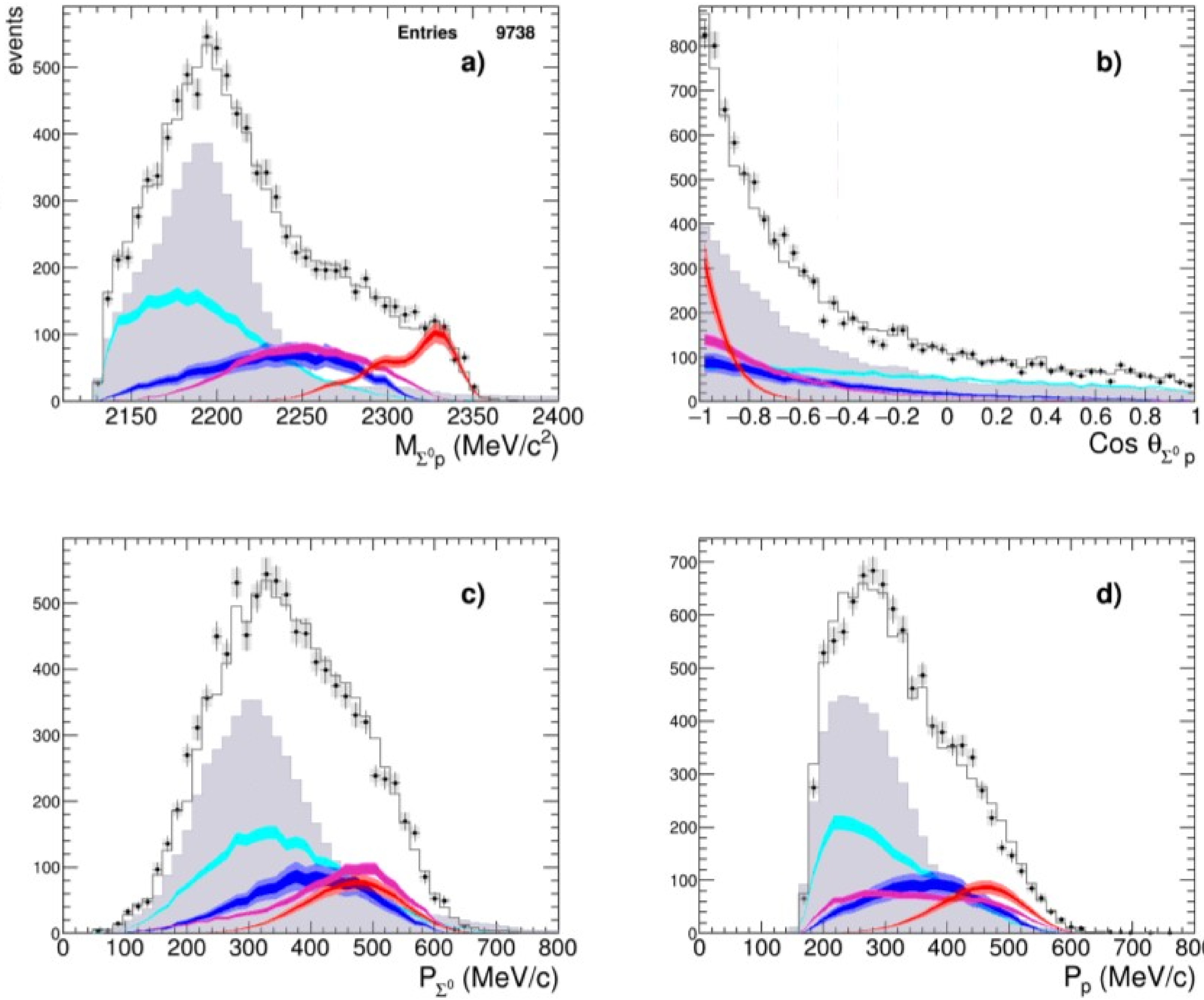

From the contributions to the fit, the yields are extracted for K- stop

Absorption results

	yield / $K^{-}_{stop} \cdot 10^{-2}$	$\sigma_{stat} \cdot 10^{-2}$	$\sigma_{syst} \cdot 10^{-2}$
2NA-QF	0.127	$\pm$ 0.019	$^{+0.004}_{-0.008}$
2NA-FSI	0.272	$\pm$ 0.028	$^{+0.022}_{-0.023}$
Tot 2NA	0.376	$\pm$ 0.033	$^{+0.023}_{-0.032}$
3NA	0.274	$\pm$ 0.069	$^{+0.044}_{-0.021}$
Tot 3body	0.546	$\pm$ 0.074	$^{+0.048}_{-0.033}$
4NA + bkg.	0.773	$\pm$ 0.053	$^{+0.025}_{-0.076}$

...is there room for the signal of a **ppK- bound state**?

Fit with ppK-

Best solution:
(best $\chi 2$ and higher yield**)**
- B.E. = 45 MeV/c2
- Width = 30 MeV/c2

$$\chi^2 = 0.807$$

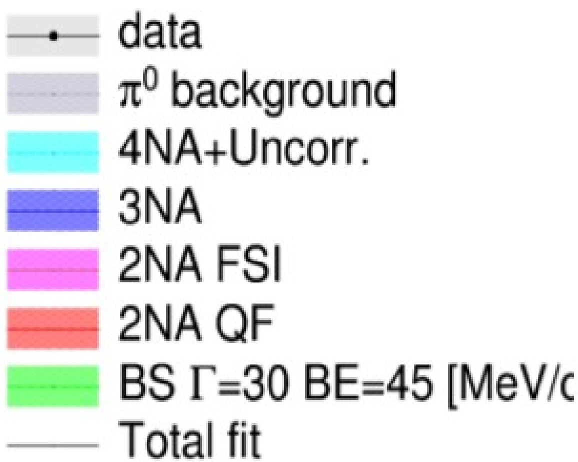

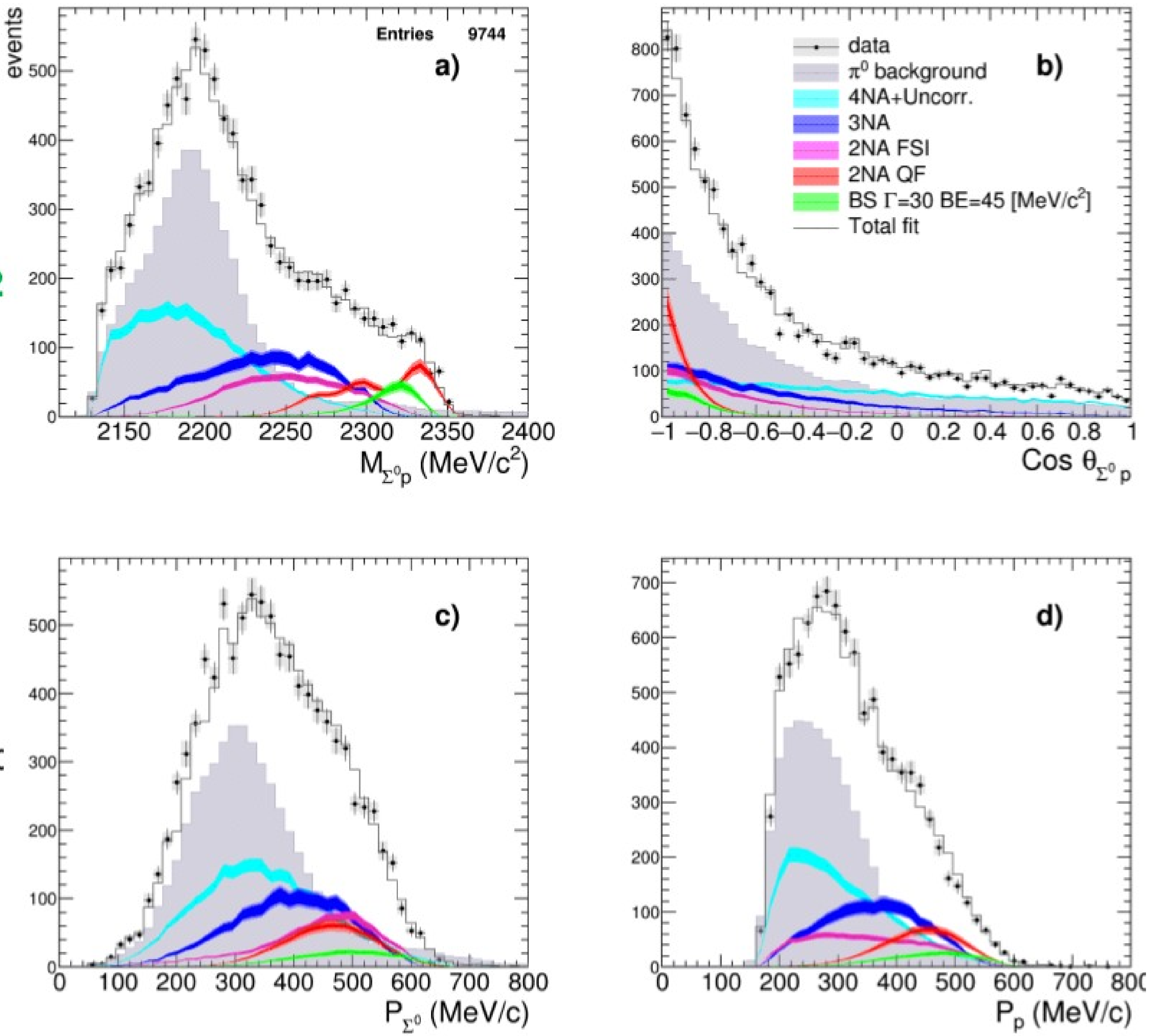

Evaluation of the significance of the ppK- signal

For B.E. = 45 MeV/c2, Width = 30 MeV/c2

$$Yield/K^{-}_{stop} = (0.044 \pm 0.009 stat^{+0.004}_{-0.005} syst) \cdot 10^{-2}$$

F-test to evaluate the addition of an extra parameter to the fit:

Significance of “signal” hypothesis w.r.t “Null-Hypothesis” (no bound state)

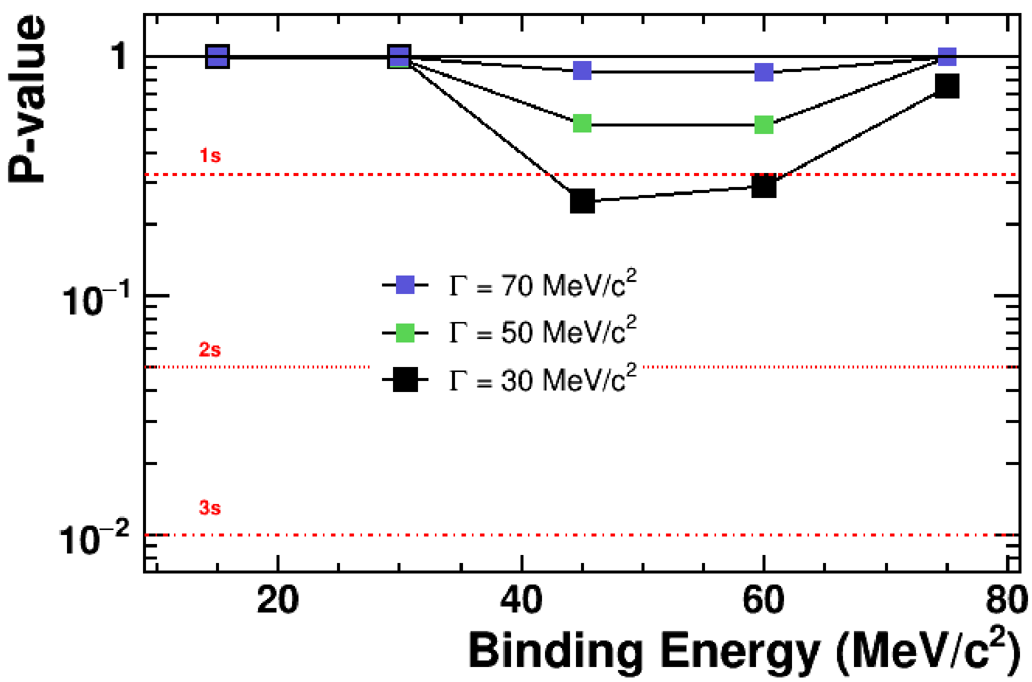

Conclusions

- 2NA-QF yield

	yield / $K^{-}_{stop} \cdot 10^{-2}$	$\sigma_{stat} \cdot 10^{-2}$	$\sigma_{syst} \cdot 10^{-2}$
2NA-QF	0.127	$\pm$ 0.019	$^{+0.004}_{-0.008}$

- Bound state ppK- yield for B.E. 45 MeV/c2 and Width 30 MeV/c2

$$Yield/K^{-}_{stop} = (0.044 \pm 0.009 stat^{+0.004}_{-0.005} syst) \cdot 10^{-2}$$

- the significance of the ppK- signal is of 1σ according to F-test

O. Vazquez Doce et al., Physics Letters B 758 (2016) 134

Λp channel

R. Del Grande PhD theis

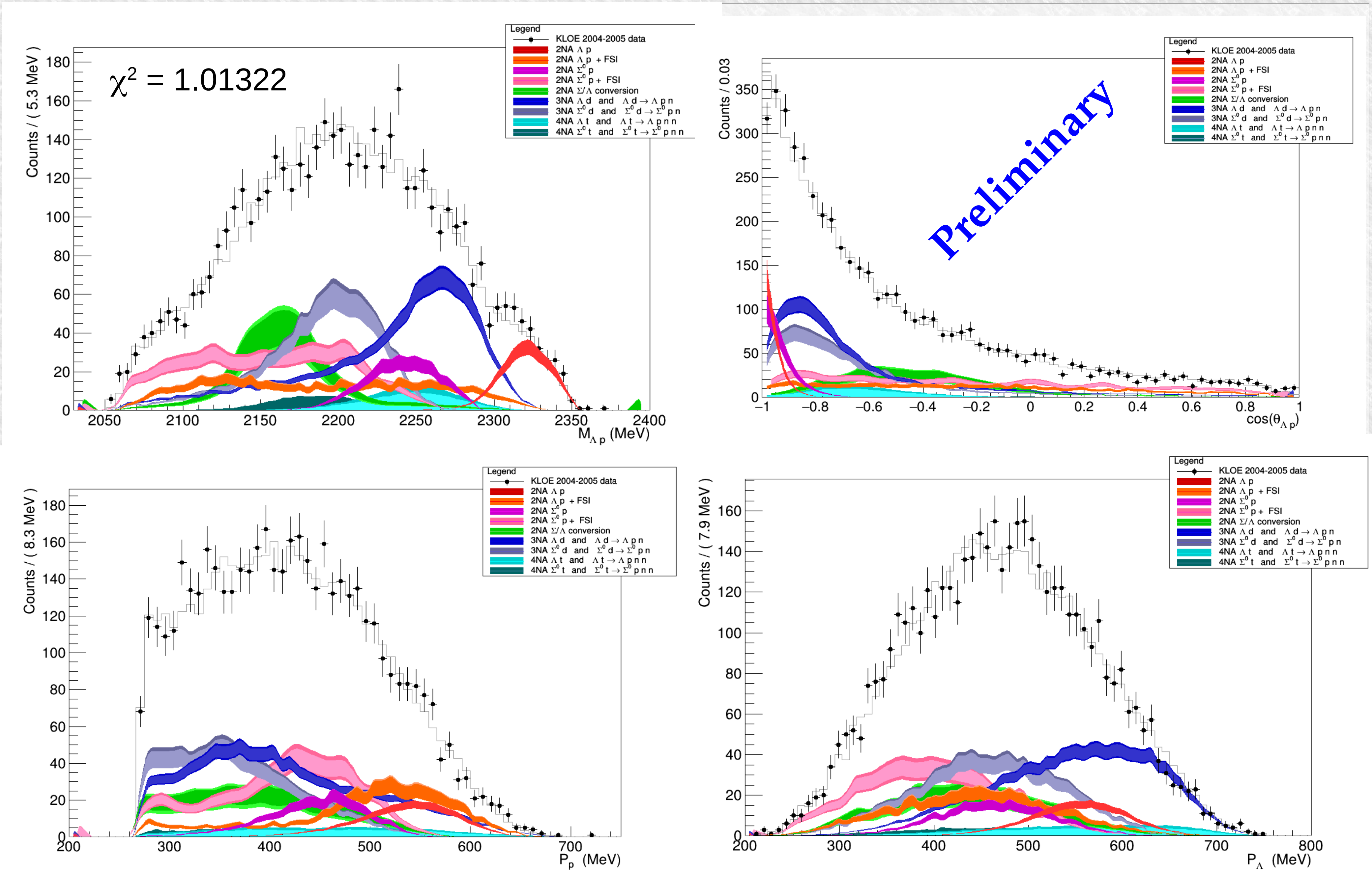

Λp channel

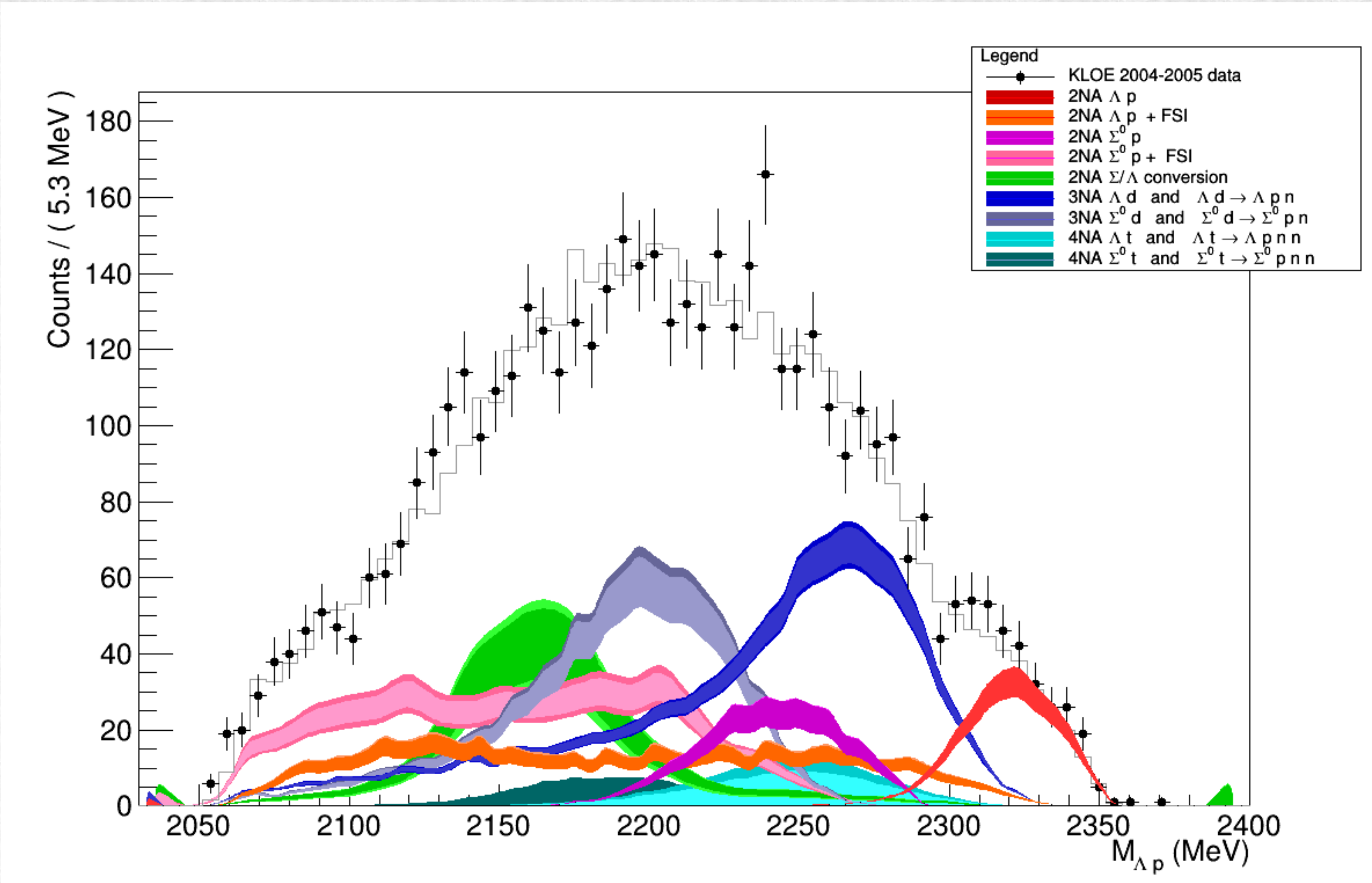

Preliminary

	yield/$K^-_{stop} \cdot 10^{-2}$	$\sigma_{stat} \cdot 10^{-2}$	$\sigma_{syst} \cdot 10^{-2}$
2NA-QF Λp	0.0493	± 0.0048	$^{+0.0045}_{-0.0076}$
2NA-QF Σ^0p	0.112	± 0.019	$^{+0.019}_{-0.016}$
2NA-FSI Λp	0.561	± 0.090	$^{+0.105}_{-0.078}$
2NA-FSI Σ^0p	3.06	± 0.71	$^{+0.50}_{-0.50}$
3NA Λpn	0.382	± 0.036	$^{+0.028}_{-0.027}$
3NA Σ^0pn	0.839	± 0.114	$^{+0.072}_{-0.112}$
4NA Λpnn	0.006	± 0.037	$^{+0.024}_{-0.010}$
4NA Σ^0pnn	$0.0076 \cdot 10^{-10}$	± 0.086	$^{+2.70}_{-0.016} \cdot 10^{-10}$
2NA-CONV	0.502	± 0.182	$^{+0.231}_{-0.266}$

	yield/$K^-_{stop} \cdot 10^{-2}$	$\sigma_{stat} \cdot 10^{-2}$	$\sigma_{syst} \cdot 10^{-2}$
2NA-QF	0.127	±0.019	$^{+0.004}_{-0.008}$
2NA-FSI	0.272	±0.028	$^{+0.022}_{-0.023}$
Tot 2NA	0.399	±0.033	$^{+0.023}_{-0.032}$
3NA	0.274	±0.069	$^{+0.044}_{-0.021}$
Tot 3 body	0.546	±0.074	$^{+0.048}_{-0.033}$
4NA + bkg.	0.773	±0.053	$^{+0.025}_{-0.076}$

Λp channel

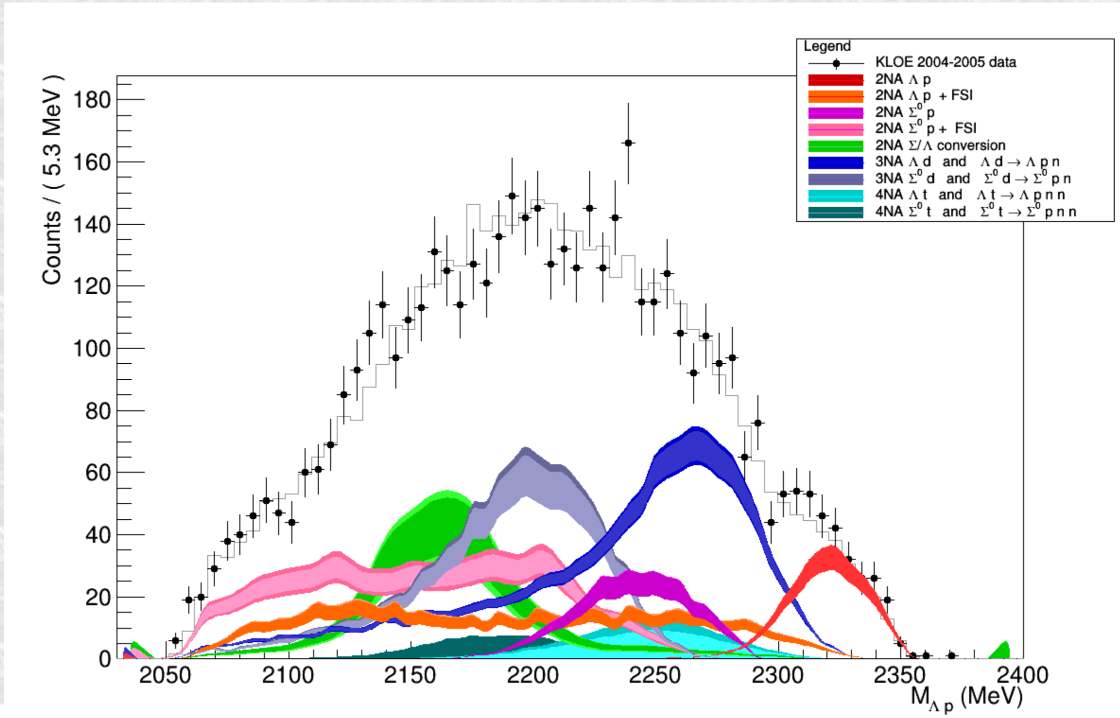

Preliminary

	yield/$K^-_{stop} \cdot 10^{-2}$	$\sigma_{stat} \cdot 10^{-2}$	$\sigma_{syst} \cdot 10^{-2}$
2NA-QF Λp	0.0493	± 0.0048	$^{+0.0045}_{-0.0076}$
2NA-QF Σ^0p	0.112	± 0.019	$^{+0.019}_{-0.016}$
2NA-FSI Λp	0.561	± 0.090	$^{+0.105}_{-0.078}$
2NA-FSI Σ^0p	3.06	± 0.71	$^{+0.50}_{-0.50}$
3NA Λpn	0.382	± 0.036	$^{+0.028}_{-0.027}$
3NA Σ^0pn	0.839	± 0.114	$^{+0.072}_{-0.112}$
4NA Λpnn	0.006	± 0.037	$^{+0.024}_{-0.010}$
4NA Σ^0pnn	$0.0076 \cdot 10^{-10}$	± 0.086	$^{+2.70}_{-0.016} \cdot 10^{-10}$
2NA-CONV	0.502	± 0.182	$^{+0.231}_{-0.266}$

	yield/$K^-_{stop} \cdot 10^{-2}$	$\sigma_{stat} \cdot 10^{-2}$	$\sigma_{syst} \cdot 10^{-2}$
2NA-QF	0.127	±0.019	$^{+0.004}_{-0.008}$
2NA-FSI	0.272	±0.028	$^{+0.022}_{-0.023}$
Tot 2NA	0.399	±0.033	$^{+0.023}_{-0.032}$
3NA	0.274	±0.069	$^{+0.044}_{-0.021}$
Tot 3 body	0.546	±0.074	$^{+0.048}_{-0.033}$
4NA + bkg.	0.773	±0.053	$^{+0.025}_{-0.076}$

$K^- \ {}^4He \rightarrow \Lambda d + n$

$K^- \ {}^{12}C \rightarrow \Lambda d + \text{Residual}$

Λ d Invariant mass
Drift Chamber GASS

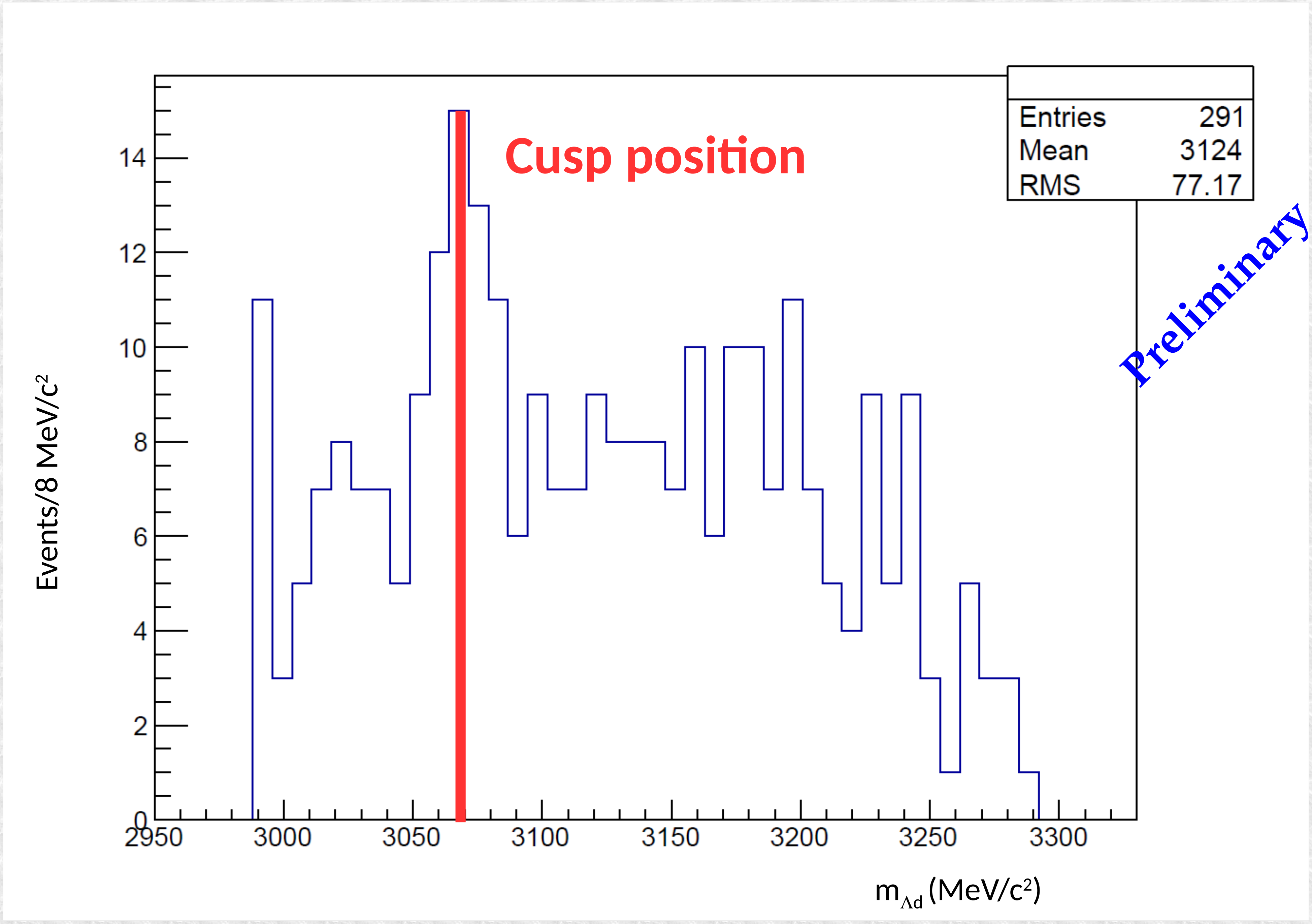

$K^- \, {}^4He \rightarrow \Lambda t$

4NA cross section and yield

Λt available data

Available data:

- in Helium :

- bubble chamber experiment
[M.Roosen, J.H. Wickens, Il Nuovo Cimento 66, (1981), 101]
K^- stopped in liquid helium, Λ dn/t search. 3 events compatible with the Λt kinematics were found

BR($K^{-4}He \rightarrow \Lambda t$) **= (3 ± 2) × 10^{-4} /K_{stop}** global, no 4NA

- Solid targets

- FINUDA [Phys.Lett. B669 (2008) 229]
(40 events in different solid targets)

Λt available data

FINUDA presented [Phys.Lett.B (2008) 229]:

- a study of Λ vs t momentum correlation and an opening angle distribution
- **40 events** collected and added together coming from different targets ($^{6,7}Li$, ^{9}Be)

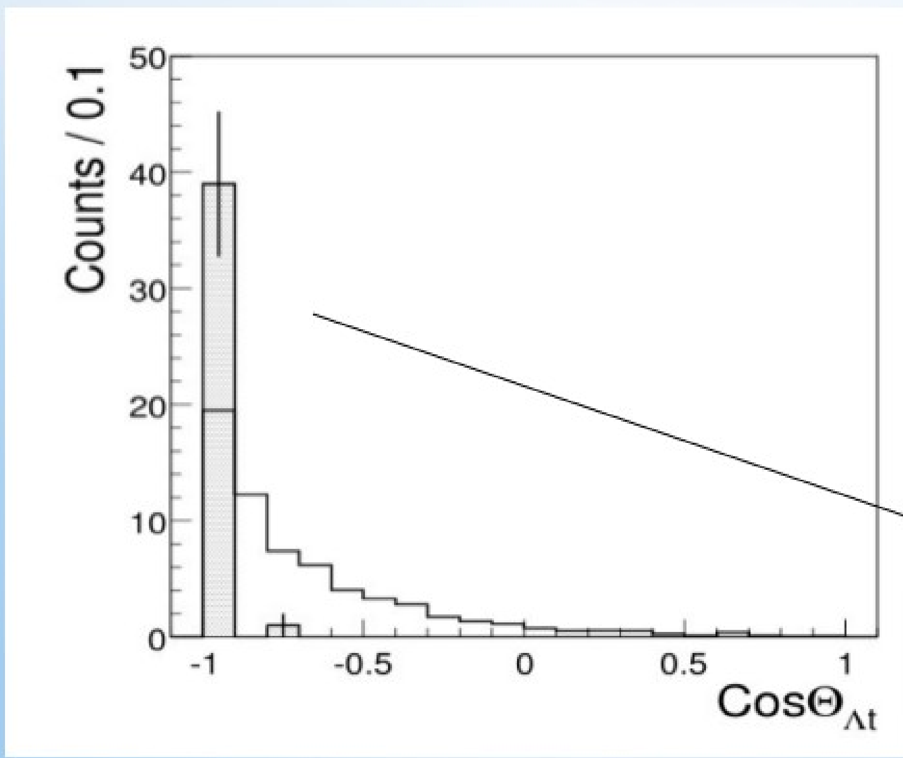

Filled histogram= data

Open histogram = Phase space simulation

(K- A → Λ t N A')

Unclear back to back topology

Λt emission yield → $10^{-3} – 10^{-4} / K^{-}_{stop}$

global, no 4NA

Experimental data only back-to-back

Λt correlation studies in ^{4}He from the DC gas : contributing processes

single nucleon absorption (1NA)

$$K^- \, {}^4He \rightarrow \Lambda \, \pi^0 \, t_{res}$$

$$K^- \, {}^4He \rightarrow \Sigma^0 \pi^0 \, t_{res} \quad , \quad \Sigma^0 \rightarrow \Lambda\gamma$$

conversion on triton:

$$K^- \, {}^4He \rightarrow \Sigma^0 \pi^0 \, t \quad , \quad \Sigma^0 t \, / \, \Lambda t$$

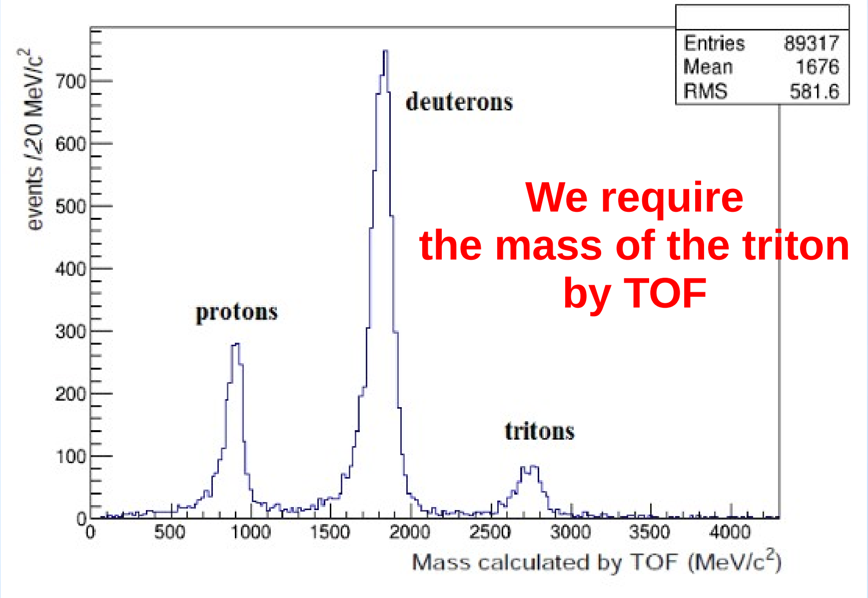

We require the mass of the triton by TOF

Tritons are spectators, too low momentum: p_t ~ Fermi momentum

<u>lower then the calorimeter threshold</u> (p_t ~ 500 MeV/c)

<u>checked by MC simulations</u>

4NA processes – K$^-$ absorbed by the **α particle:**

$$K^- \, {}^4He \rightarrow \Lambda t$$

$$K^- \, {}^4He \rightarrow \Sigma^0 t \quad , \quad \Sigma^0 \rightarrow \Lambda\gamma$$

conversion is suppressed by the Σ^0- t Back to back topology!

MC simulations: efficiency & resolution

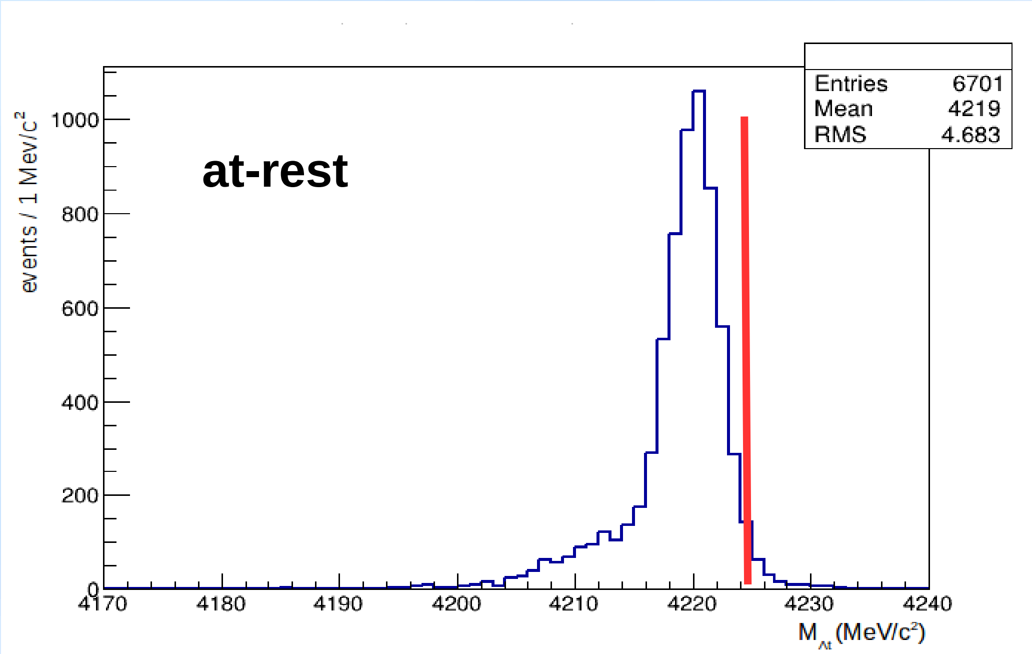

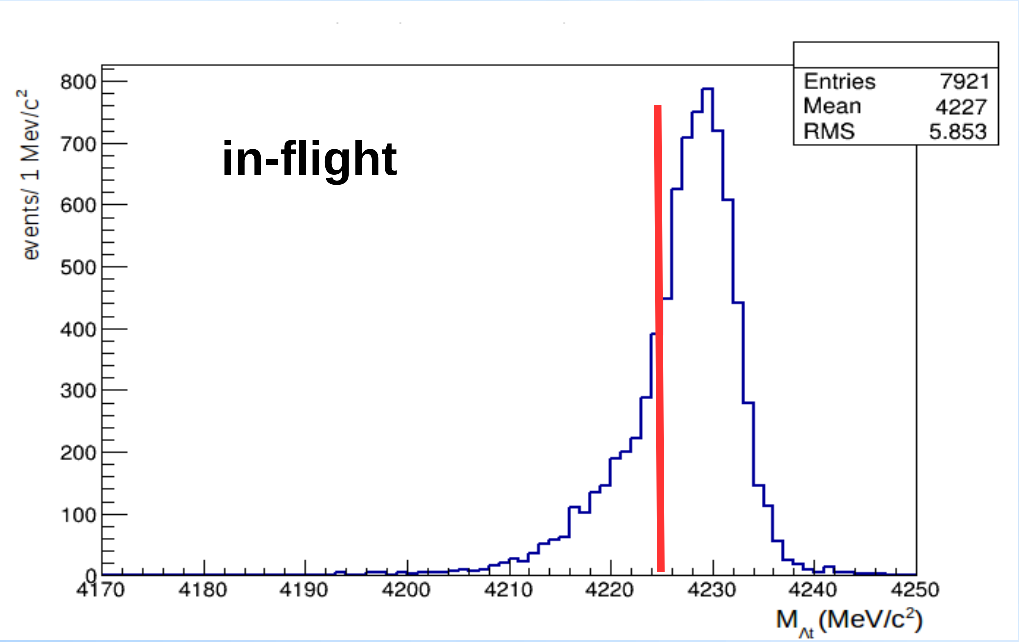

mass threshold at-rest

$M_{\Lambda t}$ invariant mass resolution = 2.2 MeV/c^2

overall <u>detection + reconstruction efficiency</u> for 4NA direct Λt production :

$$\epsilon_{4\mathrm{NA},ar,\Lambda t} = 0.0493 \pm 0.0006 \quad ; \quad \epsilon_{4\mathrm{NA},if,\Lambda t} = 0.0578 \pm 0.0006,$$

at-rest **in-flight**

Preliminary

Λt correlation studies in ^{4}He: mass, momentum and angle simulataneous fit

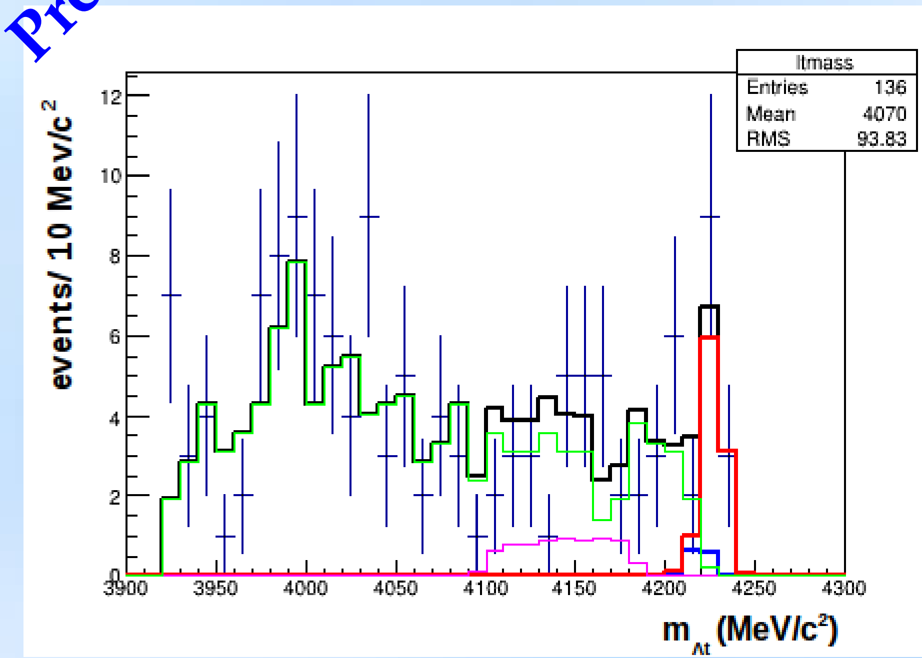

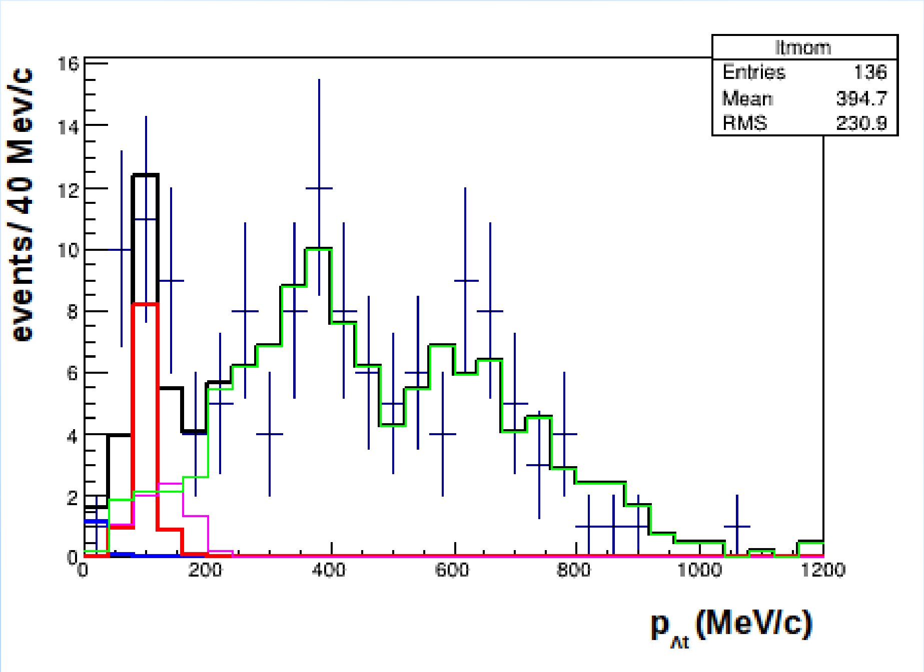

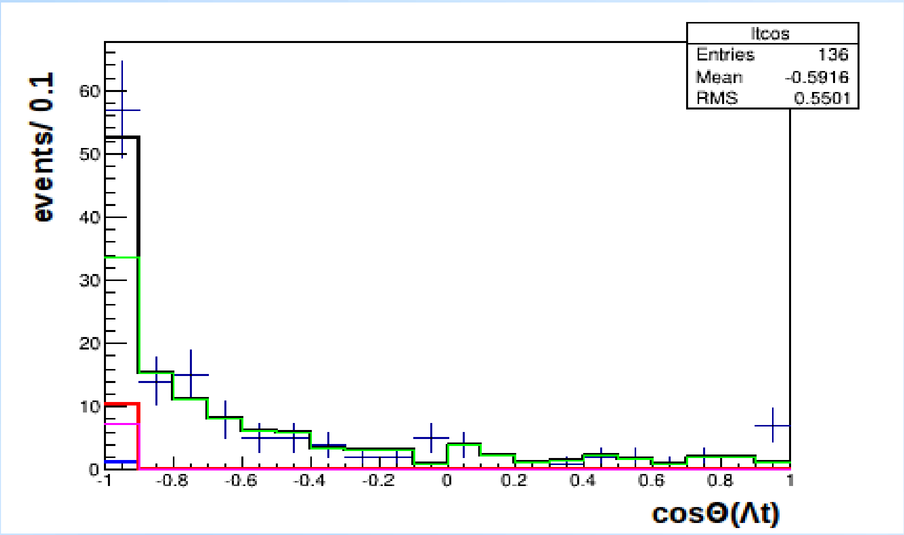

data

--- carbon data from DC wall

--- 4NA $K^- {}^4He \rightarrow \Lambda t$ in flight MC

--- 4NA $K^- {}^4He \rightarrow \Lambda t$ at rest MC

--- 4NA $K^- {}^4He \rightarrow \Sigma^0 t$, $\Sigma^0 \rightarrow \Lambda\gamma$ MC

--- 4NA $K^- {}^4He \rightarrow \Sigma^0 t$, $\Sigma^0 \rightarrow \Lambda\gamma$ MC

Λt correlation studies in ^{4}He: preliminary mass and angle momentum simulataneous fit

Preliminary

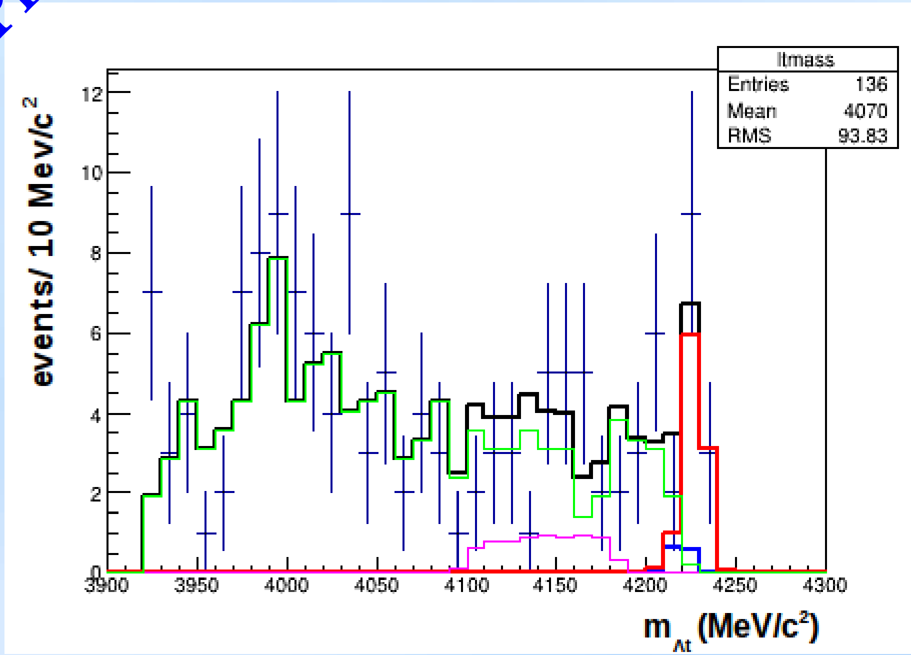

Contribution to the spectra	Parameter value
K^{-4}He $\rightarrow \Lambda t$ at rest	0.01 ± 0.01
K^{-4}He $\rightarrow \Lambda t$ in-flight	0.09 ± 0.02
K^{-4}He $\rightarrow \Sigma^0 t$ in-flight	0.05 ± 0.03
K^{-12}C $\rightarrow \Lambda t$ experimental distribution from the carbon DC wall	0.85 ± 0.06
χ^2 / ndf	0.654

Total number of events = 136

4NA K^- ^{4}He → Λt at rest → 1 ± 1 events

4NA K^- ^{4}He → Λt in flight → 12 ± 3 events

data

--- carbon data from DC wall

--- 4NA K^- ^{4}He → Λt in flight MC

--- 4NA K^- ^{4}He → Λt at rest MC

--- 4NA K^- ^{4}He → $\Sigma^0 t$, Σ^0 → $\Lambda\gamma$ MC

--- 4NA K^- ^{4}He → $\Sigma^0 t$, Σ^0 → $\Lambda\gamma$ MC

BR(K^- ^{4}He(4NA) → Λt) **< 1.3 × 10^{-4} /K$_{stop}$**

σ(100 ± **19** MeV/c) (K^- ^{4}He(4NA) → Λt) **=**

= (0.42 ± 0.13(stat) $^{+0.01}_{-0.02}$ (syst)) mb


K⁻
Thanks

Low-energy QCD in the u-d-s sector

- strong interaction is governed by QCD (color SU(3) gauge theory)

- fundamental matter fields are quarks (6 flavors & 3 colors R , G , B)

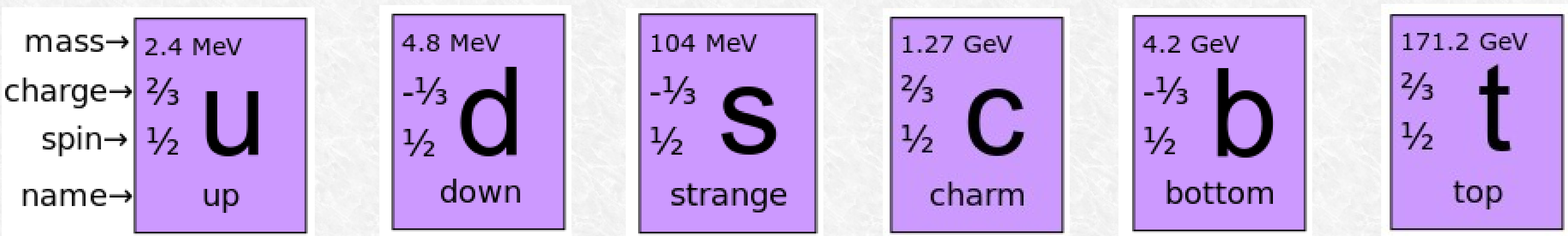

- gauge fields are 8 gluons

- in the massless limit ..

quark fields

gluon fields

$$\mathcal{L}^0_{\rm QCD} = -\frac{1}{2}{\rm tr}\,[G_{\mu\nu}G^{\mu\nu}] + \bar{q}i\gamma^{\mu}D_{\mu}q,$$

$$G_{\mu\nu} = \partial_\mu A_\mu - \partial_\nu A_\mu - ig[A_\mu, A_\nu], \qquad D_\mu = \partial_\mu - igA_\mu, \quad A_\mu = \sum_a T^a A^a_\mu,$$

Low-energy QCD in the u-d-s sector

- since the massless lagrangian can be decomposed:

$$\mathcal{L}^0_{\mathrm{QCD}} = -\frac{1}{2}\mathrm{tr}\,[G_{\mu\nu}G^{\mu\nu}] + \bar{q}_L i\gamma^\mu D_\mu q_L + \bar{q}_R i\gamma^\mu D_\mu q_R$$

left and right handed quarks: $q_L = P_L q$ $\quad$ $q_R = P_R q$

it is invariant under independent unitary transformations of L/R-handed q

chiral symmetry of QCD $SU(3)_L \times SU(3)_R$

- quark condensate breaks down the symmetry to $SU(3)_V$

$$\langle 0|\bar{q}q|0\rangle = \langle 0|\bar{q}_R q_L + \bar{q}_L q_R|0\rangle$$

SPONTANEOUS ch. symmetry breaking

- Nambu-Goldstone: *each broken symmetry introduces one massless boson in the physical particle spectrum*

Low-energy QCD in the u-d-s sector

- If we reduce to the three lightest flavors:

Light quarks **Heavy quarks**

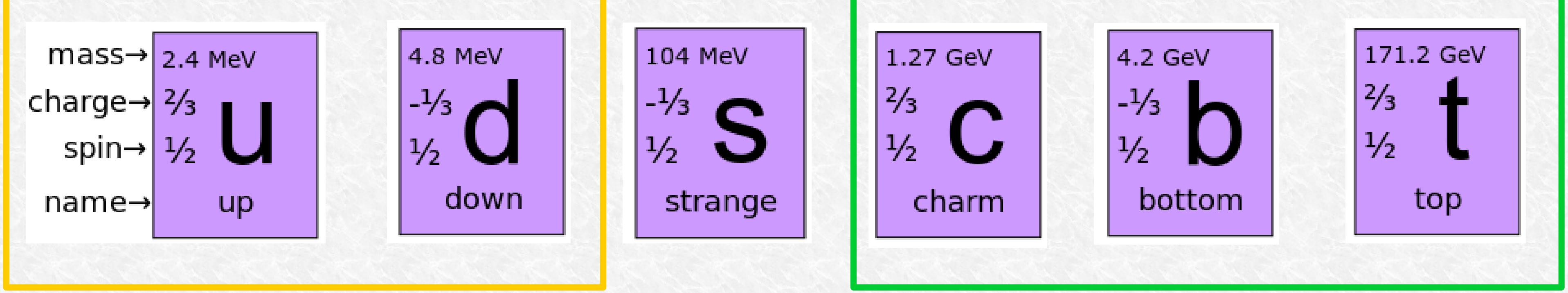

- The *approximate* N-G bosons are the lightest pseudoscalar mesons (π, K and η)

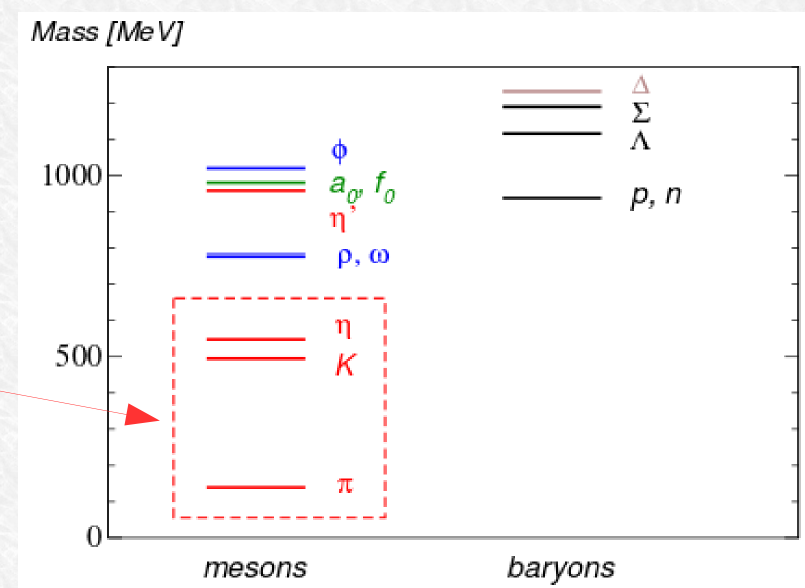

Low-energy QCD in the u-d-s sector

- Ch. symmetry is also broken by the finite quarks masses, because of the quark mass term:

$$\mathcal{L}_{QCD} = \mathcal{L}^{0}_{QCD} - \bar{q} m q, \qquad m = \begin{pmatrix} m_u & & \\ & m_d & \\ & & m_s \end{pmatrix}$$

m_u, m_d ~ few MeV ; m_s ~ 100 MeV

EXPLICIT ch. symmetry breaking

- s quarks are intermediate between light and heavy → test of the interplay among spontaneous and explicit ch. sy. breaking in low-energy QCD

- At low-energy the non-perturbative effect of the strong interaction causes color confinement → asymptotic degrees of freedom are hadrons instead of quarks and gluons.

Low-energy QCD in the u-d-s sector

- CHIRAL PERTURBATION THEORY

a chiral Lagrangian with effective degrees of freedom *U* takes the place of the QCD Lagrangian:

$$\exp\{iZ\} = \int \mathcal{D}q\mathcal{D}\bar{q}\mathcal{D}A_\mu \exp\left\{i\int d^4x\mathcal{L}_{QCD}\right\} = \int \mathcal{D}U \exp\left\{i\int d^4x\mathcal{L}_{eff}\right\}$$

lowest excitations (pseudoscalar mesons):

$$\Phi = \begin{pmatrix} \frac{1}{\sqrt{2}}\pi^0 + \frac{1}{\sqrt{6}}\eta & \pi^+ & K^+ \\ \pi^- & -\frac{1}{\sqrt{2}}\pi^0 + \frac{1}{\sqrt{6}}\eta & K^0 \\ K^- & \bar{K}^0 & -\frac{2}{\sqrt{6}}\eta \end{pmatrix}$$

with chiral field $U(\Phi) = \exp\left\{\frac{i\sqrt{2}\Phi}{f}\right\}$

the counting rule is defined considering the meson momentum small respect to the ch. sy. Breaking scale $4\pi f \sim 1$ GeV.

Similar for the baryon fields:

$$B = \begin{pmatrix} \frac{1}{\sqrt{2}}\Sigma^0 + \frac{1}{\sqrt{6}}\Lambda & \Sigma^+ & p \\ \Sigma^- & -\frac{1}{\sqrt{2}}\Sigma^0 + \frac{1}{\sqrt{6}}\Lambda & n \\ \Xi^- & \Xi^0 & -\frac{2}{\sqrt{6}}\Lambda \end{pmatrix}$$

Why AMADEUS & DAΦNE?

Neutron detection efficiency

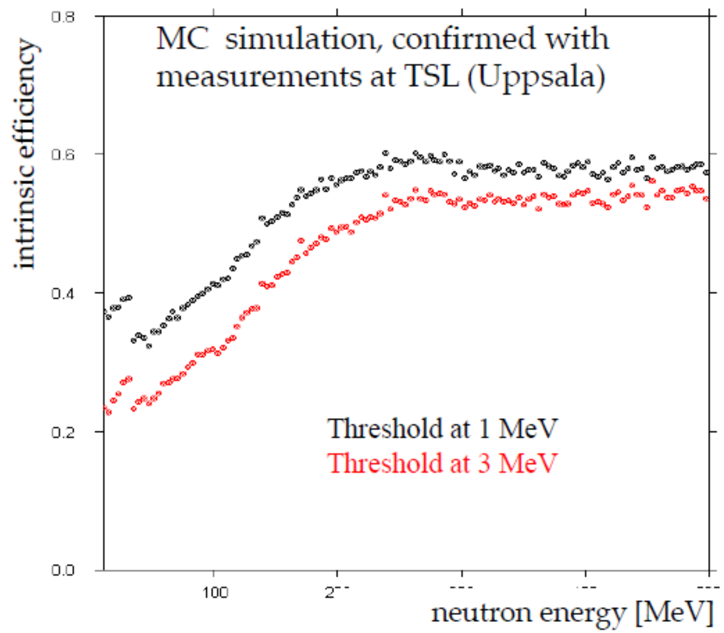

LNF Nov. 10, 2014

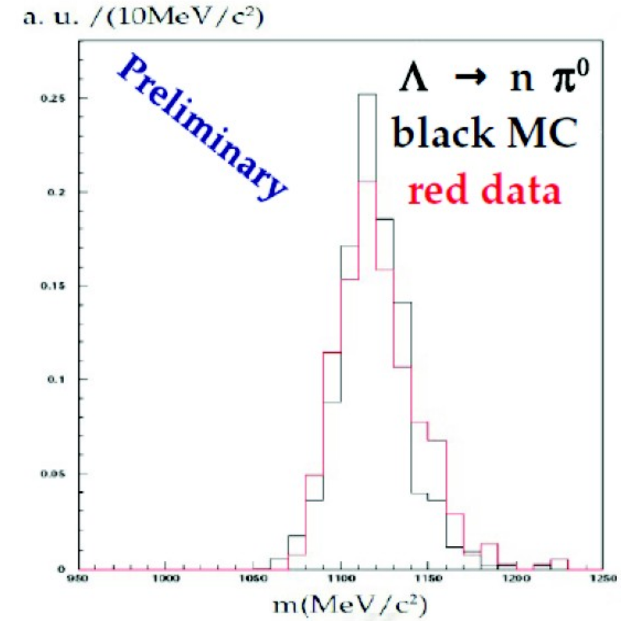

Fig. 1. *$n\pi^0$ invariant mass spectrum measured by the KLOE EMC, the red line corresponds to data, the black one corresponds to a Monte Carlo simulation of the $\Lambda \to n\pi^0$ decay, reconstructed in the KLOE calorimenter.*

KLOE

- 96% acceptance,
- optimized in the energy range of all charged particles involved
- good performance in detecting photons (and neutrons checked by kloNe group (M. Anelli et al., Nucl Inst. Meth. A 581, 368 (2007)))

future AMADEUS physics case

proposal in preparation
you are kindly invited to participate

Conclusions and Future Perspectives

Future → AMADEUS DEDICATED SETUP

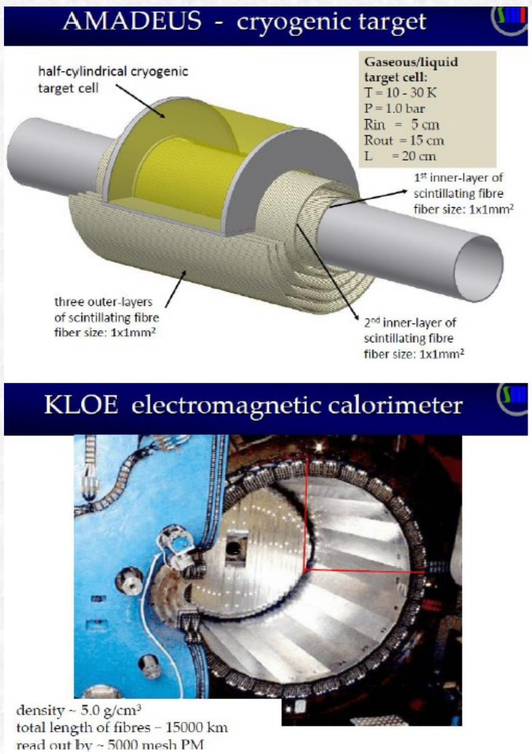

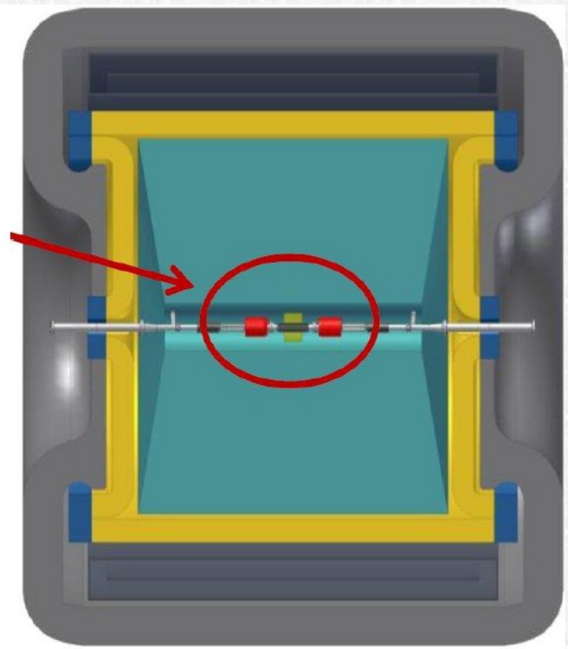

Reuse the KLOE apparatus with dedicated inner solid target (Li, Be, ^{12}C) and cryogenic gaseous target (^4He, ^3He, d)

Scientific Case:

- Investigation of the Λ(1405) properties through the $K^- d \rightarrow (\Sigma\pi)^0 n$ reaction;
- Investigation of YN(NN) two and three body interaction;
- K^- N elastic and inelastic scattering cross section below 100 MeV;
- Study of neutron rich hypernuclei.

Y-N/NN interaction essential impact on the case of NEUTRON STARS

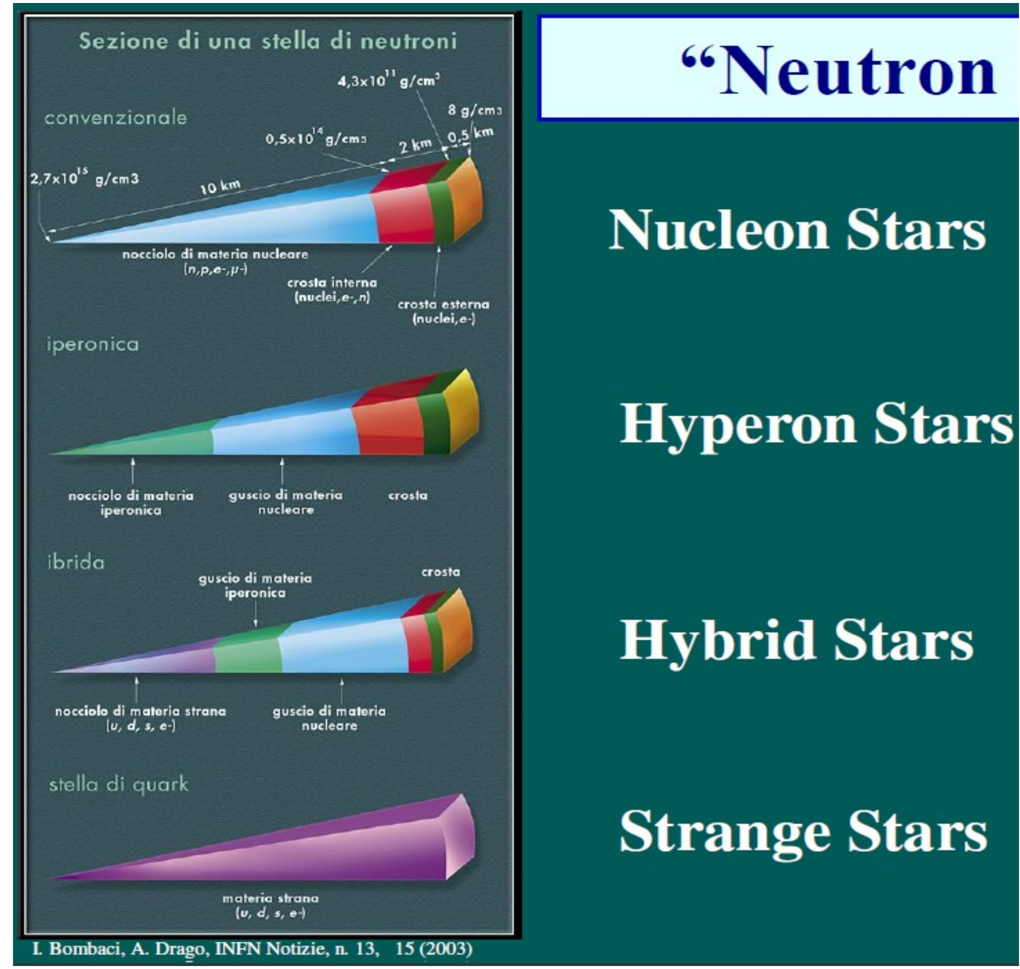

Microscopic approach to hyperonic matter EOS

input

2BF: nucleon-nucleon (NN), nucleon-hyperon (NY), hyperon-hyperon (YY)
e.g. Nijmegen, Julich models

3BF: NNN, NNY, NYY, YYY

Hyperonic sector: experimental data

1. YN scattering (very few data)
2. Hypernuclei

No experimental information on Σ^0-N/NN interaction

Λ-neutron matter

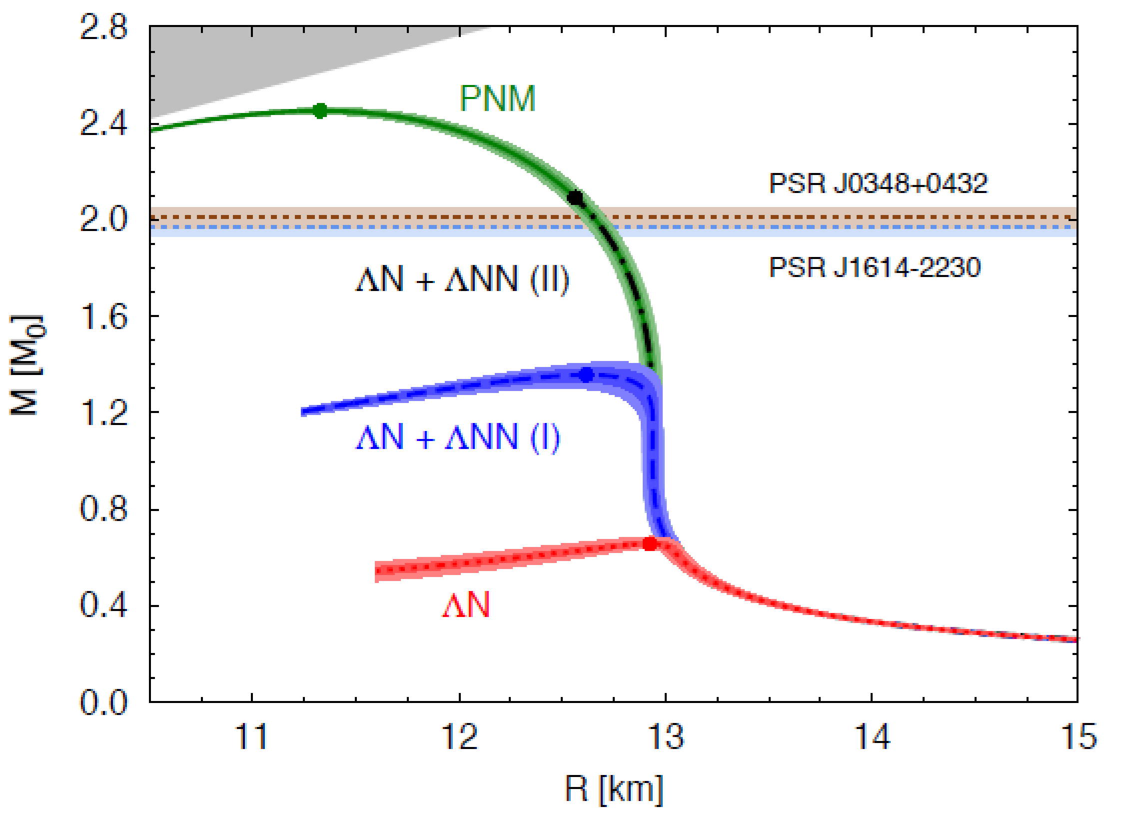

Lonardoni, Lovato, Gandolfi, Pederiva, PRL (2015)

Drastic role played by ΛNN. Calculations can be compatible with neutron star observations.

Note: no $v_{\Lambda\Lambda}$, no protons, and no other hyperons included yet...

No experimental information on Σ^0-N/NN interaction

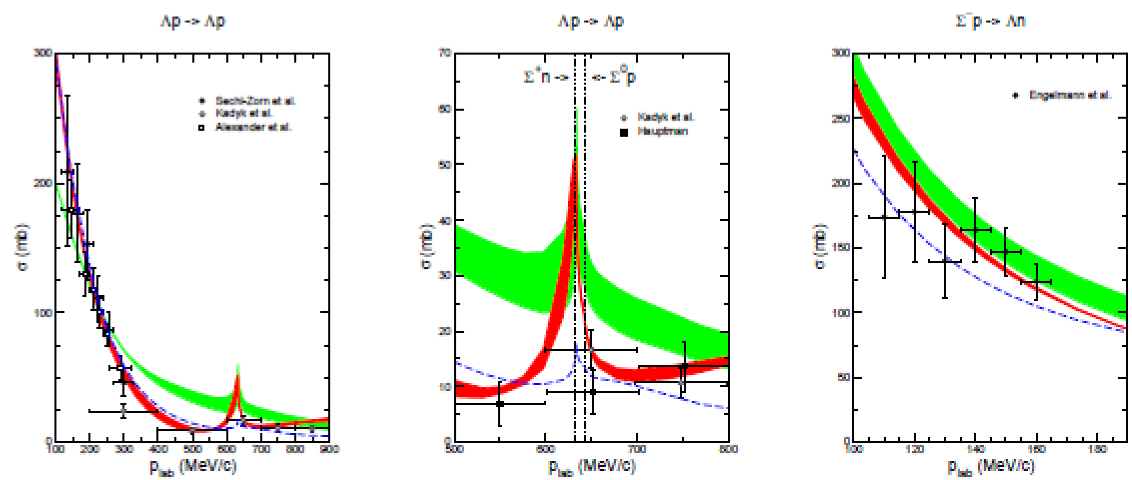

Nucl. Phys. A 915 (2013) 24-58

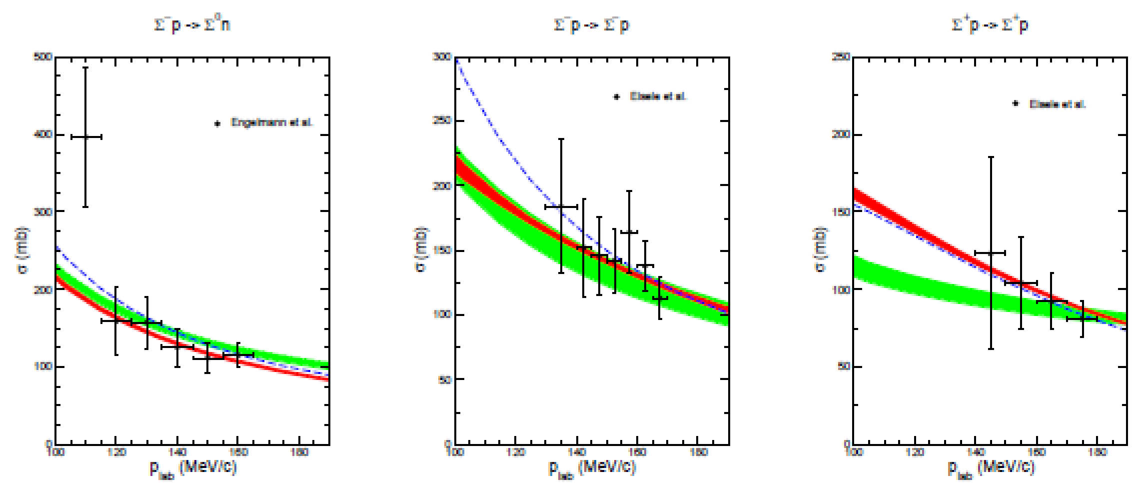

Figure 2: "Total" cross section σ (as defined in Eq. (24)) as a function of p_{lab}. The experimental cross sections are taken from Refs. [52] (filled circles), [53] (open squares), [65] (open circles), and [66] (filled squares) ($\Lambda p \to \Lambda p$), from [54] ($\Sigma^- p \to \Lambda n$, $\Sigma^- p \to \Sigma^0 n$) and from [55] ($\Sigma^- p \to \Sigma^- p$, $\Sigma^+ p \to \Sigma^+ p$). The red/dark band shows the chiral EFT results to NLO for variations of the cutoff in the range $\Lambda = 500, \ldots, 650$ MeV, while the green/light band are results to LO for $\Lambda = 550, \ldots, 700$ MeV. The dashed curve is the result of the Jülich '04 meson-exchange potential [36].

$$(K^- ppn) + n \rightarrow \Sigma^0 d + n$$

3NA in ^{4}He

for the investigation of the

Σ^0-N & Σ^0-(NN) interaction

3NA - (K^- ppn) + n $\rightarrow$ Σ^0 d + n

3NA can be followed by two possible elastic FSI

1) n d $\rightarrow$ n d we may take advantage of the well known σNN data

2) Σ^0 n/d $\rightarrow$ Σ^0 n/d from which to estract information on Σ^0-N , Σ^0-(NN) interaction.

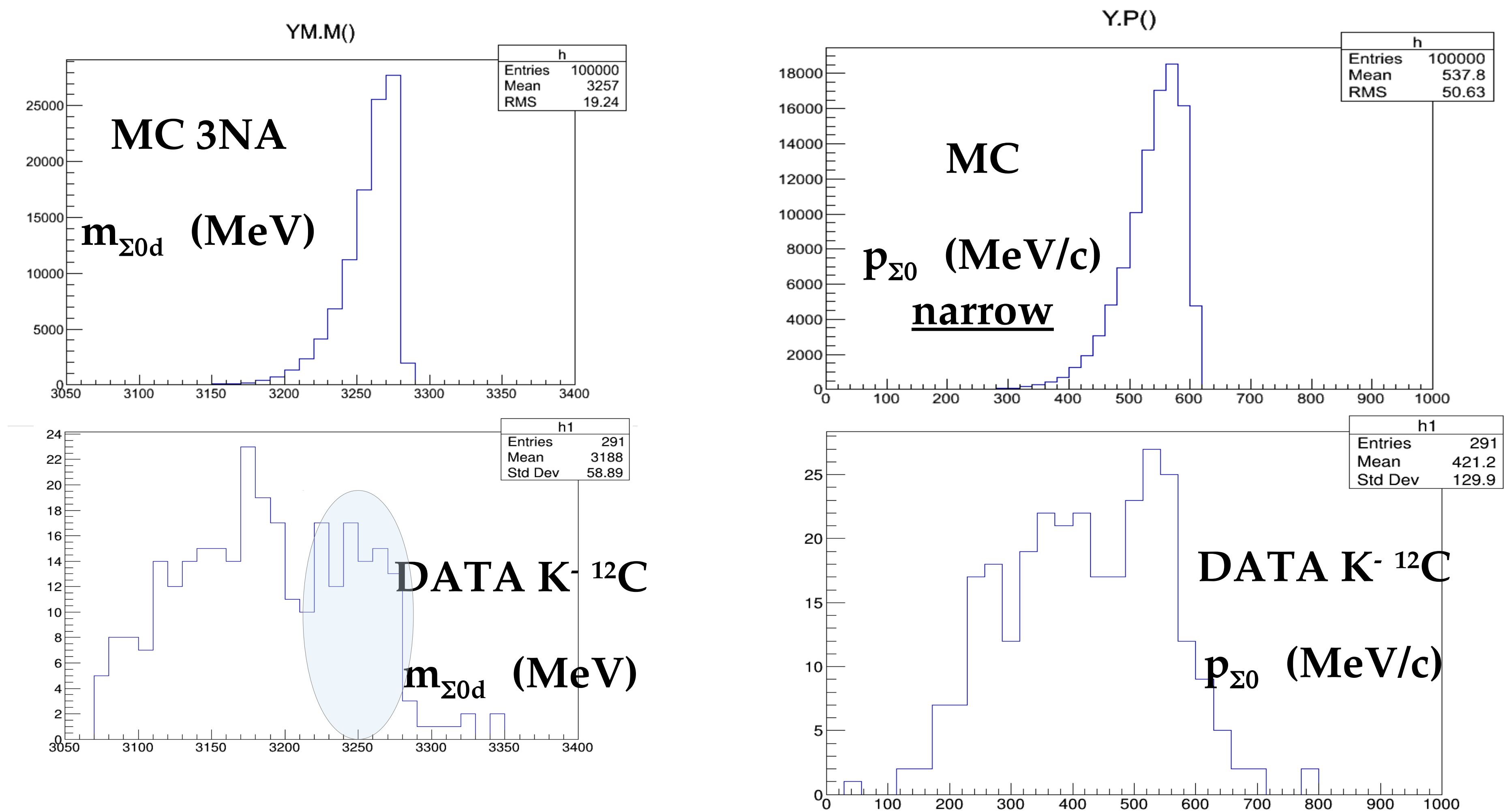

2NA - $(K^- pn) + d \rightarrow \Sigma^0 n + d$

2 possible elastic FSI

1) $n\,d \rightarrow n\,d$ we may take advantage of the well known σ_{NN} data

2) $\Sigma^0 d/n \rightarrow \Sigma^0 d/n$ *hopefully well separated in the lower energy part of the final state phase space*

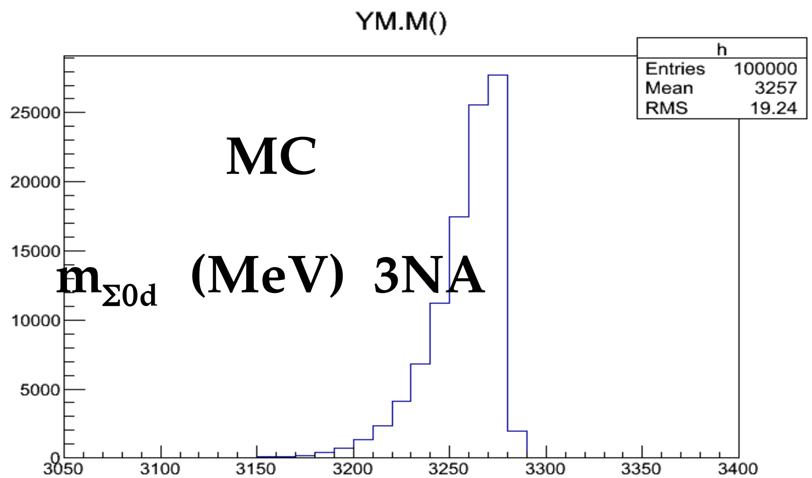

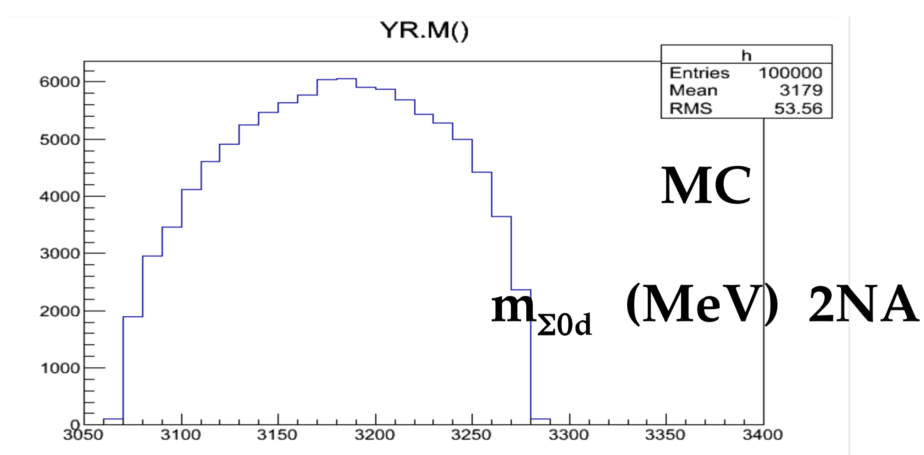

Accurate model of the:

$$(K^- \, ppn) + n \rightarrow \Sigma^0 \, d + n$$

3NA in ^{4}He

+

$$\Sigma^0 \, d/n \rightarrow \Sigma^0 \, d/n \quad \text{FSI}$$

is needed to extract the corresponding cross sections from the measured shapes.


K⁻
Thanks

How search the kaonic bound states?

Production schemes for kaonic bound states:

- K^- absorption experiments: the K^- beams are produced first and then captured from the target nuclei.

Examples:

$$K^- + {}^3He \rightarrow (K^-pp) + n$$
$$(K^-pp) \rightarrow \Lambda + p$$
$$(K^-pp) \rightarrow \Sigma^0 + p$$

$$K^- + {}^4He \rightarrow (K^-ppn) + n$$
$$(K^-ppn) \rightarrow \Lambda + d$$
$$(K^-ppn) \rightarrow \Sigma^0 + d$$

- p-p collisions: proton beam interacts with hydrogen targets.

Example:

$$p + p \rightarrow (K^-pp) + K^+$$
$$(K^-pp) \rightarrow \Lambda + p$$
$$(K^-pp) \rightarrow \Sigma^0 + p$$

- pion induced reactions: pion beams collides with nuclear targets
- photoproduction: photon beams collides with nuclear targets

How search the kaonic bound states?

Analysis procedures to study kaonic nuclear clusters:

- Missing mass spectroscopy: during the formation process of a cluster, by determining the energy and momentum of the partecipating spectator protons or spectator neutrons the mass of the formed object could be determined and so, the binding energy and width of the formed cluster.

  Example: $\mathbf{K^-} + \mathbf{{}^3He} \rightarrow (K^-pp) + \mathbf{n}$

- Invariant mass spectroscopy: all the decay products of the cluster have to be detected and their 4-momentum has to be determined. This allows the recostruction of the invariant mass of the decaying cluster and hence the calculation of the binding energy and width of this object.

  Example: $K^- + {}^3He \rightarrow (K^-pp) + n$

  → $\mathbf{\Lambda + p}$

  → $\mathbf{\Sigma^0 + p}$

Search for the K^-pp bound state

AMADEUS:

- Invariant mass spectroscopy
- K^- absorption experiment → **Backgrounds**: the competiting processes in the search for kaonic bound states are the so-called single and multi-nucleon absortion processes.

EXAMPLE

Let us suppose we want to search the signal of K^-pp bound state in K^- interactions in ^4He through the Λp decay channel

$$K^- + {}^4He \to \Lambda + p + n + n$$

$$K^- + \text{"pp"} \to K^-pp \to \Lambda + p$$

→ This is the process we want to search

2NA: $K^- + \text{"pp"} \to \Lambda + p$

3NA: $K^- + \text{"ppn"} \to \Lambda + p + n$

4NA: $K^- + \text{"ppnn"} \to \Lambda + p + n + n$

$K^- + \text{"pp"} \to \Sigma^0 + p$

$\Sigma^0 + n \to \Lambda + n$

Σ^0 to Λ conversion processes

Experimental studies in the Λp decay channel

- through K^- absorption experiments $K^- X \rightarrow \Lambda\, p\, X'$

FINUDA at DAΦNE (X= ^{6}Li, ^{7}Li, ^{9}Be)
[M. Agnello et al., PRL94, 212303, 2005]

E-549 at KEK (X= ^{4}He)
[T. Suzuki et al., MPLA,23,2520, 2008]

Invariant mass spectroscopy

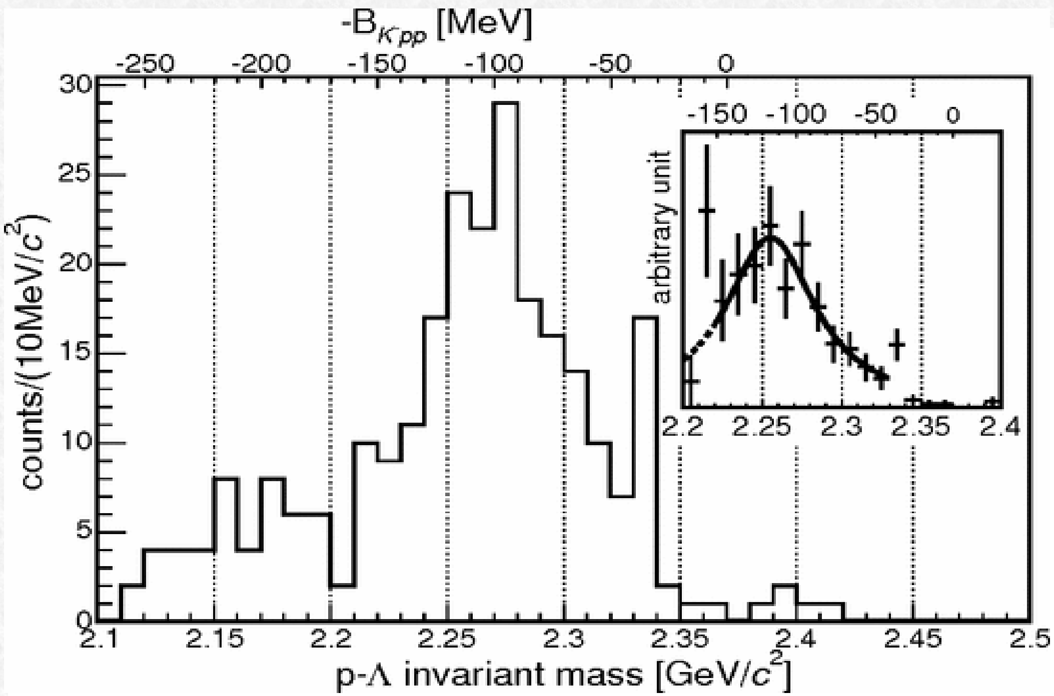

$B = 115^{+6}_{-5}\,(\text{stat})^{+3}_{-4}\,(\text{sys})$ MeV
$\Gamma = 67^{+14}_{-11}\,(\text{stat})^{+2}_{-3}\,(\text{sys})$ MeV

Missing mass spectroscopy

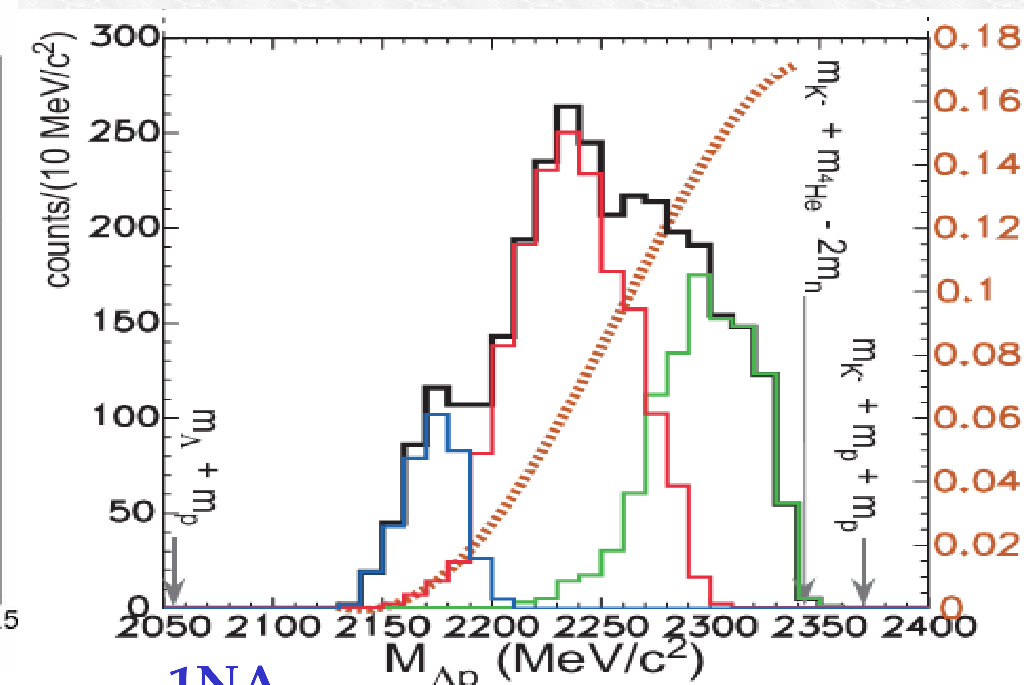

1NA
ΣN/ΛN - DBKNS
2NA

Experimental studies in the Λp decay channel

- through pp collisions

T. Yamazaki et al. Phys.Rev.Lett.104,(2010)

DISTO $pp \to p K^+ \Lambda$

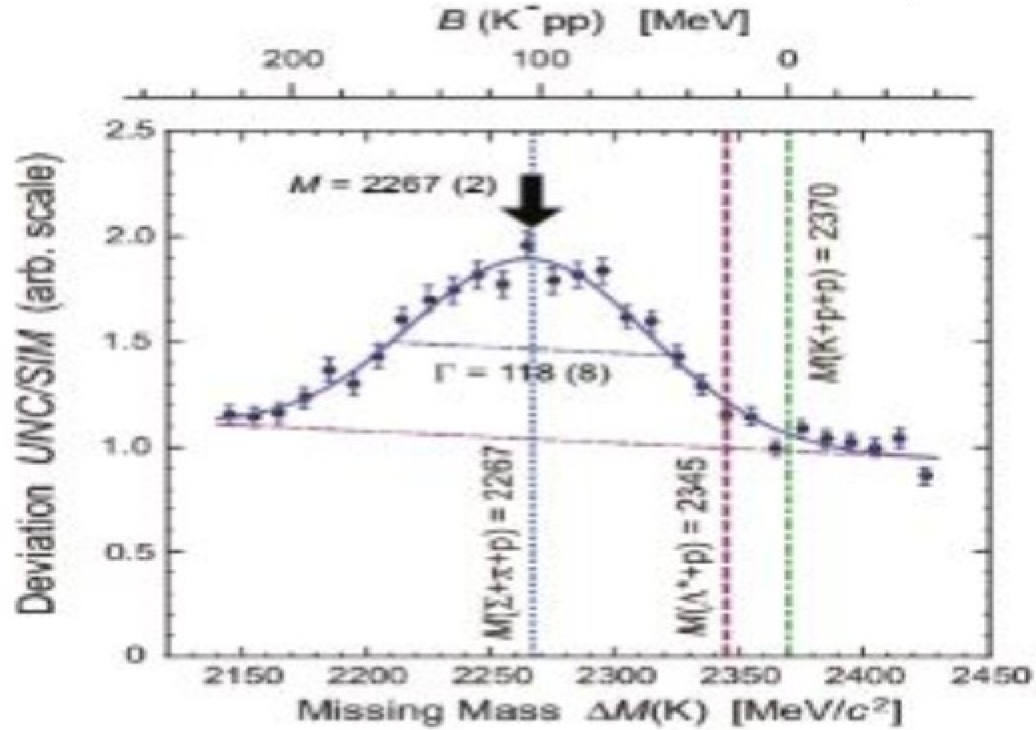

$B(ppK^-)$ = 103 $MeVc^{-2}$
$\Gamma(ppK^-)$ = 118 $MeVc^{-2}$

G. Agakishiev et al., Phys.Lett. B742 (2015) 242-248

HADES $pp \to pK^+\Lambda$ @ p = 2.85 GeV

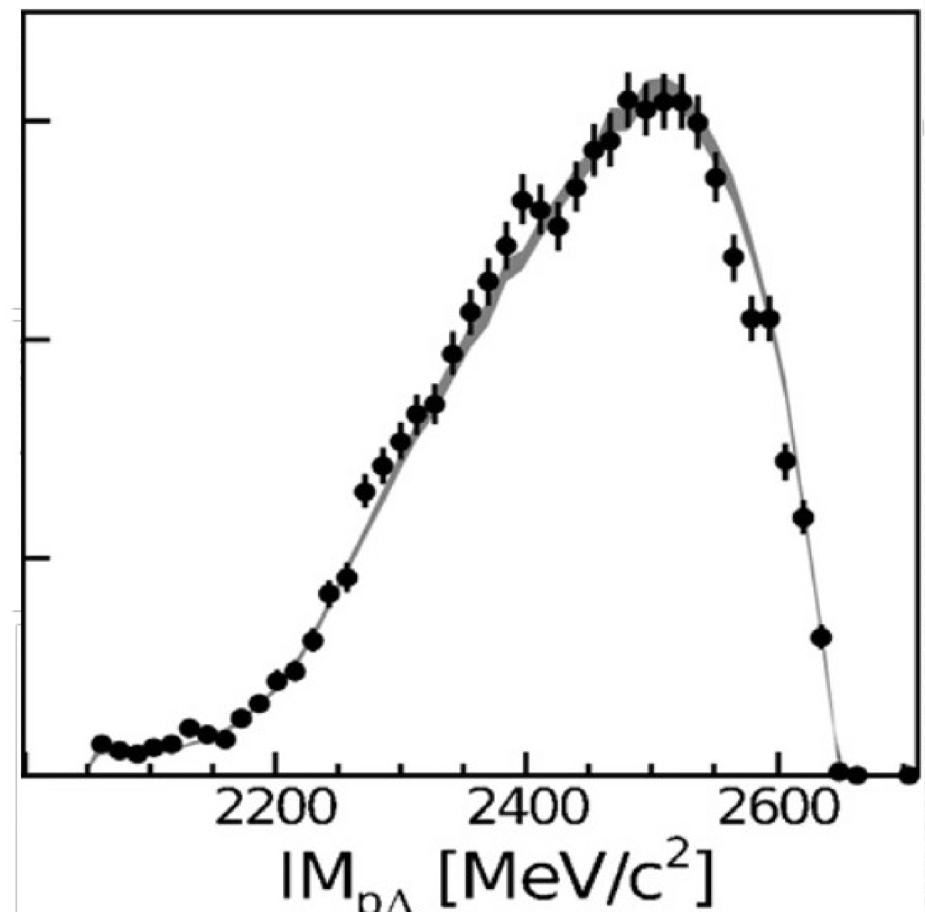

Experimental studies in the Λp decay channel

A.O. Tokiyasu et al., Phys. Lett. B 728 (2014) 616-621

LEPS/SPring-8: d(γ,K⁺π⁻) @ Eγ=1.5-2.4 GeV

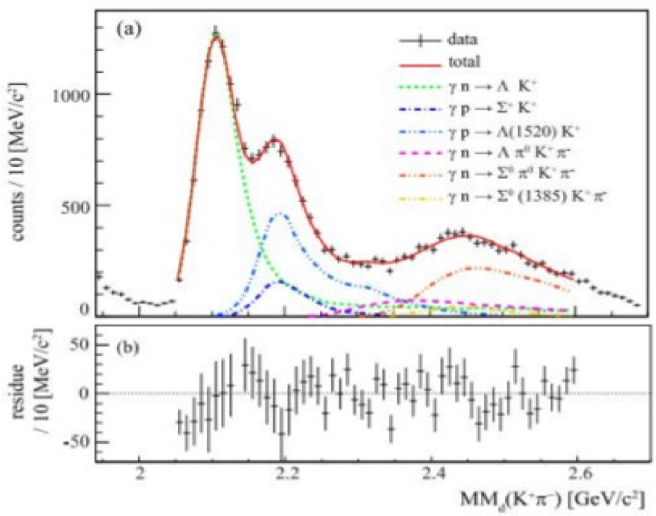

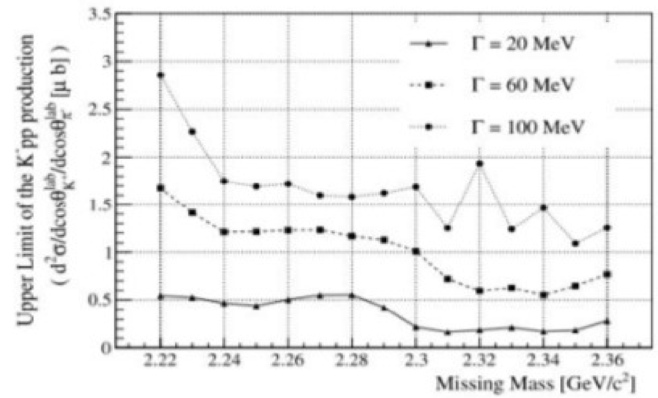

formation upper limit

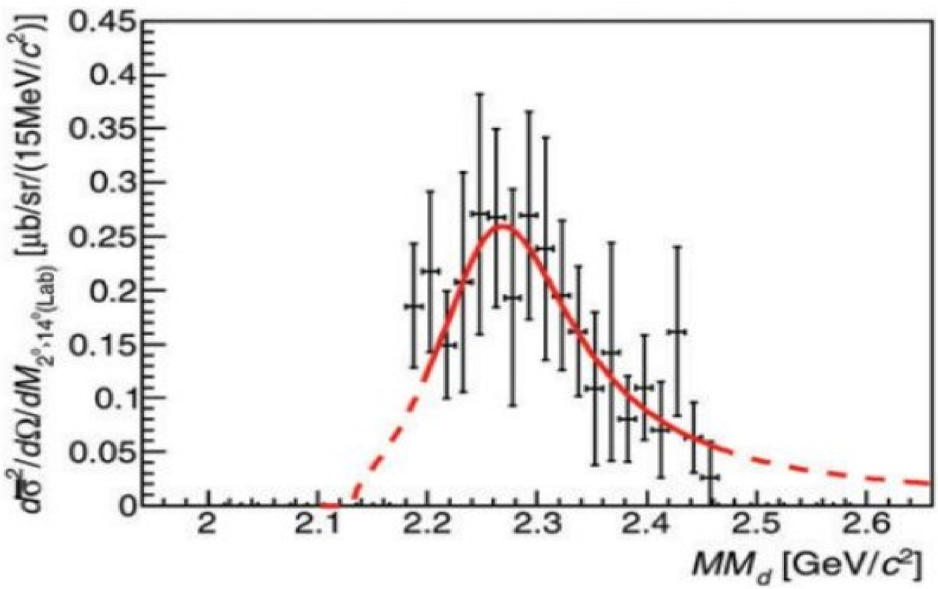

Y. Ichikawa et al., PTEP 2015, 021D01

J-PARC E27: d(π⁺, K⁺) @ 1.69 GeV/c

B =95 +18 −17 (stat.) +30 −21 (syst.) MeV

Γ = 162 +87 −45 (stat.) +66 −78 (syst.) MeV

How deep can an antikaon be bound in a nucleus?

K^-pp bound state

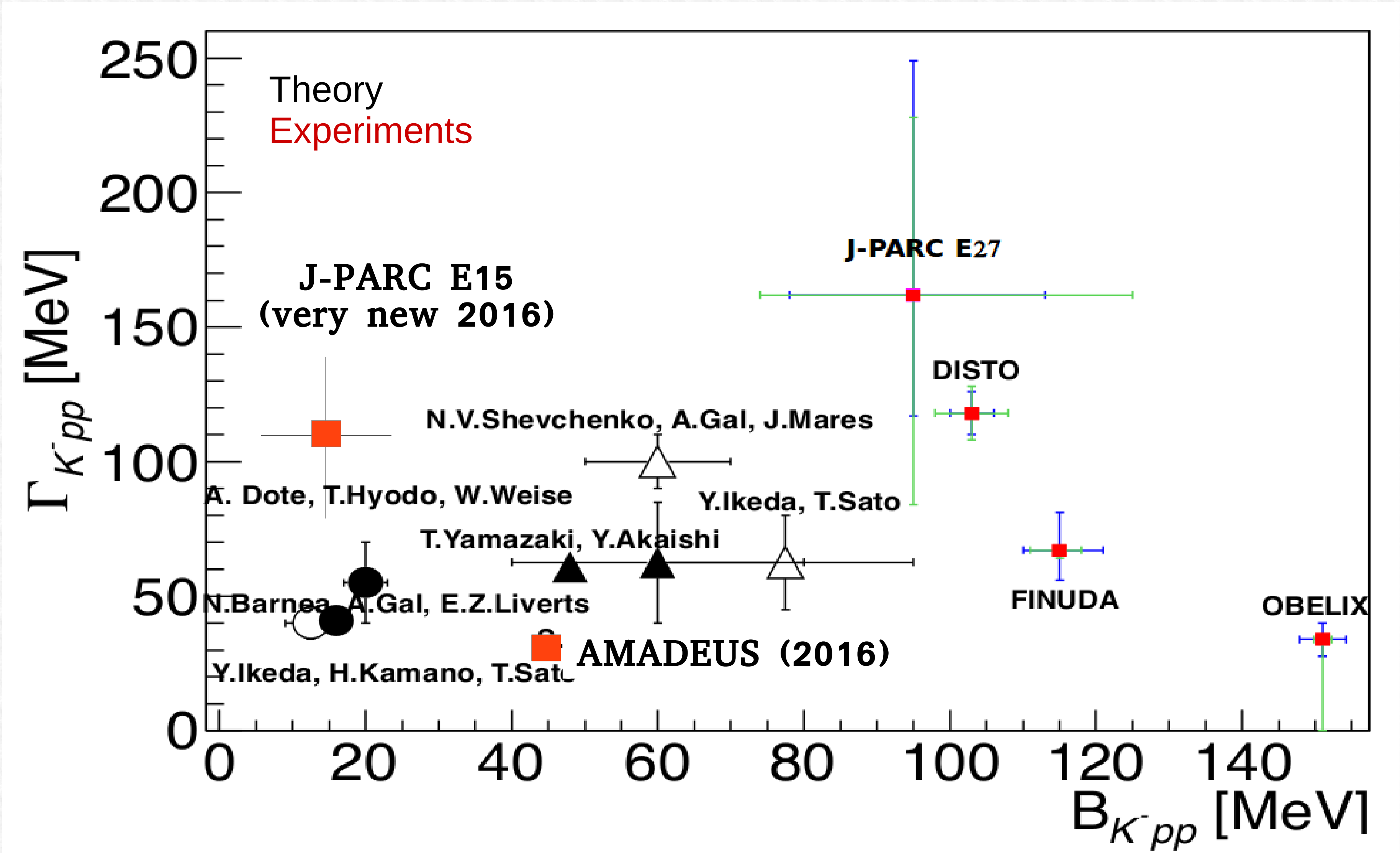

[from the talk of T. Nagae at HYP2015, Sep. 10, 2015]

Λ(1116) the signature of K^- hadronic interaction

The **presence of a Λ(1116) is the signature of K^- absorption** and is the starting point of the performed analysis:

reconstruction of the Λ decay vertex: Λ(1116) → $p\pi^-$ (BR ~ 64 %)

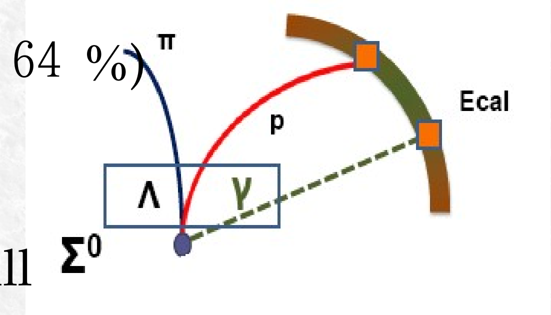

requests:

- vertex with at least two opposite charged particles
- spatial position of vertex inside DC, or in DC entrance wall
- tracks with dE/dx > 95 ADC counts.

First positive tracks are requested to have an associated cluster in the calorimeter and the correct *E* - *p* relation, lack of low momentum protons!

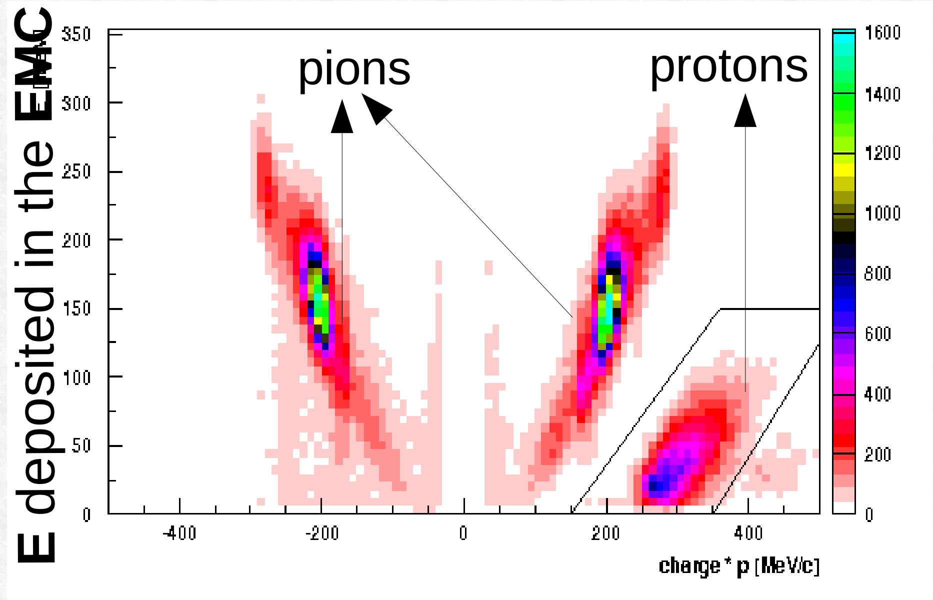

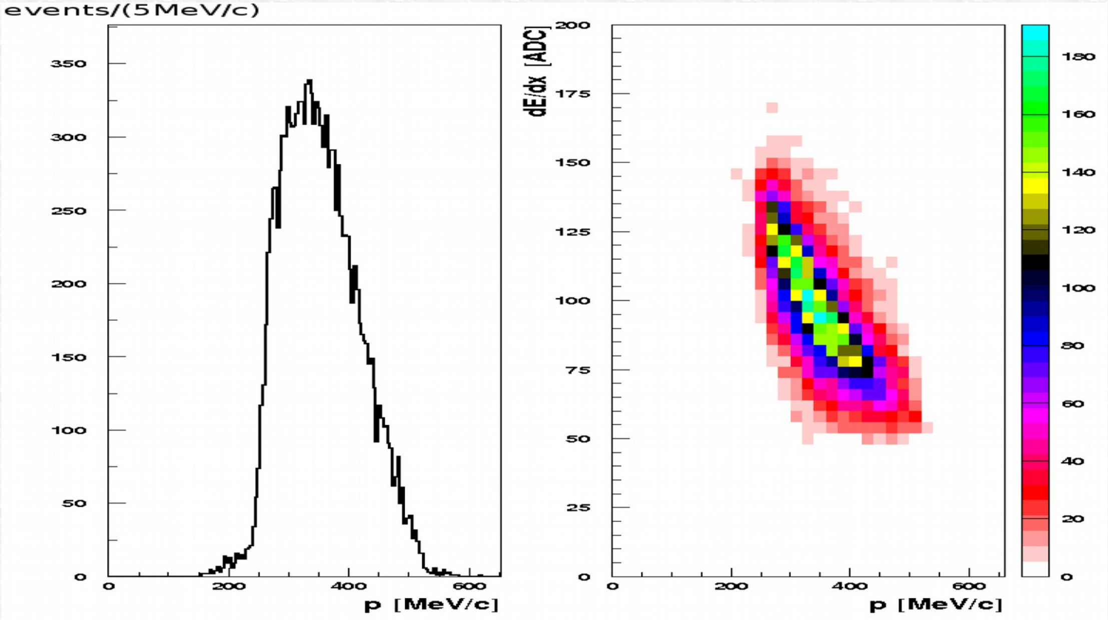

Λ(1116) the signature of K^- hadronic interaction

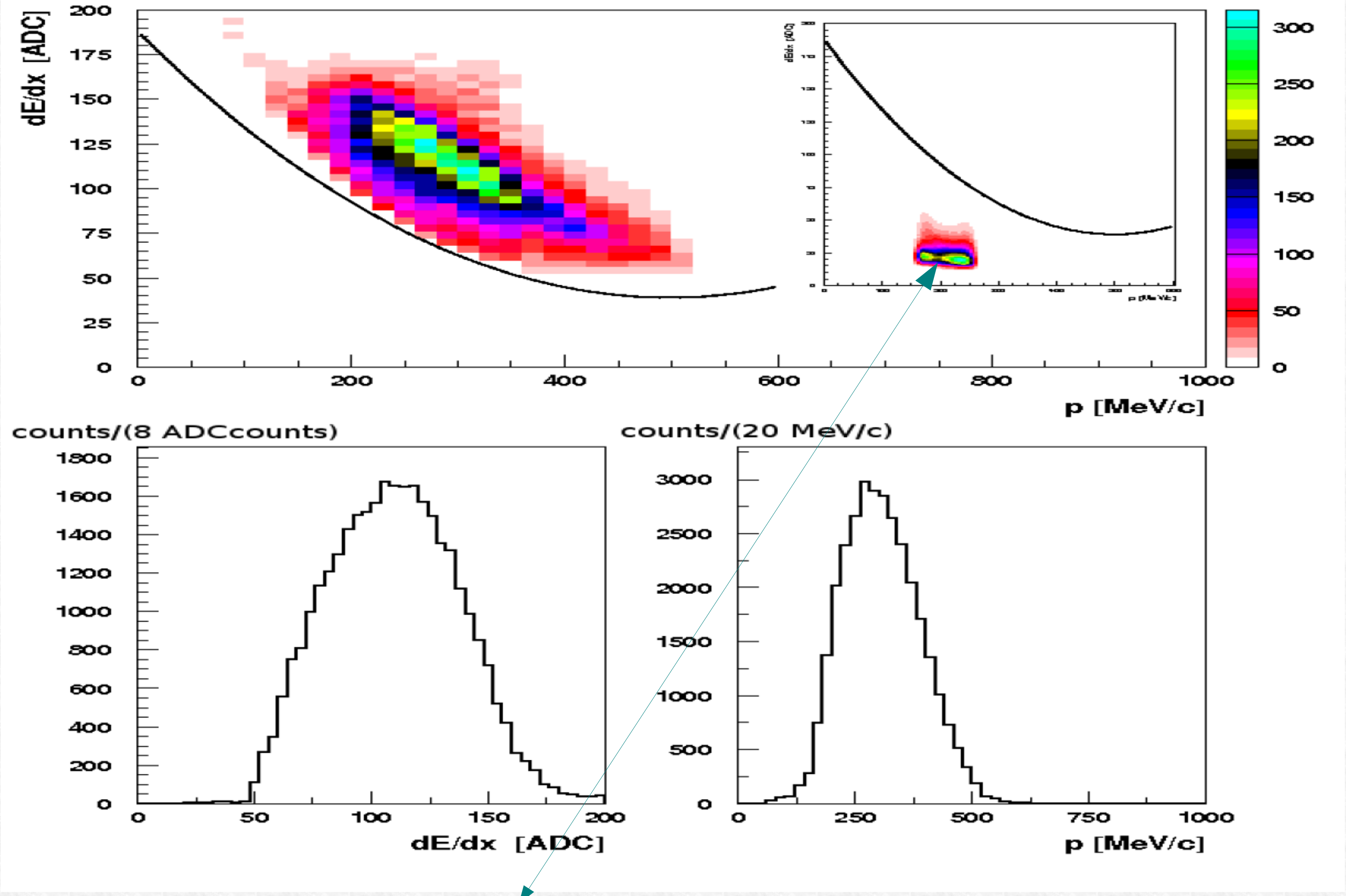

A clear separation with respect to pions (from K^+ two body decay) is evident.

Λ(1116) the signature of K⁻ hadronic interaction

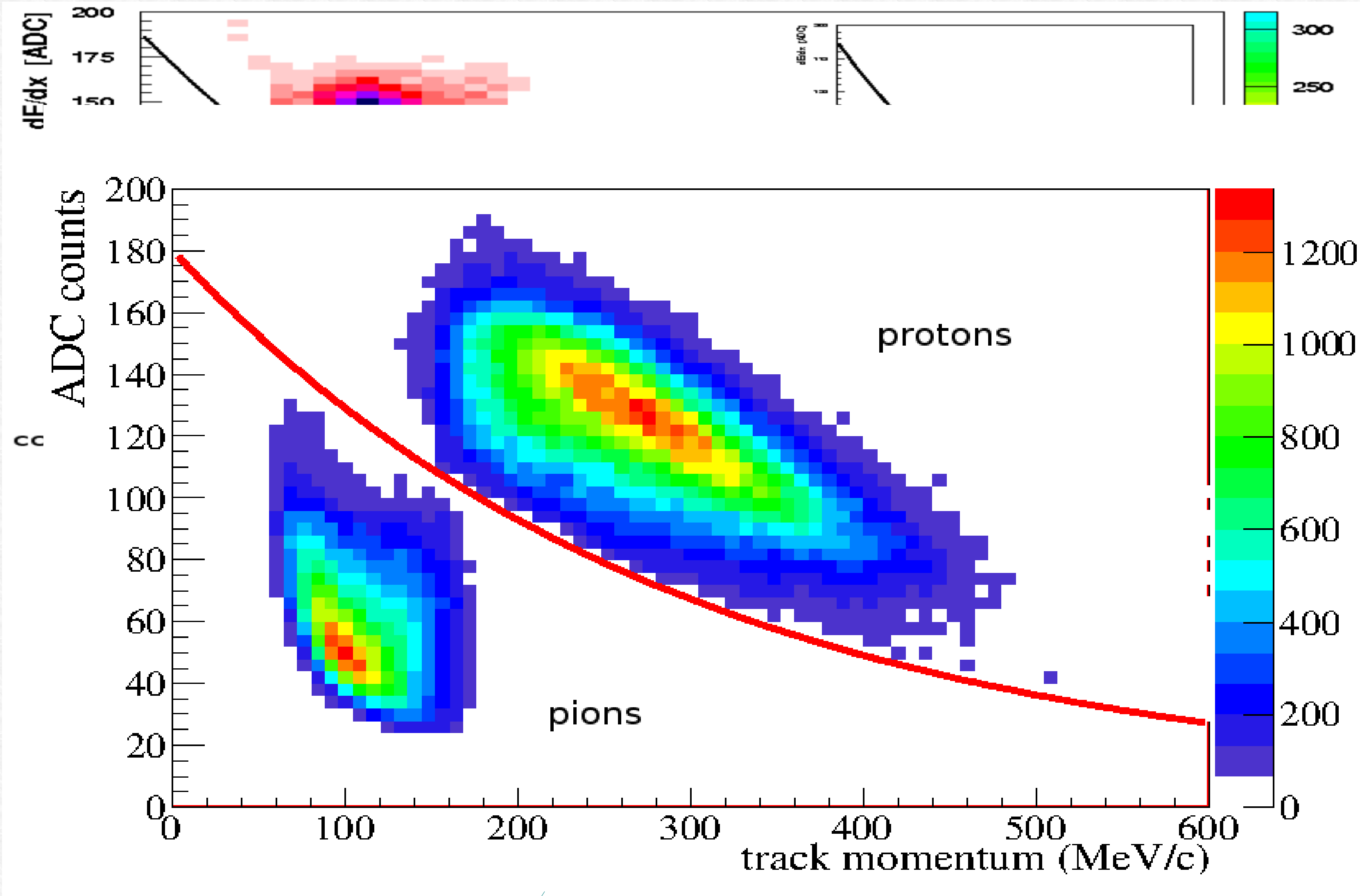

A clear separation with respect to pions (from K^+ two body decay) is evident.

$\Lambda(1116)$ the signature of K^- hadronic interaction

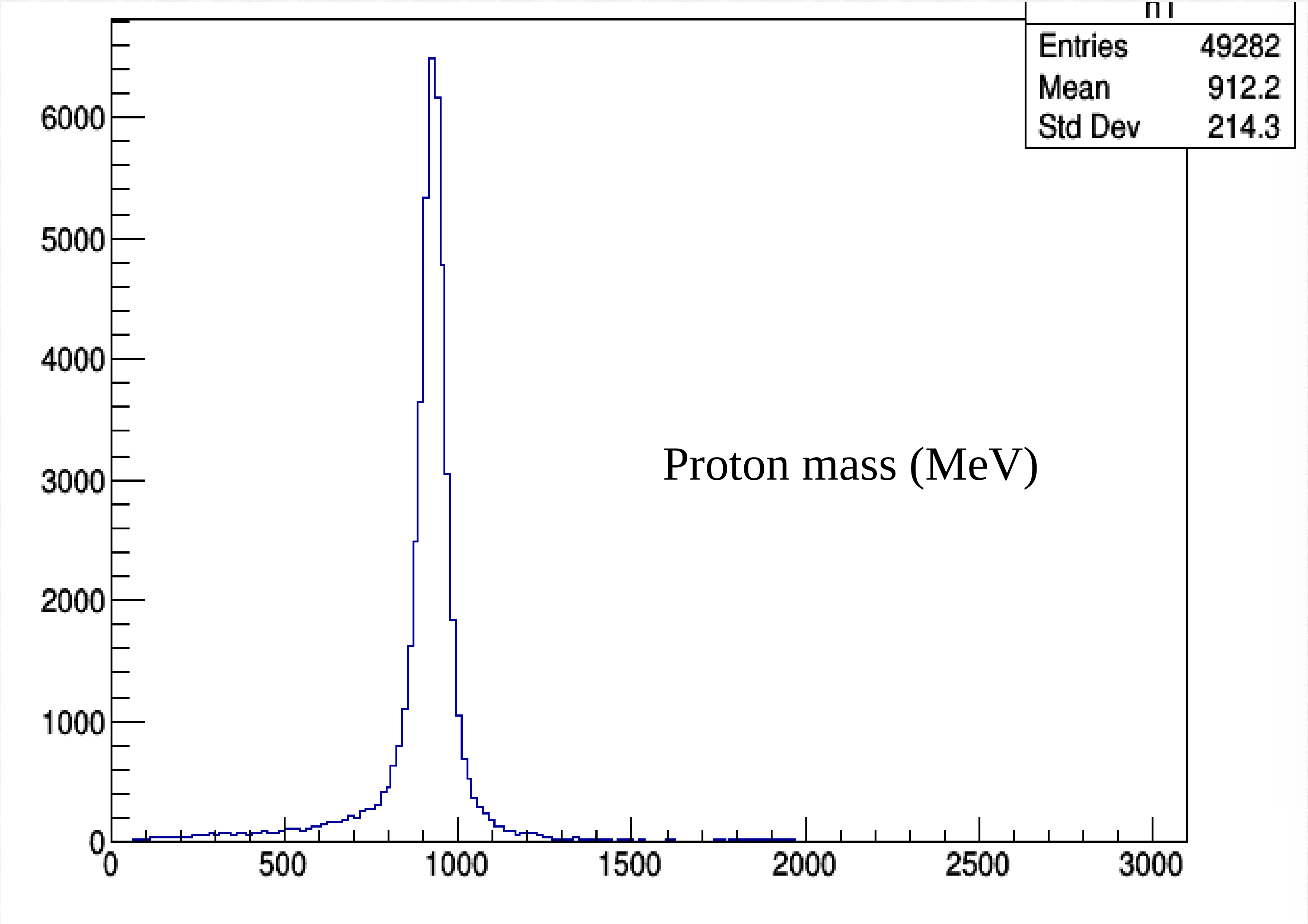

Λ(1116) the signature of K^- hadronic interaction

1st Step: $\Lambda \rightarrow p + \pi^-$ identification (BR = 63.9 ± 0.5 %)

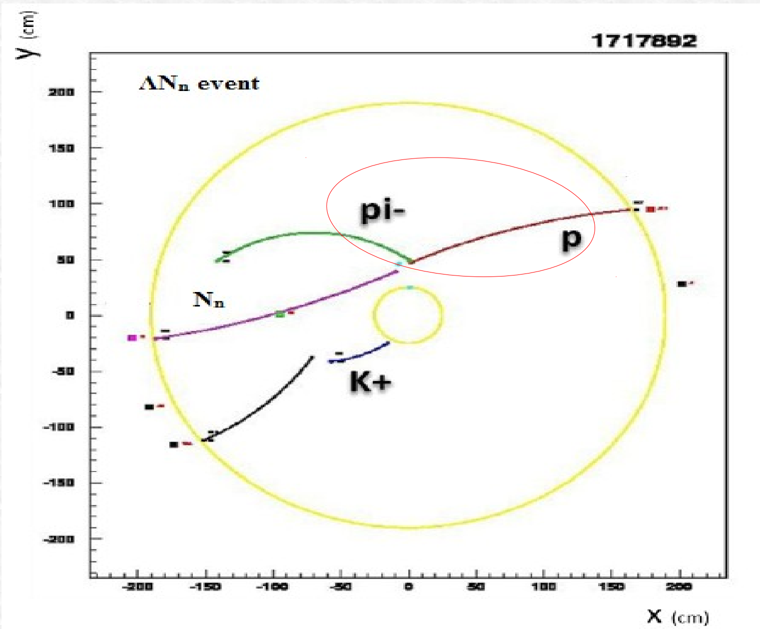

dE/dx information in the DC wires

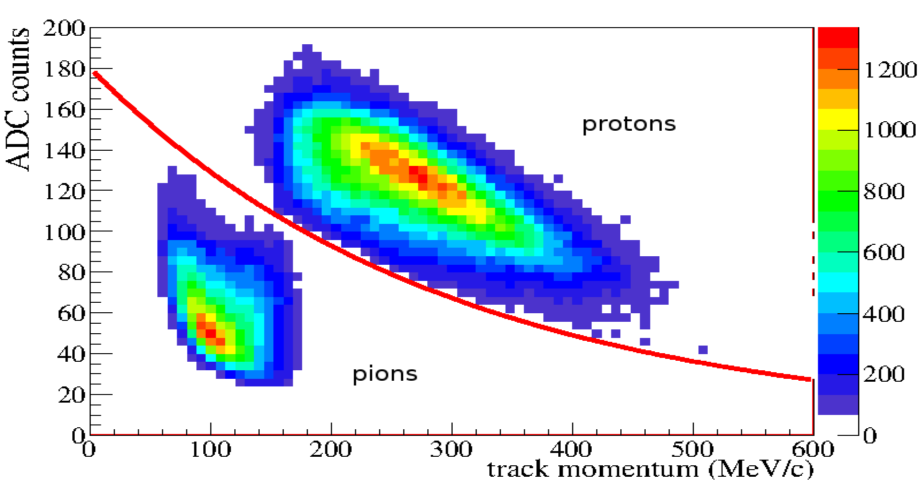

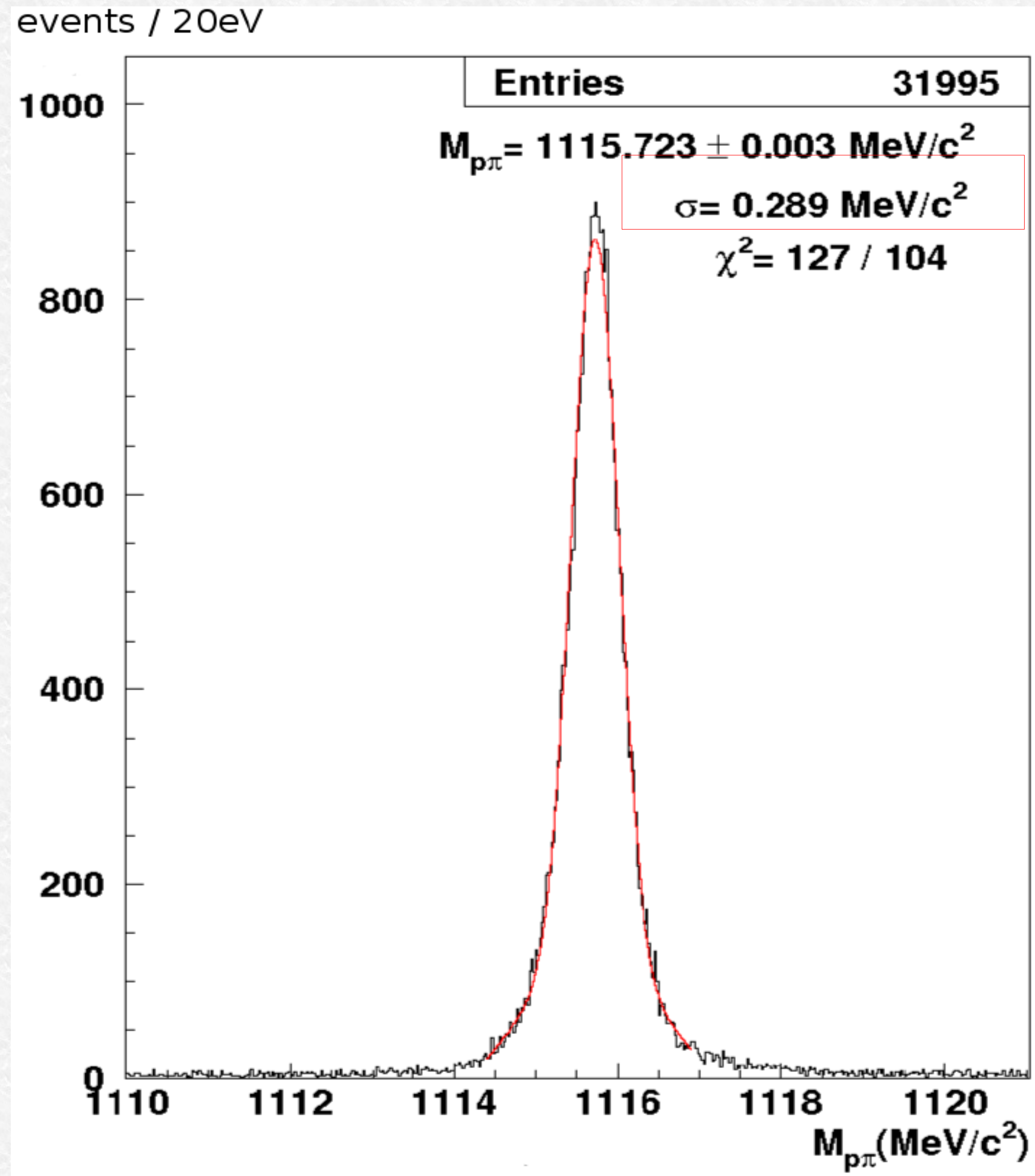

Hadronic interaction vertex recostruction

1st Step: $\Lambda \rightarrow p + \pi^-$ identification
(BR = 63.9 ± 0.5 %)

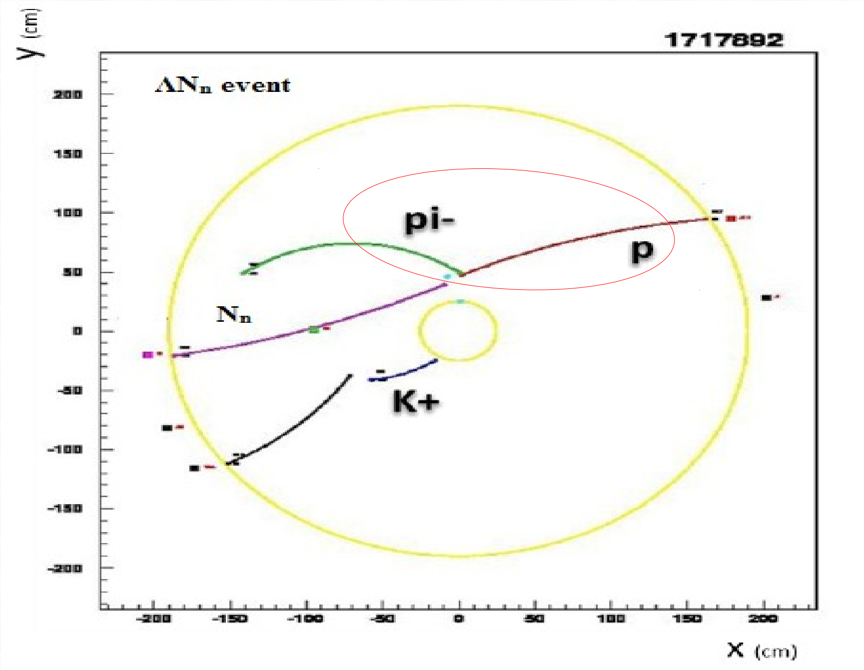

2nd Step: **hadronic interaction vertex** searched extrapolating backwards the Λ path and an extra positive track

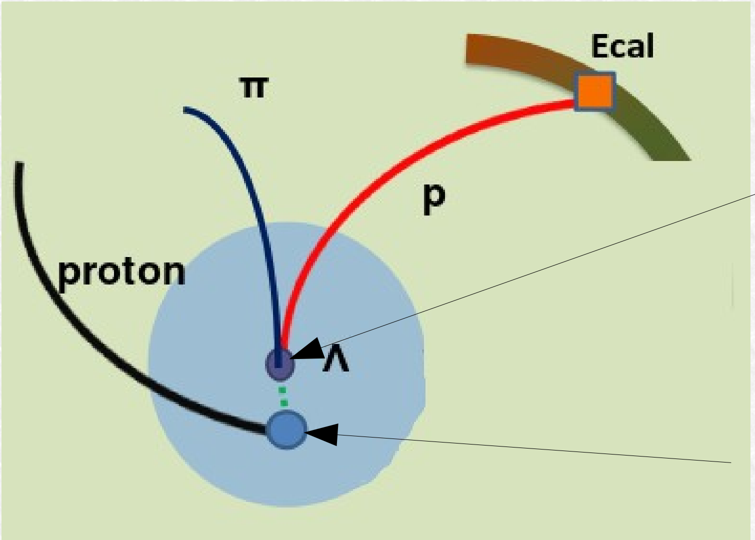

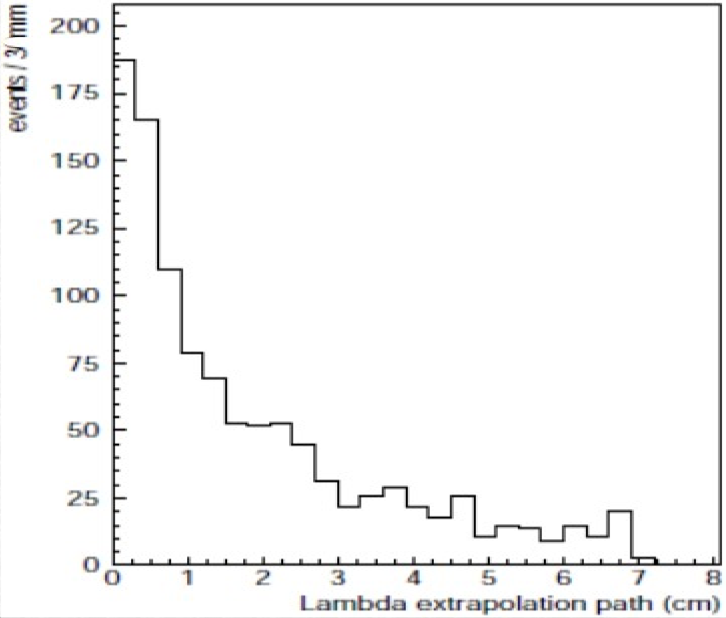

Hadronic interaction vertex recostruction

For the selected Λp events, a check in the mass of the proton track can be done if it is associated with a cluster in the calorimeter, and one of the two particles from the lambda decay has as well an assiciated cluster. To calculate their mass by time of flight we use the time of the cluster (t_{cl}) of the lambda decay product and the time of the interaction (t_i):

$$t_i = t_{cl} - (path_t / v_t) - (path_l / v_l)$$

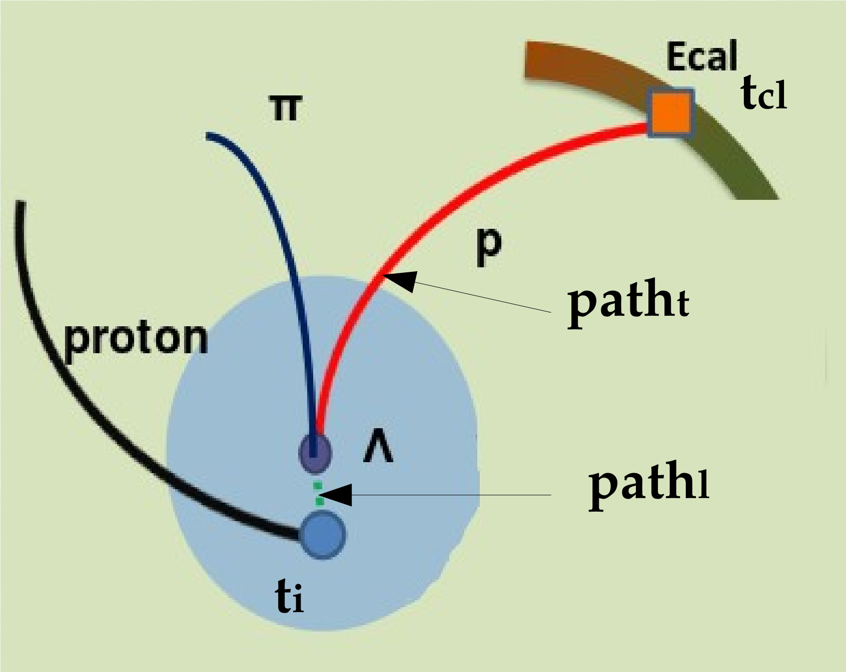

Using the time of the proton cluster in the calorimeter and $path_p$ we calculate the proton velocity v_p. The mass is calculated using the information of the proton momentum p_p:

$$mass = p_p \cdot \sqrt{1/(v_p^2/c^2)}$$

Hadronic interaction vertex recostruction

Resolutions:

From MC simulations of
K^- absorption in ^4He

p_Λ	0.49 ±
p_p	2.63 ±
$M_{\Lambda p}$	1.10 ±
r_{vertex}	0.12

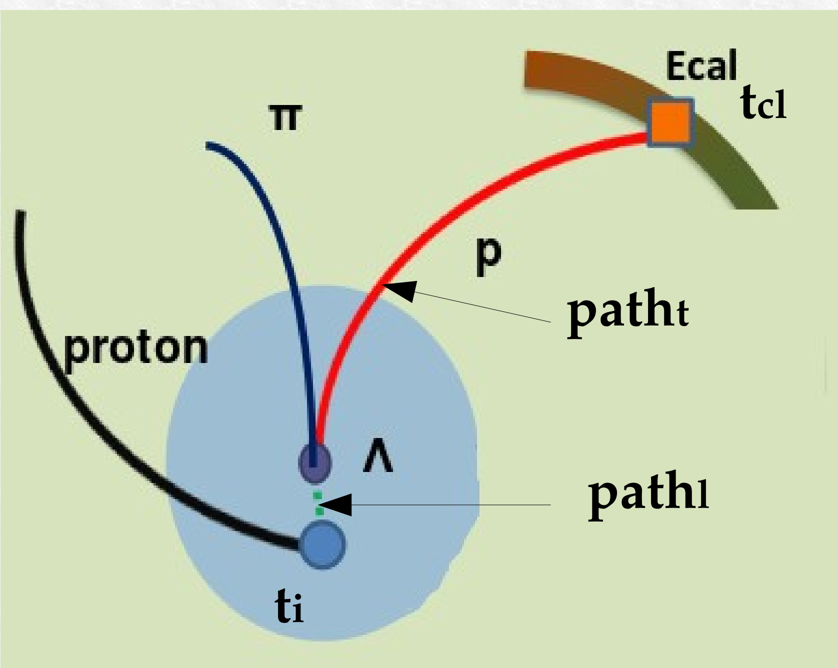

Extra-proton mass

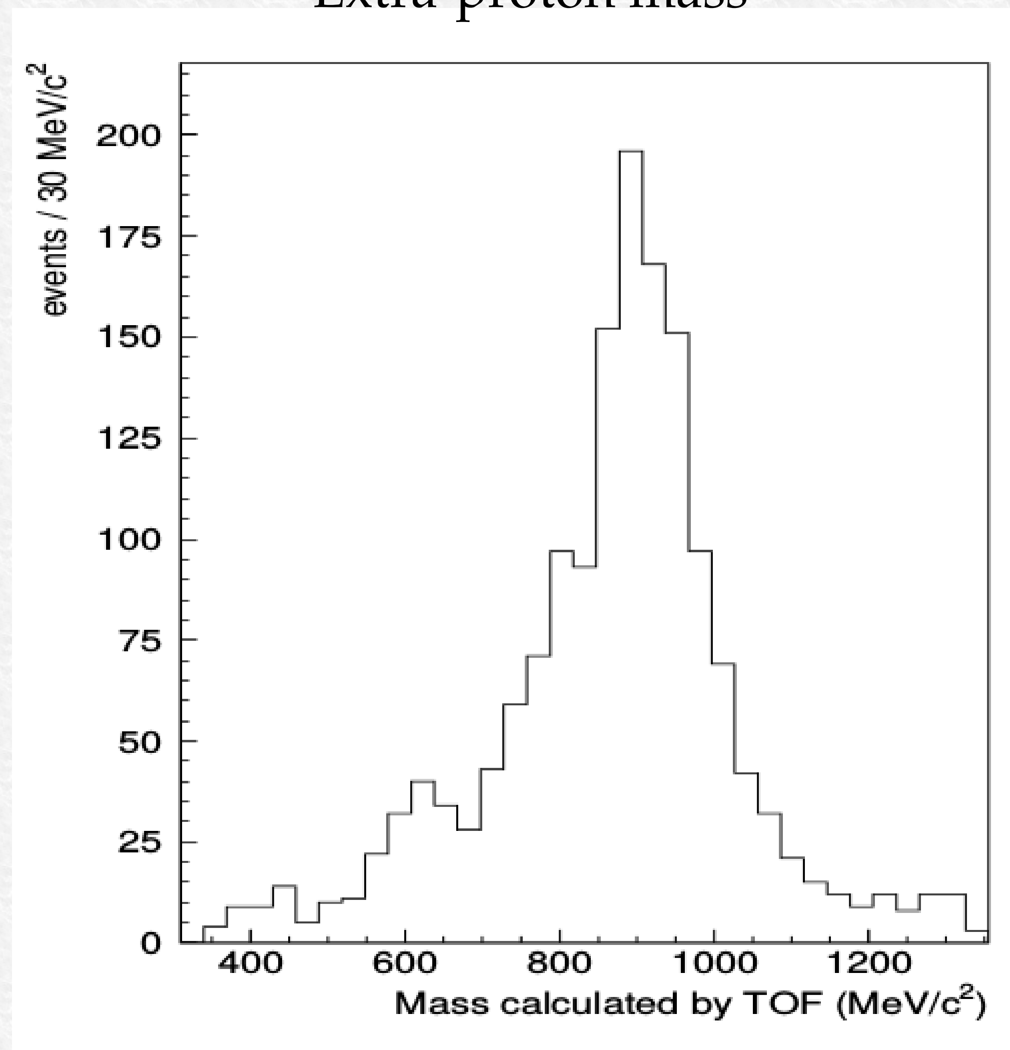

Hadronic interaction vertex recostruction

Additional photon signal at the hadronic vertex is required to select Σ^0**p events.**

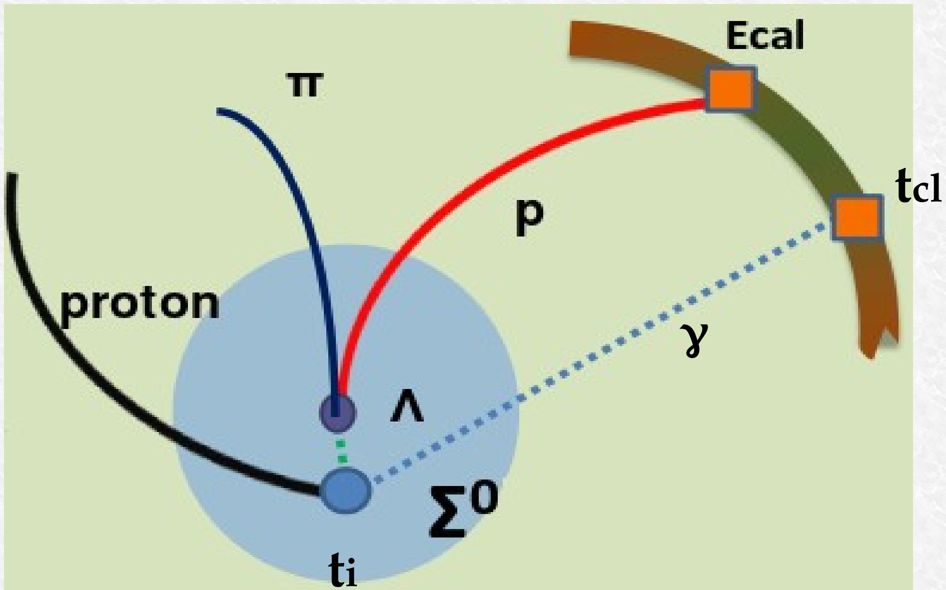

The photon candidate selection:

1. search for neutral clusters in the calorimeter
2. calculate the hadronic interaction time ti, using the time time of the cluster of one of the lambda decay particles
3. calculate the distance between the hadronic vertex and the cluster position
4. the requirement is

$$Time\ of\ flight = t_{cl} - t_i = path_\gamma / c$$

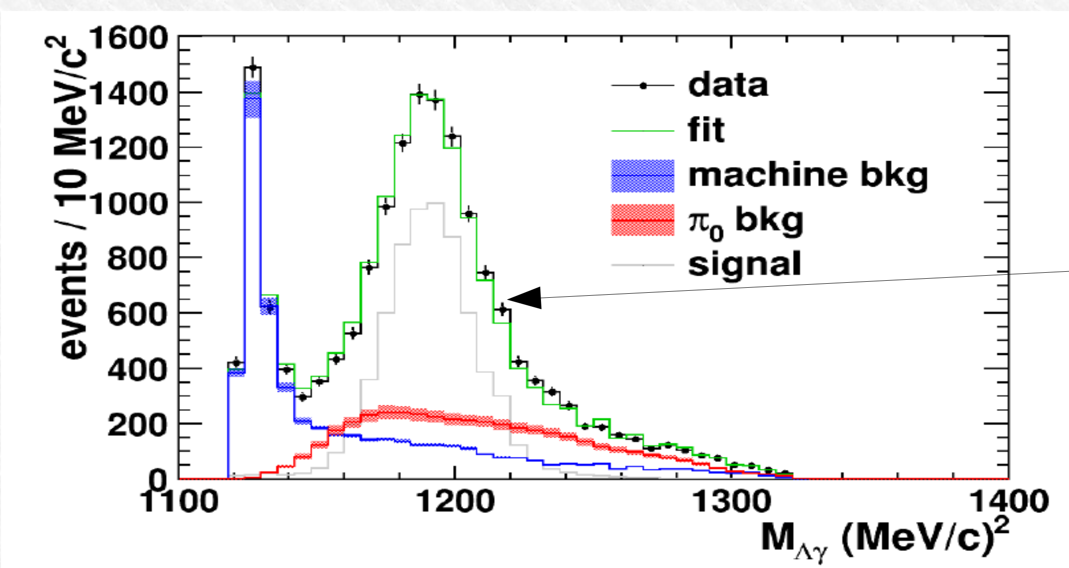

$$\Sigma^0 \rightarrow \Lambda + \gamma$$

Hadronic interaction vertex

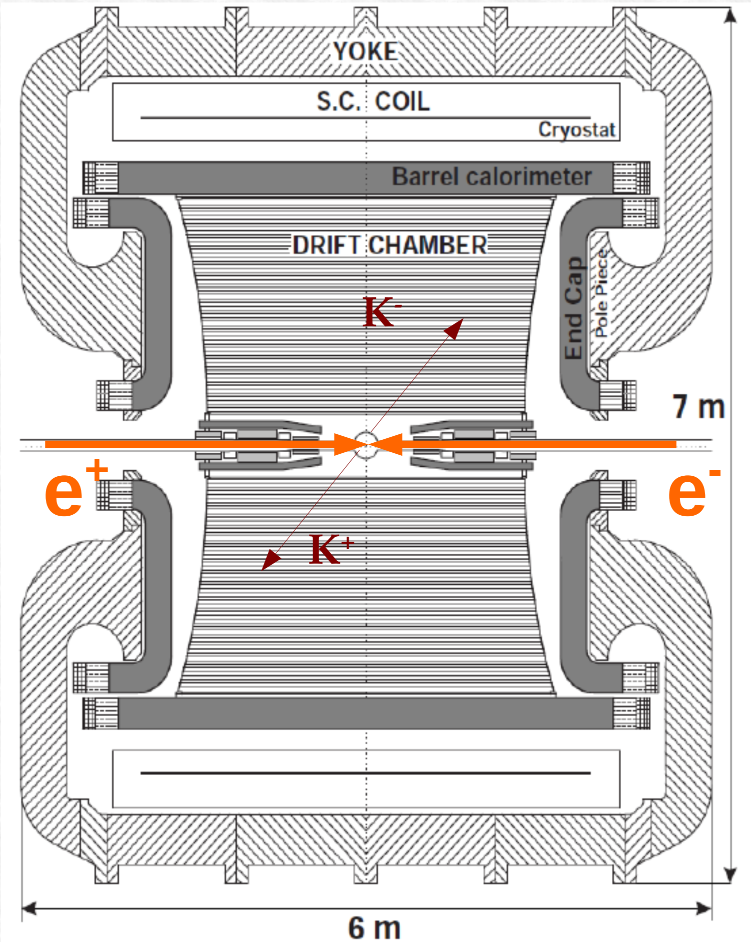

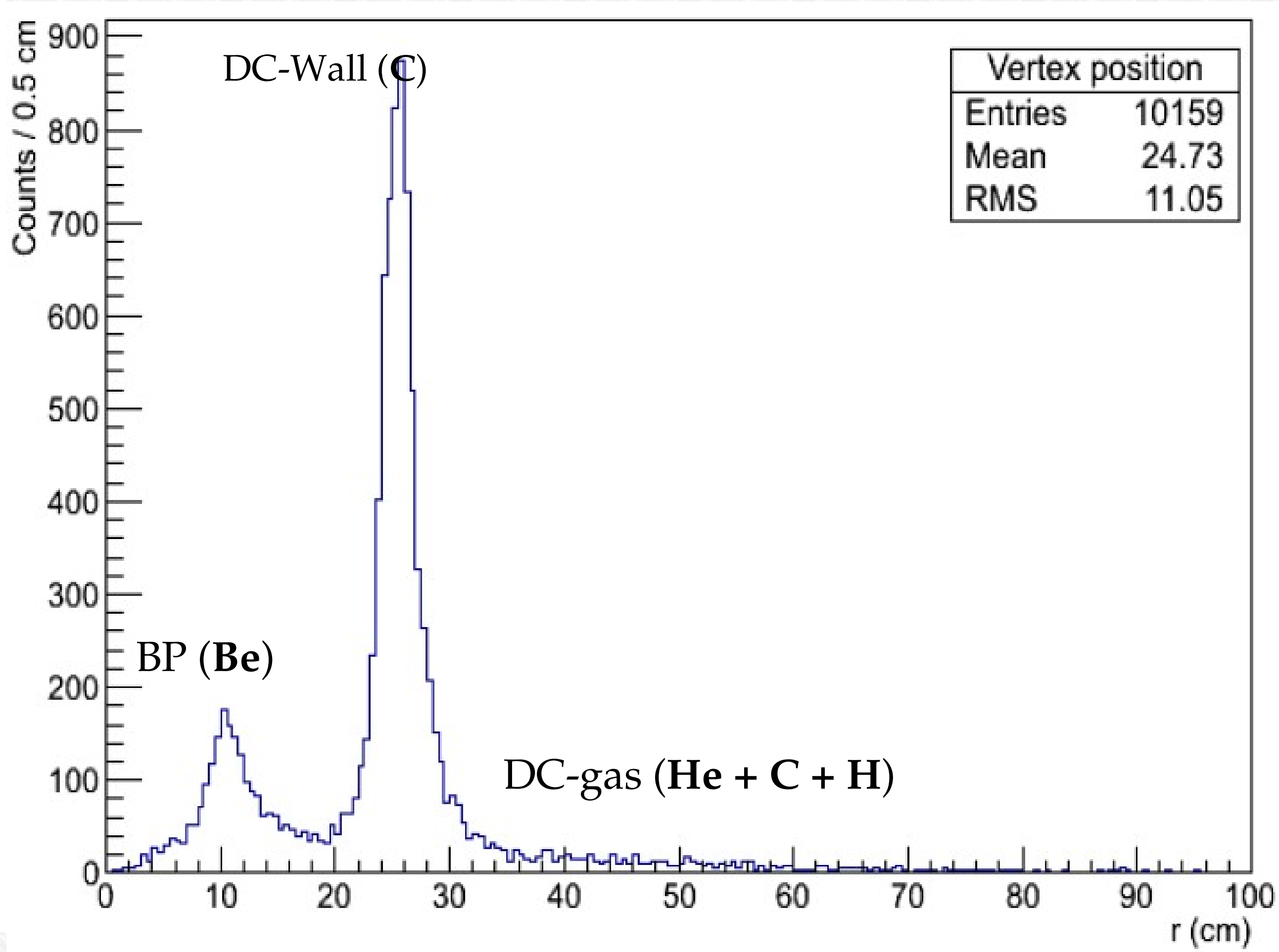

Events:

AT-REST (K$^-$ absorbed from atomic orbit)

IN-FLIGHT (p_K~100MeV)

Deuteron and triton identification

Selection in masses obtained by Time of Flight

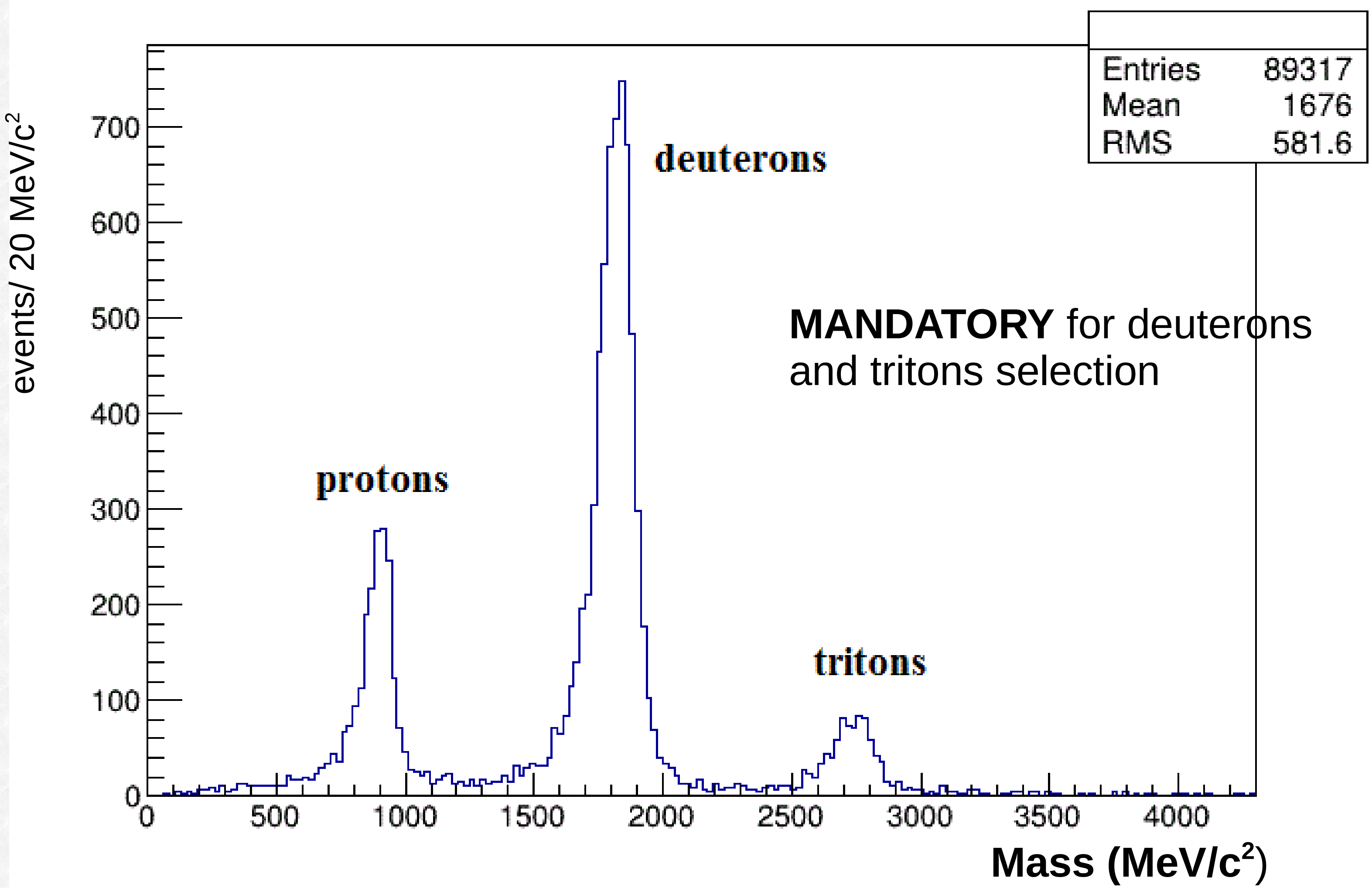

MANDATORY for deuterons and tritons selection

Λp channel

MC Simulations

2NA Λp-QF

- **Mode11: $K^- + {}^{12}C \rightarrow \Lambda + p + {}^{10}Be$**
- **Mode12: $K^- + {}^{12}C \rightarrow \Lambda + p + 2\,{}^{4}He + 2\,n$**
- Mode13: $K^- + {}^{12}C \rightarrow \Lambda + p + 4\,p + 6\,n$
- Mode14: $K^- + {}^{12}C \rightarrow \Lambda + p + {}^{4}He + 4\,n + 2\,p$
- **Mode15: $K^- + {}^{12}C \rightarrow \Lambda + p + {}^{4}He + 2\,t$**
- **Mode16: $K^- + {}^{12}C \rightarrow \Lambda + p + {}^{4}He + {}^{3}He + 3\,n$**
- Mode17: $K^- + {}^{12}C \rightarrow \Lambda + p + {}^{8}Be + 2\,n$